Sonoprocessing:
from Concepts to Large-scale Reactors

Daniela Meroni[a], Ridha Djellabi[a,*], Muthupandian Ashokkumar[b], Claudia L. Bianchi[a], Daria C. Boffito[c,d,*]

[a] Dipartimento di Chimica, Università degli Studi di Milano, Via Golgi 19, 20133 Milano, Italy

[b] School of Chemistry, University of Melbourne, Parkville, VIC 3010, Australia

[c] Polytechnique Montréal, Département de Génie Chimique, C.P. 6079, Montréal H3C 3A7, Canada

[d] Canada Research Chair in Intensified Mechano-Chemical Processes for Sustainable Biomass Conversion, Department of Chemical Engineering, Polytechnique Montréal, C.P. 6079, Succ. CV, H3C 3A7 Montréal, Québec, Canada

* Corresponding authors: ridha.djellabi@unimi.it, daria-camilla.boffito@polymtl.ca

Authors' bio:

Dr. Daniela Meroni received her PhD in Chemical Sciences in 2013. During this period, she was a visiting student in the groups of Prof. Dirk Poelman at Ghent University and of Prof. Ulrich S. Schubert at Jena University. She was then awarded Post-doctoral fellowships in the groups of Prof. G. Cappelletti and Prof. S. Ardizzone at the University of Milan. In 2015 she was awarded the *Debut in Research* ENI award. From 2017, she is a Research Associate in the Department of Chemistry at the University of Milan. Her research interests include the application of ultrasound to environmental remediation and synthesis.

Dr Ridha Djellabi received his PhD from Badji-Mokhtar University (Annaba, Algeria) in Analytical Chemistry and Environment. He conducted a part of his thesis research at University of Milan, Italy. He carried out a postdoctoral research at LSRE-University of Porto, Portugal. After that, Ridha worked at RCEES, Chinese Academy of Sciences (Beijing, China) and Shenzhen University (Shenzhen, China). Currently, Ridha works at University of Milan. His research focuses mainly on the intensification of advanced oxidation processes and eco-friendly materials design towards environmental pollution abatement. He is the author of more than 55 papers and 6 book chapters. ORCID: 0000-0002-1475-5565

Prof. Muthupandian Ashokkumar (Ashok) is a Physical Chemist who specializes in Sonochemistry and is a senior academic staff member of the School of Chemistry, University of Melbourne. He is currently the Assistant Deputy Vice-Chancellor International at the University of Melbourne. Ashok is a renowned sonochemist, with about 25 years of experience in this field. He is the Editor-in-Chief of *Ultrasonics Sonochemistry*, an international journal devoted to sonochemistry research with a Journal Impact Factor of 7.491). He has edited/co-edited several books and special issues for journals; published ~450 refereed papers (**H-Index: 68**) in high impact international journals and books; and delivered over 200 invited/keynote/plenary lectures at international conferences and academic institutions.

Prof. Claudia L. Bianchi is full professor of Industrial chemistry at the University of Milan. Author of numerous original research papers on International Journals with IF in applied material science and environmental catalysis (H-index: 46), 2 patents, and several chapters in books. Her expertise relates to heterogeneous catalyst design mainly applied to environmental remediation. Recent research aimed to fabricate active and selective solid catalysts at micro/nano-scale in sono/photodegradation processes substantially for pollution control and environmental compliance in both water and gas phases, exploiting the sunlight. She has approached chemical engineering and manufacturing with Process Intensification techniques such as ultrasound to reduce the energy requirements of the syntheses in a liquid phase and confer definite structural-morphological and chemical properties to powders. LCA calculations are often on the basis of her recent research, to determine the environmental impact of products.

Daria C. Boffito is Associate Professor in Chemical Engineering at Polytechnique Montréal since 2016, whereby she is the head of the Engineering Process Intensification and Catalysis (EPIC) research group. She holds the Canada Research Chair in Intensified Mechanochemical Processes for Sustainable Biomass Conversion. She received Canadian and International prizes, including the Emerging Leaders in Chemical Engineering (Canadian Society for Chemical Engineering - CSChE), the NSERC Banting postdoctoral fellowship, the PBEEE FRQNT scholarship, GreenTalents2012 (German government), and The Australia Awards Endeavour Research Fellowship (2011, Australian government). She completed a Ph.D. in Industrial Chemistry at the University of Milan in 2013. Besides sonochemistry, her research interests include Process Intensification, heterogeneous catalysis, and biomass conversion. She is the Executive Editor of *Ultrasonics Sonochemistry*, an international journal devoted to sonochemistry research with a Impact Factor of 7.491. Prof. Boffito is also active in the field of scientific communication. She coauthored one book on how to redact scientific papers, posters, and presentations. Prof. Boffito collaborates with Canadian and foreign companies in the field of oil and gas, material synthesis, biomass conversion, and process inetsnification technologies.

Abstract

Intensification of ultrasonic processes for diversified applications, which include environmental remediation, extractions, food processes, synthesis of materials among others, has received attention from both the scientific community and industry. The mechanistic pathways involved in intensification of ultrasonic processes that include the ultrasonic generation of cavitation bubbles, radical formation upon their collapse, and the possibility of fine-tuning operating parameters for specific applications are all well documented in the literature. However, the scale-up of ultrasonic processes with large-scale sonochemical reactors for industrial applications remains a challenge. In this context, this review provides a complete overview of the current understanding of the role of operating parameters and reactor configuration on the sonochemical processes. Experimental and theoretical techniques to characterize the intensity and distribution of cavitation activity within sonoreactors are compared. Classes of laboratory and large-scale sonoreactors are reviewed, highlighting recent advances in batch and flow-through reactors. Finally, examples of large-scale sonoprocessing applications have been reviewed, discussing the major scale-up and sustainability challenges.

Table of Content

1. Introduction

Ultrasound, a developing technology for chemical and processing applications, is classified as a process intensification approach. Process intensification comprises a pool of innovative approaches that improves process efficiency, and provides opportunities for feedstock substitution, energy transition, in particular for the electrification of the chemical industry.

Ultrasound is sound waves of frequencies above 20 kHz, *i.e.*, the upper audible limit of human hearing. Ultrasound is generally classified into low frequency (20-100 kHz, corresponding to wavelengths in water between 7.4 cm and 1.5 cm), intermediate frequency (100 kHz-1 MHz, corresponding to a 15-1.5 mm wavelength range in water) and high frequency (1-10 MHz, with wavelength in water down to *ca.* 150 μm). In a liquid medium, ultrasound waves induce the growth of bubbles (cavities) via nucleation of pre-existing dissolved gas bubbles or gas sacs trapped in solid impurities, at surfaces or appositely machined pits. Ultrasound imposes on the formed bubbles an oscillatory sound (pressure) field, which causes cycles of high pressure, compressing the gas within the bubble, and low pressure, forcing the bubble to expand. Under the effect of the ultrasound field, bubbles tend to grow via rectified diffusion of dissolved gases and solvent molecules to the oscillating bubble[1] and coalescence of bubbles[2]. When a bubble reaches the (frequency dependent) resonance size (usually in the range of micrometers), it couples strongly to the acoustic field and grows to a maximum in a single acoustic cycle [3]. At this point, it implodes, fragmenting into smaller bubbles that can either dissolve or repeat the process (**Figure 1**). Overall, the phenomenon of ultrasound-induced nucleation, growth and collapse of micro-bubbles is referred to as acoustic cavitation. Under specific experimental conditions, a single bubble may continue to grow and collapse without fragmentation and repetitively undergo growth and collapse for each acoustic cycle (single bubble cavitation).

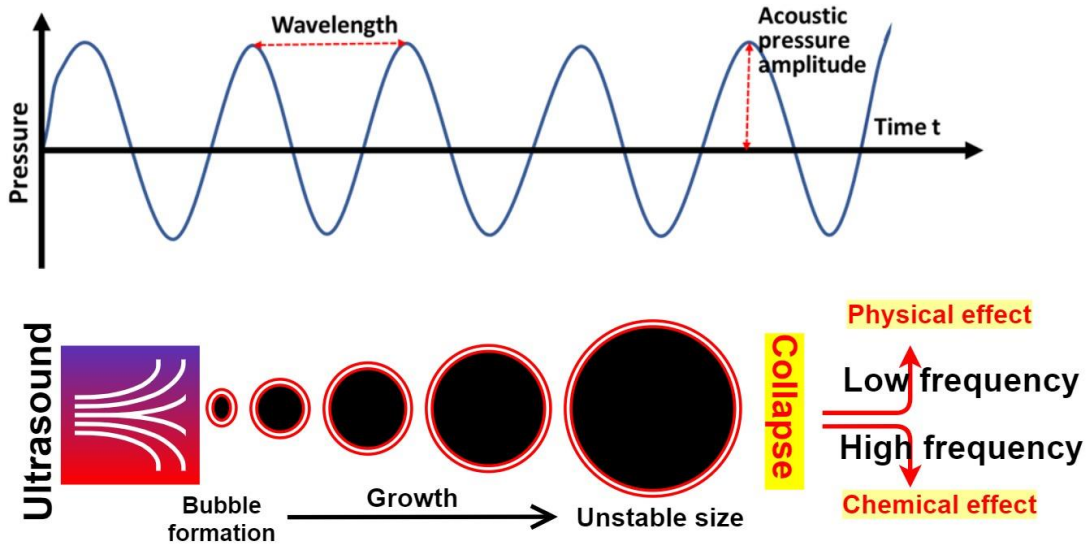

Figure 1. Schematic representation of the acoustic cavitation process.

For most of the oscillation cycles, there is a possibility for an almost unrestricted heat exchange between the bubble and the exterior [4]. However, at the end of the bubble collapse, when the velocity of the wall collapse approaches speed of sound, negligible heat transfer to the liquid medium occurs, leading to a near adiabatic heating of the bubble content [5,6]. Extreme conditions can be achieved at the end of the bubble collapse [7], with temperature of few thousands K and pressure up to several thousand bar [7-9], leading to the formation of active radical species (such as hydroxyl radicals due to the decomposition of water molecules), which can activate sonochemical reactions [10]. These hotspots within the collapsing bubbles give rise also to light emission (sonoluminescence) [11]. Moreover, the bubble implosion creates shock waves within the liquid: these shock waves, on the one hand, promote mass transfer by strong turbulent mixing, while on the other hand, they accelerate suspended solid particles causing violent collisions, which can induce fragmentation of brittle materials (sonofragmentation), exfoliation of layered materials, and agglomeration of malleable materials [12,13] . When the bubble collapse occurs asymmetrically, usually at boundaries or surfaces, high speed liquid jets (called microjets) propagate from the bubble towards the nearby surface, leading to surface erosion, pitting, and deformation phenomena. Nevertheless, microjets can also be utilized for cleansing, metal surface activation and surface engineering[14]. Moreover, ultrasound irradiation

during the crystallization step can generate crystal seeds (sonocrystallization), thereby decreasing the induction time, increasing crystallization yields, promoting selectivity towards a desired crystal morphology, and resulting in smaller crystals with more uniform size distribution [13,15-17].

Due to the extreme and transient phenomena produced during acoustic cavitation, ultrasound has been adopted for the intensification of physical and chemical processes in numerous fields, including:

- synthesis of chemicals [18-21] and materials [22-27], where sonication can accelerate reaction rates, boost yield and selectivity, enable the use of milder reaction conditions, shorten reaction time, enhanced nanoparticles dispersion during decoration of a matrix [28,29], promote crystallization [30] and control particle morphology [31-33];
- wastewater treatment by disinfection and degradation of recalcitrant pollutants, also in combination with other advanced oxidation techniques [34-41];
- electroanalysis by promoting mass transfer efficiency and accelerate analytical response [42-44];
- food industry and biotechnology [45-48] for extraction, homogenization, emulsification, foam control in bioreactors, cell disruption, and promotion of enzymatic reactions;
- pharmaceutical industry where sonocrystallization can be used as alternative for the conventional approach of crystal seeding to induce nucleation in a reproducible way [49].
- cleaning, leaching, textile processing, biofuel production, in polymer chemistry and in the petrochemical industry, etc.[50,51].

Despite the numerous studies and proven advantages over conventional alternatives, cavitation-based technologies are mostly restricted to laboratory-scale and industrial applications are limited due to scalability issues. Moreover, the sonochemical process efficiency is limited by the acoustic impedance of the system, secondary effects (such as streaming, heating and bulk mixing) and other effects (*e.g.* noise emission, erosion of emitter and reactor surface, sound-field attenuation, by-product formation). A dense cloud of bubbles usually generates in the vicinity of the emitter. These bubbles incorporate into a fluid stream

in motion, which is termed *acoustic streaming* [52]. Acoustic streaming is the steady state fluid flow caused by the absorption of acoustic oscillations and can be visually observed near sound emitters and can be visualized by particle image velocimetry as streams of fluid originated from the emitting surface. Acoustic streaming can decrease the number of acoustic cavitation phenomena, hence the acoustic activity [52].

As a matter of fact, cavitation is a complex phenomenon, which is affected by numerous parameters, including the ultrasound operating conditions and medium properties, and reactor geometry. These parameters often display a non-linear and interlinked effects on the performance of the sonochemical system: an optimal set of parameters for one application will often fail to yield the same performance when applied to another. Nonetheless, general trends can be identified for individual parameters and a range of characterization methods of the cavitation phenomenon and its effects can guide the optimization.

The purpose of this review is to provide an overview on the parameters involved in the experimental design and optimization of sonoreactors. Although most of the literature investigating the role of individual operating parameters is based on lab-scale studies and theoretical investigations, the lessons we draw from these studies are instrumental in guiding the development of large-scale reactors. Sonoreactors for processing large volumes especially suffer from issues such as the erosion of sonicator surfaces at high power intensities required for industrial operations and wide variations in the energy dissipation rates in the reactor. Some of these issues can be addressed by combining mapping techniques for the characterization of the cavitation activity and numerical methods to simulate the acoustic pressure distribution. The main methods and experimental procedures for the characterization of the cavitation activity in sonoreactors are presented in **Section 3**, along with numerical methods adopted to simulate the acoustic pressure distribution. The most common reactor geometries in practice have also been discussed with a view to distinguishing batch and continuous configurations. In this respect, a special emphasis is given to the reactor characteristics and limitations with respect to a desired application. We have reviewed current and emerging applications, highlighting their advantages, limitations and on-the-market solutions. Finally, the key issue

of the actual sustainability of sonoprocessing technologies is discussed, with reference to environmental and energy aspects, as well as cost analysis.

Although other means to achieve cavitation exist (namely hydrodynamic cavitation), the present review focuses only on acoustic cavitation. The interested readers can find recent overviews of hydrodynamic cavitation reactors in refs [36,53].

2. Guidelines for experimental parameters

2.1 Ultrasound physical characteristics

2.1.1 Frequency

The frequency of the sound field influences the pressure cycle, affecting the bubble population in terms of:

- *number of bubbles*: increasing the frequency leads to a higher number of antinodes, hence increasing the number of cavitation bubbles, as represented in **Figure 2**.
- *bubble size and size distribution*: according to the Minnert equation, the resonance size of a bubble is inversely proportional to the applied ultrasound frequency:

  $$f = \frac{1}{2\pi R}\left(\frac{3\gamma p}{\rho}\right)^{1/2} \qquad (1)$$

  where f is the resonant frequency in Hz, R is the radius of the bubble in meters, γ is the polytropic coefficient, *p* is the ambient pressure in kPa, and ρ is the fluid density in kg/m^3. In the case of water at atmospheric pressure, the equation simplified to:

  $$f R \approx 3.26 \text{ m/s} \qquad (2)$$

  Experimentally, it has been reported that with an increase in frequency, average size of bubbles becomes smaller and the size distribution becomes narrower (**Figure 3**). This can be understood considering the duration of the rarefaction phase, during which cavitation bubbles grow, is inversely proportional to ultrasound frequency. Therefore, a higher frequency entails a shorter expansion phase during oscillation growth, leading to a lower amount of vapor diffusing into the bubble and resulting in smaller bubbles [6].

- *time of collapse*: at higher frequency, the oscillation period is shorter, hence collapse and fragmentation occur more quickly. For instance, if ultrasound irradiation at 20 and 500 kHz are compared in otherwise constant conditions (10 W/cm^2 ultrasound intensity in air saturated water), the bubble average diameter is 330 and 13 μm and the collapse duration is 10 and 0.4 μs, respectively [54].

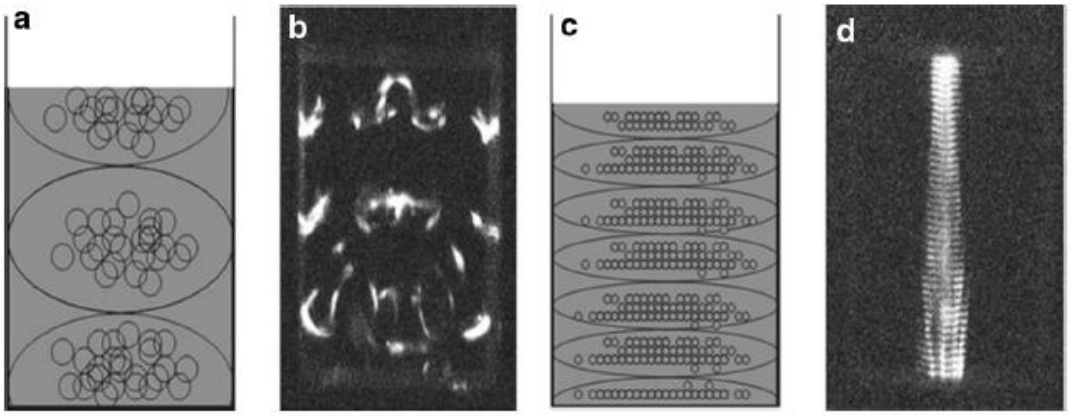

Figure 2. (a, c) Schematic illustration representing the effect of standing waves at different frequencies on the number of bubbles: low (a) and high frequency (c). (b, d) Sonoluminescence profile images at 37 (b) and 440 kHz (d). Reprinted with permission from Ref [55] .

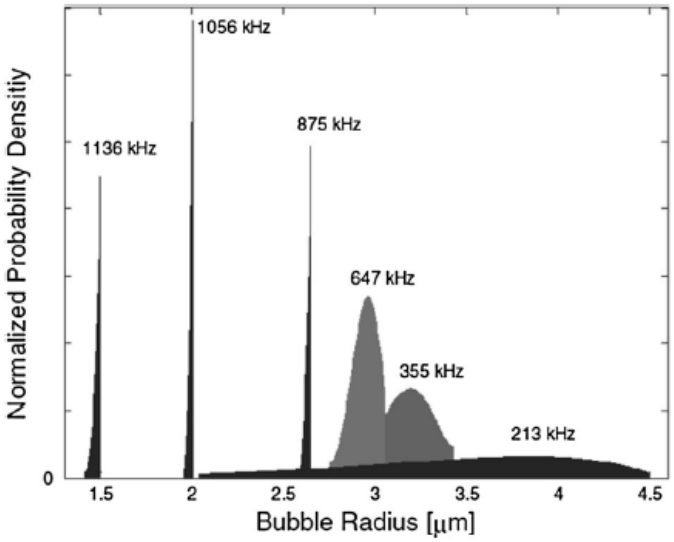

Figure 3. Bubble size distributions at different frequencies at 1.5 W (for 875, 1056 and 1136 kHz, data have been scaled down by a factor of 4); reprinted with permission from Ref [56].

These phenomena have important consequences in terms of the cavitation activity:

- *Generation of radical species*: The size of the collapsing bubble affects the maximum temperature reached during implosion. In particular, theoretical calculations predict that the maximum temperature is proportional to the maximum bubble radius for frequencies greater than 16 kHz [56]. However, larger bubbles obtained at lower frequencies contain a larger amount of water vapor due to the longer acoustic period [57]. As a result, the temperature during collapse at low frequency is decreased by heat consumption by endothermic chemical reactions [58]. Both effects (collapse temperature and vapor composition inside the bubble) have a crucial role on the amount of radicals generated at bubble collapse [59].

  On the grounds of what is discussed above, the number of primary radicals generated per collapsing bubble is larger at lower frequencies. However, the observed, overall radical yield depends also on the total number of bubbles, which is larger at higher frequencies. As a result, the radical yield increases with frequency up to a maximum value, which is generally in the range 200–600 kHz [60-65], then decreases with a further frequency increase due to the already discussed shorter oscillation time and reduction in collapse intensity.

- *Prevalence of physical or chemical effects*: At low frequencies (20 - 100 kHz), cavitation bubbles are relatively few although large in size: hence, cavitation at low frequency results mainly in physical effects on liquid circulation and turbulence, whereas chemical effects are less significant.

  Indeed the intensity of cavitation collapse decreases with an increase in ultrasound frequency [66]. At high frequency, cavitation is more difficult to be induced since cycles of compression-rarefaction can be too short to enable bubble nucleation and growth. As a result, with increasing frequency, larger power intensities are required to generate cavitation.

  Low frequency operation is thus preferred for applications where intense physical effects are required, such as in extraction, cell disruption, textile processing, polymer degradation, etc. At frequencies up to 500 kHz, the increased number of bubbles promote

the overall radical yield and chemical effects become more prominent [19]. As a result, frequencies in the range from few hundreds of kHz to 1 MHz should be selected for applications such as chemical synthesis and pollutant degradation in wastewater treatment. For these applications, the optimal frequency often depends on a balance between chemical effects (responsible for radical formation) and physical effects (which promote mass transfer) [19].

Figure 4 summarizes the frequency range best suited for different applications; it should be noted that the exact optimal frequency is reactor and system specific [67].

These selection criteria are valid for single frequency operation. It should be noted that an alternative approach makes use of a combination of same or different frequencies (multi-frequency operation) to enhance the overall cavitation activity thanks to synergistic enhancements [68,69].

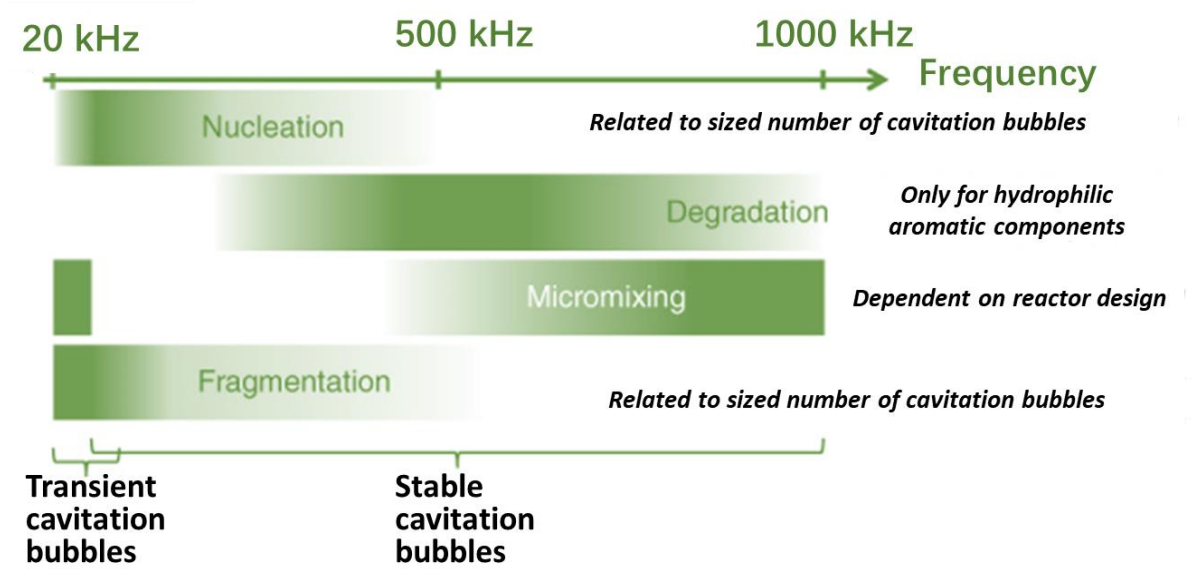

Figure 4. Schematic of the optimal frequencies for several cavitation-induced processes: dark colors indicate elevated process rates; redrawn with permission from [49].

2.1.2 Acoustic power

The acoustic power is related to the pressure amplitude of the sound wave and should supply the pressure needed for cavitation (cavitation threshold). Increasing the acoustic power increases the number and size of cavitation bubbles, the maximum bubble collapse temperature

and the sonochemical yield [64]. For instance, in sonochemiluminescence experiments, the increasing light intensity with power clearly displays how higher power amplitudes yield more chemically active bubbles: luminol reacts with the •OH radicals formed upon implosion of the acoustic bubbles, generating light emissions (**Figure 5**). Studies using chemical dosimetry (see **Section 3.2**) have shown that, irrespective of the chosen dosimeter, sonochemical efficiency increases with acoustic power [70].

However, increasing the acoustic power promotes cavitation activity only up to an optimum level, beyond which either marginal effects or even reduced performances are observed [71-74]. The optimum value depends on the reactor configuration and on the specific application. For instance, when working with high viscosity liquids such as oils, higher amplitudes are generally required with respect to aqueous solutions.

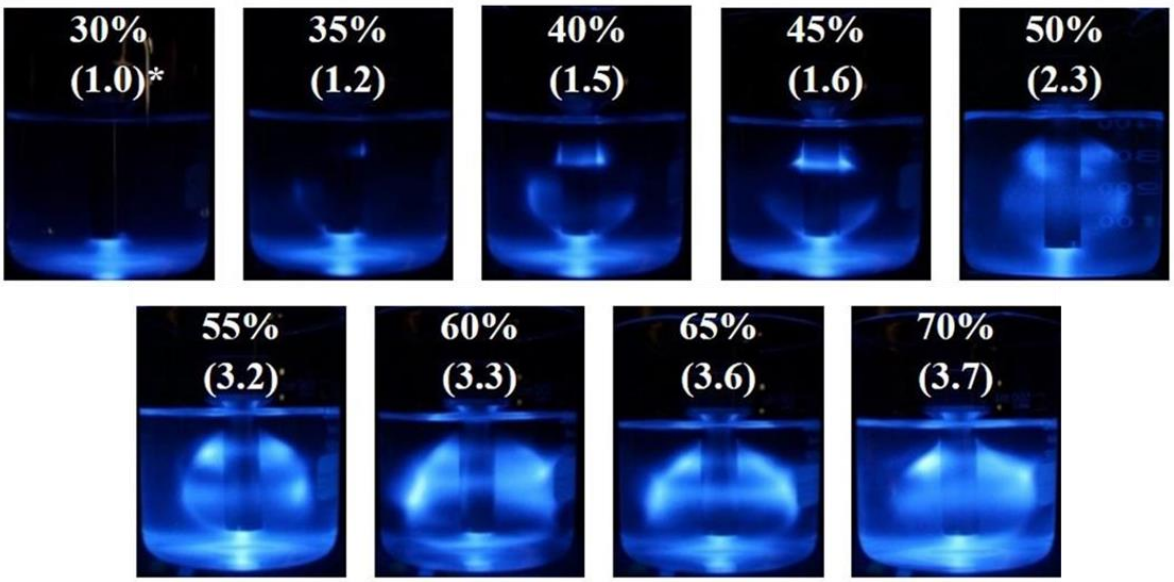

Figure 5. Sonochemiluminescence as a function of power intensity in multibubble sonochemiluminescnece; adapted with permission from [75].

The occurrence of an optimum value of power dissipation can be attributed to shielding and acoustic decoupling effects [76]. The former effect is related to the large number of bubbles formed at high-pressure amplitude, which leads to the formation of bubble clouds around the transducer surface and at antinode regions. These bubble clouds can absorb or scatter the

incident sound waves resulting in attenuation of the sound field and decreased energy transfer. Decoupling losses refer to change in acoustic impedance of the medium due to the increased bubble presence, which lowers the energy transfer efficiency from the ultrasound source to the liquid.

The determination of the optimum power value for a specific application and experimental conditions is thus a crucial step to optimize the process while minimizing the operating costs. In addition, it should be noted that operating at high power can cause a rapid deterioration of the ultrasonic transducer, resulting in poor ultrasound transmission through the liquid media and liquid contamination.

2.2 Operating parameters and reactor characteristics

2.2.1 Transducer type

A transducer converts electric current into acoustic vibrations. Generally, transducers are based on piezoelectric materials, driven by a power amplifier, which is seeded by a signal generator. Two common types of transducers are ultrasonic plates and ultrasonic horns (**Figure 6**). The ultrasonic horn, mostly in rod form with shrinking diameter toward its end, is directly submerged into the medium to generate ultrasonic cavitation; it is also known as sonotrode, ultrasonic probe or disintegrator. More details about the sonotrode types available are discussed in **Section 4**.

The bubble dynamics and distribution depend strongly on the type of ultrasonic source. Plate transducers deliver sound wave diffusely, giving rise mainly to stable (repetitive transient) cavitation due to standing wave formation, where active bubbles are localized at the antinodes. In **Figure 6a** sonochemilumiscence emission characteristics distinguish two zones with different acoustic activity peculiarities: the zone with the travelling wave field is characterized by a higher macroscopic acoustic pressure in the lower region (closer to the transducer), but lower chemical activity (lower $^{\bullet}OH$ radicals concentration); the zone farther from the transducer displays a standing wave with zones of higher chemical activity than the travelling wave area, despite a lower acoustic pressure. Conversely, horn transducers generate a

concentrated ultrasound irradiation, leading to a conical zone of highly concentrated cavitation activity just under the sonotrode tip (**Figure 6b**). The intense cavitation activity promotes radical production and induces violent agitation of the liquid medium, but the layer of bubbles generated at the transducer surface impedes the sound wave propagation, decreasing the energy efficiency of the process.

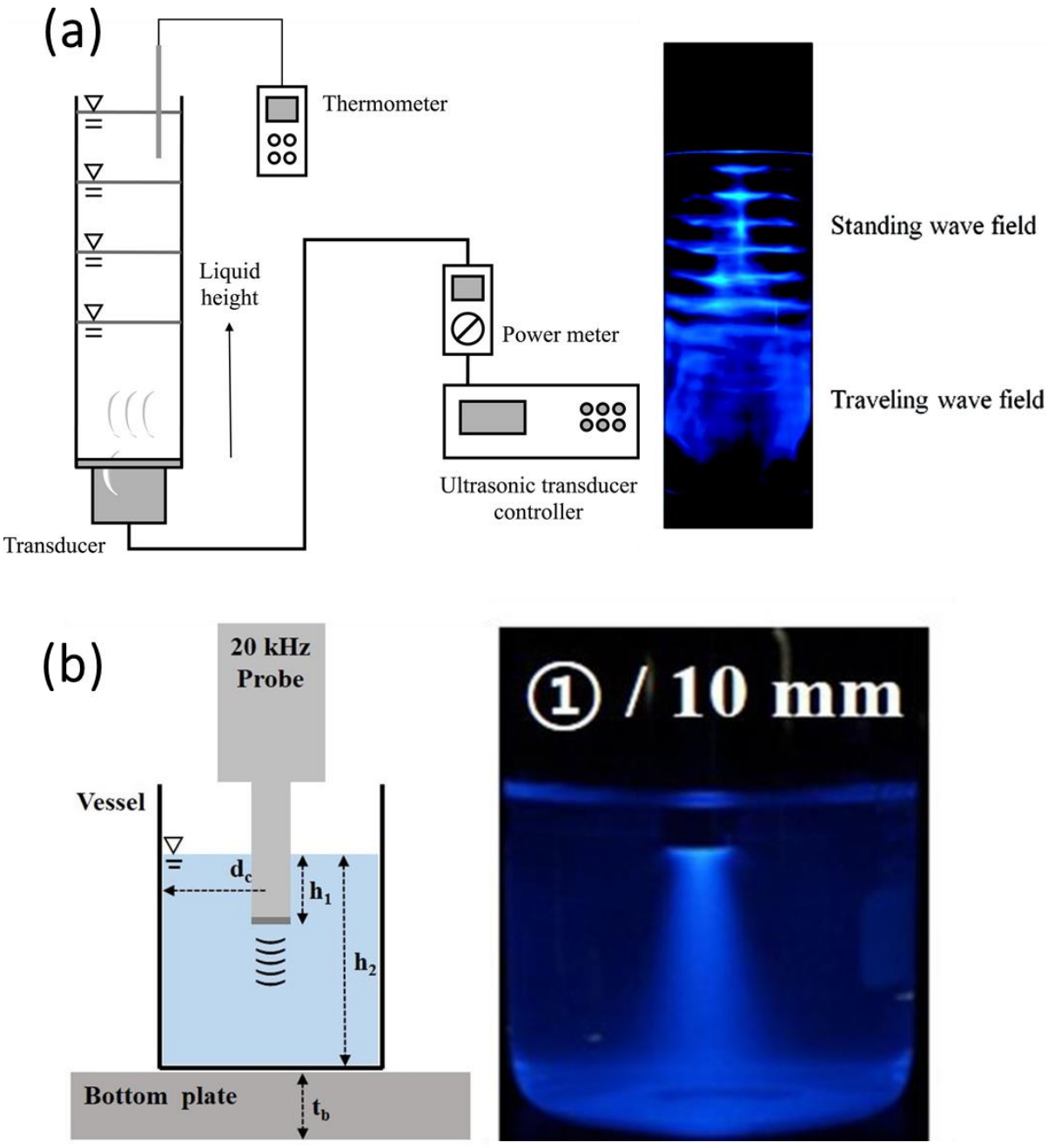

Figure 6. Experimental setup and sonochemiluminescence images of reactors based on a plate transducer (a) and horn transducer (b); reprinted with permission from [77] (a) and [75] (b).

2.2.2 Material of transducers

The choice of the transducer material is critical for reactor designs where the transducer is in direct contact with the solution, such as ultrasonic horns. In this respect, the material of choice of probe emitters is usually a titanium alloy (Ti-6Al-4V), owing to its good fatigue strength, excellent acoustic properties, and good surface hardness. Nevertheless, this material suffers

erosion during usage, leading to the release of metal particles into the liquid medium and ensuing sample contamination [78]. For applications requiring high amplitude and harder surface, titanium horns can be coated with materials such as polytetrafluoroethylene, titanium nitrides, carbides or nickel [79]. Less costly alternatives include stainless steel, hastelloy and aluminum. To overcome sample contamination issues, probe tips made of quartz, Pyrex, or polymers [80] can be used, although these materials present some limits especially at high amplitudes. These materials have also the advantage of being compatible with microwave (MW) irradiation, hence they can be adopted in ultrasound-MW combined treatments [81]. Alternatively, an indirect sonication strategy can be selected, where ultrasound is irradiated through the walls of the sample container, such as in cup-horn setups (see **Section 4.1**). The latter approach does not benefit from high intensity focused ultrasound directly in contact with the sample.

2.2.3 Reactor configuration

Cavitation activity is non-homogeneous in nature. This entails that, beside active cavitation areas, dead zones exist within sonochemical reactors. Dead zones are areas where no transient cavitation can be observed and only non-cavitation behavior (*e.g.*, bubble motion, acoustic streaming, etc.) can be detected.

The distribution of active and dead zones within a sonoreactor as well as the total cavitationally active volume are related to the reactor configuration. The latter plays a pivotal role on ultrasound attenuation, *i.e.*, a decrease in pressure intensity as a function of the distance from the transducer. Sound wave attenuation occurs due to absorption, reflection and refraction as sound waves propagate through the liquid medium, contributing to the spatial variability of cavitation intensity. The attenuation factor, α, is proportional to the square of frequency, hence, attenuation is much higher at higher frequencies:

$$\alpha = \frac{8\Pi^2 \mu f^2}{3\rho c^3} \qquad (3)$$

where μ is the viscosity of bulk liquid, f is the ultrasound frequency, ρ is the liquid density and c is the speed of sound in liquid.

The major parameters in reactor design include:

- **Vessel/transducer diameter ratio**: In the case of horn transducers, attenuation of ultrasound waves occurs both radially and axially. As a result, the vessel diameter should guarantee enough space to the oscillating probe to avoid unwanted collisions with the container walls, while minimizing the distance between the horn and the vessel walls to reduce radial attenuation. Thangavadivel and coauthors reported that a vessel/transducer ratio of 1.45 optimized sonochemical and acoustic energy transfer efficiency across a range of liquid heights [82].
- **Number and position of transducers**: In order to promote a uniform distribution of the cavitation activity, multiple transducers can be used to dissipate the total power using a larger irradiation surface. The use of multiple transducers is especially crucial in large-scale reactors, where a single transducer would fail in dissipating the entire required power with good efficacy due to the inherent limitations in the construction materials of piezoelectric elements. A multiple transducer setup also enables a multiple frequency operation. The optimum number of transducers depends on the power requirement, reactor volume, and dimensions of each. The position of the transducers in the reactor should maximize the active cavitation area and intensity. The transducer number and position also affect the hydrodynamic behavior and the mixing characteristics in the reactor, which are crucial aspects especially in physical processing applications. More details about this point will be provided in **Section 4**.
- **Shape of the reactor**: Sound waves are reflected by solid surfaces. In order to reduce attenuation, the thickness of the vessel should be optimized (**Figure 7**). In addition, the shape of the container has been reported to play a crucial role on sound wave attenuation. When the transducer is placed close to the bottom of the reactor, flat-bottomed vessels are generally the reactors of choice. However, Fukunaga et al. [83] have recently showed that while the fragmentation performance in a flat bottom vessel largely depends on the horn position, it varies much less in a spherical bottom vessel. They concluded that spherical bottom vessels provide a large areas of high acoustic pressure regions regardless of the horn position. Also, Capelo et al. [84] reported that containers with conical,

fan-shaped and spherical bottoms gave rise to better extraction efficiency with respect to flat bottom ones.

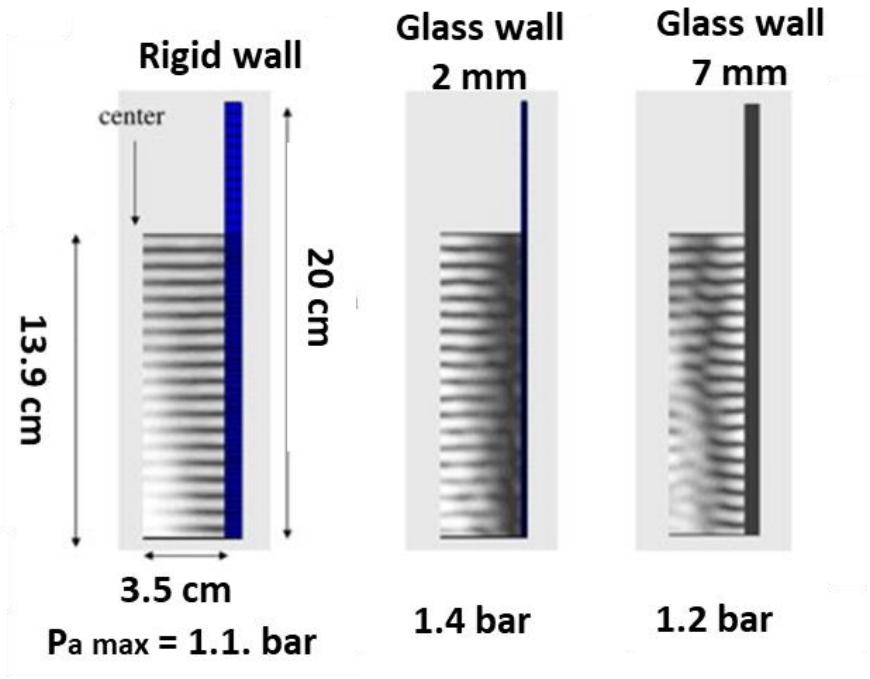

Figure 7. The calculated spatial distribution of the acoustic amplitude for rigid wall, and glass wall of 2 and 7 mm in thickness; reprinted with permission from [85].

2.2.4 Liquid height and transducer immersion depth

The immersion depth of the transducer horn or, in the case of plate transducers, the liquid height greatly influences the reflection of incident sound waves from the walls of reactors and liquid surface. Such reflections can cause the formation of hot spots of cavitation activity in regions far from the horn tip [86] or close to the liquid surface in plate transducer set-ups [87].

Placing the transducer horn close to the reactor bottom has been shown to increase reflection of sound waves[88,89], extending the active cavitation areas (as shown by sonochemiluminescence images, **Figure 8**). On the other hand, by placing the horn tip far from the bottom of the vessel, attenuation of the sound waves increases, which reduces the ultrasound reflection. The strong reflection at the bottom is due to the vicinity of the probe to the boundary. In this case, not only the overall acoustic zone increased in volume, but also the chemical activity was higher in case of a deeper position of the probe: the concentration of

•OH radicals at 60 mm of immersion depth was seven times higher than that observed at immersion depths < 30 mm (**Figure 8**).

In the case of plate transducers, Laborde et al. [90] reported that optimal liquid height matches an odd multiple of the fourth of the wavelength so that the air/water interface falls at an anti-node point [91], thus reinforcing the standing wave component. Asakura et al. [87] reported an optimal sonochemical efficiency when liquid height was 15 times the wavelength.

Indeed, the optimal value seems to depend on geometrical and operating parameters [82,88,91,92] as well as on the type of application, especially when liquid flow or foam formation are desired [93,94].

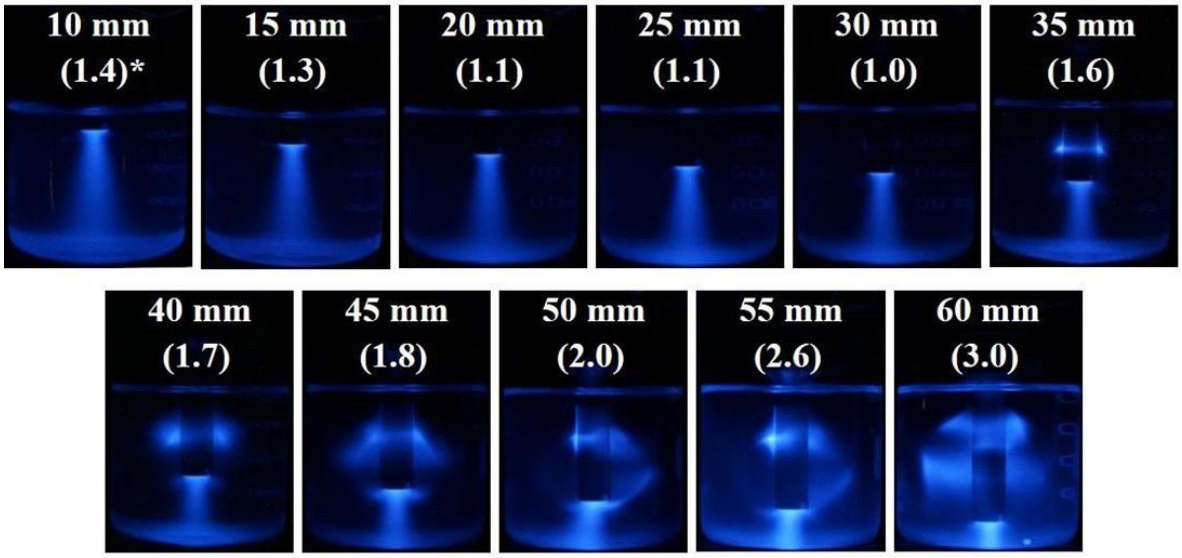

Figure 8. Sonochemiluminescence images at different probe immersion depths; reprinted with permission from [75].

2.2.5 Signal type and duty cycle

The ultrasound signal can be delivered in a continuous, pulsed or sweeping modes. When a continuous signal is applied, sound waves may produce an excessive amount of bubbles, which can agglomerate in clouds; these bubble clouds can attenuate the sound wave, resulting in a lower cavitational efficiency. Continuous irradiation can also result in bubble growth via coalescence, which can promote degassing of the liquid medium.

Other sonication modes allow overcoming these issues. Beside frequency sweeping, which is less common and shows mixed performance [95], pulsed sonication presents a series of advantages with respect to continuous operation: lower erosion of the transducer, more limited local temperature rise [96], lower coalescence and signal attenuation, increased zones of active cavitation [97]. The explanation of these effects might reside in the movement of the bubbles during the off time of the pulsed signal, during which bubbles can move away from one another or migrate from the antinodes [98]. In this respect, the choice of the duty cycle is crucial to optimize these effects [97,99]. The optimum value of duty cycle is dependent on the reactor configuration and type of application.

2.2.6 Liquid flow

Liquid flow can play numerous fundamental roles in sonochemical reactors: it has been reported to limit coalescence and clustering of cavitation bubbles, preventing degassing of the solution [100,101], shown to disperse bubbles from dead zones [102], it can promote bubble collapse, increasing the overall cavitation activity and can increase mass transfer [103].

It should be noted that, without stirring or circulation pumping, ultrasound-assisted reactions can suffer poor reaction kinetics and overall yield [104], since ultrasound-induced liquid circulation cannot provide uniform bulk mixing, especially for large scale operations and heterogeneous systems [105].

However, it has been reported that an optimal flow rate exists for sonochemical reactions, which offers good conversions at reduced energy consumptions [100,106,107]. This value depends on the individual system and applied parameters, in particular the applied frequency, power and adopted method to promote liquid flow [100,108]. For instance, the shape, size and position of a stirrer can affect the sound field, possibly reducing the cavitation areas. Moreover, in certain power and frequency conditions, excessive liquid circulation has been reported to negatively affect sonochemical yield by preventing the wave propagation and reducing the standing wave portion of the field [109].

2.3 Medium characteristics

2.3.1 Solvent

It is important the choice of a suitable liquid medium having the following physico-chemical parameters:

- **Viscosity**: higher viscosities induce an increase in cohesive forces within a liquid, raising the cavitation threshold [110]. Moreover, high viscosity liquids are responsible for a more severe attenuation of the sound wave intensity, reducing the active cavitation zones and the process yield (see **Equation 3**). As a result, liquids with lower viscosity are preferable and, alternatively, amplitudes should be increased when working with high viscosity liquids.
- **Vapor pressure**: solvents with low vapor pressure are generally preferred as they lead to stronger cavitational effects with respect to high vapor pressure liquids. This can be explained considering that the vapor content of bubbles increases with the vapor pressure of the liquid: a higher vapor content lowers the energy released during the collapse (cushioning effect) and, consequently, hampers cavitation activity [111].
- **Surface tension**: liquids with high surface tension provide more resistance to nucleation of cavitation bubbles [112], but after nucleation surface tension tends to stabilize the growth of the bubbles, which are then more likely to grow to active size. As a result, high surface tension solvents, such as water, present higher cavitation intensity. The surface tension can be modulated by addition of surfactants and/or electrolytes (see next points).

2.3.2 Solution temperature

Solution temperature strongly affects the physicochemical features of the liquid medium. In particular, higher solution temperatures cause a decrease in both liquid viscosity and surface tension, while increasing the vapor pressure. In addition, higher temperatures decrease gas solubility in the liquid, limiting the number of available cavitation nuclei. As a result, increasing temperature has generally a negative impact on cavitation intensity.

Conversely, a temperature increase can promote the reaction kinetics via conventional reaction mechanisms, so an optimum temperature exists depending on the specific system [19].

Considering that ultrasound irradiation causes the release of substantial heat to the medium, systems for temperature control (*e.g.*, jacketed reactors, Rosett cells, flow reactors) are usually applied to limit temperature rise, which could also cause the degradation of thermolabile compounds/specimen.

2.3.3 Static pressure

Working with higher static pressures leads to a shift of the cavitation threshold to higher acoustic pressure [113]. However, once the cavitation threshold is reached, the intensity of the cavitation bubble collapse can be enhanced. Experimental and theoretical studies have shown an initial promoting effect of increasing the static pressure on sonochemical yields, up to an optimum value above which a detrimental effect is observed [114-116].

2.3.4 Dissolved gases

As cavitation bubbles form starting from gas (vapors) dissolved in the liquid, the presence of dissolved gas bubbles facilitates cavitation, while degassing inhibits nucleation and reduces sonochemical yields.

It should be noted that sonication can cause degassing of the liquid medium: when bubbles grow by coalescence to a size greater than the resonance size, they oscillate out of phase and move towards the nodes, becoming inactive due to the decrease in pressure variance [117]. These inactive bubbles, often called degas bubbles, eventually float to the liquid surface, causing a loss of dissolved gas in the liquid medium. Therefore, gas bubbling into the medium can be used to maintain a sustained cavitation.

Gas bubbling can also be exploited to control the composition of cavitation bubbles in order to modulate the sonochemical response. The maximum temperature reached in a collapsing bubble depends on the thermal conductivity of the gas and vapors present within the bubble; a higher thermal conductivity translates into lower temperatures due to the quicker heat dissipation to the liquid medium. In this respect, argon enables to achieve high temperatures

in the collapsing bubble [118], hence it is bubbled into the liquid medium to promote pyrolytic reactions [119]. At the other end of the scale, pure CO_2 bubbling is known to have a quenching effect on sonochemical processes [120].

2.3.5 Salt addition

The presence of electrolytes in the liquid medium is known to impact sonochemistry. In particular, salt content causes the bubble size to decrease [121], inhibits bubble coalescence [122,123], and the sonochemical yields vary with the electrolyte content [124,125]. However, the mechanisms underlying these effects are still debated. As a matter of fact, the addition of salt has multiple effects. Electrolytes reduce the gas solubility (salting out effect) [126], limiting the population of active bubbles. On the other hand, salt addition increases the surface tension and viscosity of the liquid, which have been linked to lower vapor content within the bubbles and consequently to a higher intensity of the bubble collapse. Finally, it should be noted that, depending on the chemical nature of the ions, electrolytes can elicit new chemical reactions, such as chlorides and bicarbonates, which are known to act as radical scavengers [127].

2.3.6 Dispersed solids

The addition of dispersed solids, such as powders, has mixed effects on the cavitation activity [128]. A promoting role of the presence or generation of solid particles on cavitation has been suggested [129-131] due to powder surface and pores acting as source for cavitation nuclei. On the other hand, other studies reported a decrease in cavitation activity upon addition of solid particles, possibly due to attenuation of sound waves via scattering [132].

2.3.7 Surfactants

Surfactants, as the name suggest, adsorb preferentially at interfaces. As a result, during acoustic cavitation, surfactant molecules in solution tend to adsorb at the bubble-liquid interface. The presence of surfactants, particularly ionic ones, at the bubble interface is known to reduce bubble coalescence [133], resulting in cavitation bubbles of smaller size. Conversely, when a single bubble is considered, the growth rate is higher in surfactant solutions compared to pure water [134]. This phenomenon has been attributed to an increased resistance to mass

transfer during the compression phase of rectified diffusion. In this respect, surfactants with a longer chain length showed higher growth rates, in keeping with their greater mass transfer resistance [135], whereas the type of surfactant headgroup played a notable role only at high surface loadings [135].

3. Characterization methods of ultrasound systems

Cavitation activity has a non-homogeneous and dynamic nature, utterly dependent on the operating parameters and reactor design (see **Section 2**). In order to identify the active and dead zones in a sonochemical reactor and to optimize the design parameters, it is fundamental to characterize the cavitation activity in sonochemical reactors.

Cavitation activity can be experimentally quantified by means of primary effects, such as temperature or pressure changes ensuing bubble collapse, using techniques like calorimetry, thermal mapping and hydrophone measurements. Alternatively, secondary effects can be monitored, such as radical formation, acoustic streaming or microjets, using characterization methods such as chemical dosimetry, sonochemiluminescence, fluorescence measurements, electrochemical diffusion, particle image velocimetry, and aluminum foil erosion. Other methods include quantification of radical species by electron paramagnetic resonance spin traps [136], polymer degradation [137-139], high-speed cameras [140,141], Laser Doppler Anemometry (LDA), also known as Laser Doppler Velocimetry (LDV) [142] and laser tomography [143,144]. As summarized in **Table 1**, the provided information varies with the characterization technique, both in terms of spatial resolution (global characterization of the whole system *vs.* mapping techniques) and of its qualitative/quantitative nature.

Beside experimental characterizations, numerical simulations can support data interpretation and guide the optimization of acoustic field distribution inside the sonoreactor. In this respect, most of the literature aims at modeling acoustic pressure distribution by solving the Helmholtz equation for the linear propagation of sound waves. This latter aspect will be only briefly treated in this review. The interested readers can find a recent overview on numerical methods for the simulation of acoustic pressure in sonoreactors at reference [85].

3.1 Physical methods

3.1.1 Calorimetry

Ultrasound waves propagating in a liquid are absorbed and, and to a lesser degree, scattered by the medium. Sound wave absorption results in energy transfer to the liquid, increasing the temperature of the liquid medium. Measuring the change in the bulk temperature of the liquid medium provides information about the total amount of energy entering the reactor.

The effective calorimetric power (P_{cal}) can be calculated from the temperature increase of a weighted amount of ultrapure water as a function of sonication time (**Figure 9a,b**) according to Equation 4:

$$P_{cal} = mC_p \frac{dT}{dt} \qquad (4)$$

where *m* is the liquid mass, C_p is the specific heat capacity of the liquid (4.184 J g^{-1} K^{-1} for water) and *dT/dt* is the rate of liquid temperature increase [145]. The effective calorimetric power can be used to quantify the energy transfer efficiency of the sonochemical reactor.

Gogate at al. [146] proposed a modification of this equation to distinguish between the energy actually utilized to raise the bulk liquid temperature, from the energy absorbed by the reactor components (walls and transducers), which can account to 5% of the overall energy consumption, and energy lost to ambient air by convection, which is significant especially when large reactors are considered. They proposed the following Equation 5:

$$P_{cal} = \left(mC_p\Delta T\right)_{liquid} + \left(m_i C_{pi}\Delta T\right)_{innerreactorwall} + (hA\Delta T) \qquad (5)$$

where *m* is the mass of liquid, C_p is specific heat of liquid at constant pressure, ΔT is change in temperature, m_i is the mass of reactor/transducers, C_{pi} is the specific heat of the reactor material, *h* is the convective heat transfer coefficient and *A* is the area of heat transfer. The interested readers can find more information about the modeling and experimental determination of the convective heat transfer coefficient in sonoreactors in ref. [147].

Special care must be taken when investigating power dissipation in immiscible reaction systems (such as in emulsification operations), since the amount of energy dissipated in those systems corresponds to the sum of the energy dissipated in each individual phase [148].

The power determined according to the calorimetric method can be used to determine the energy efficiency of the system as the ratio between the power dissipated in the system and the supplied electrical power.

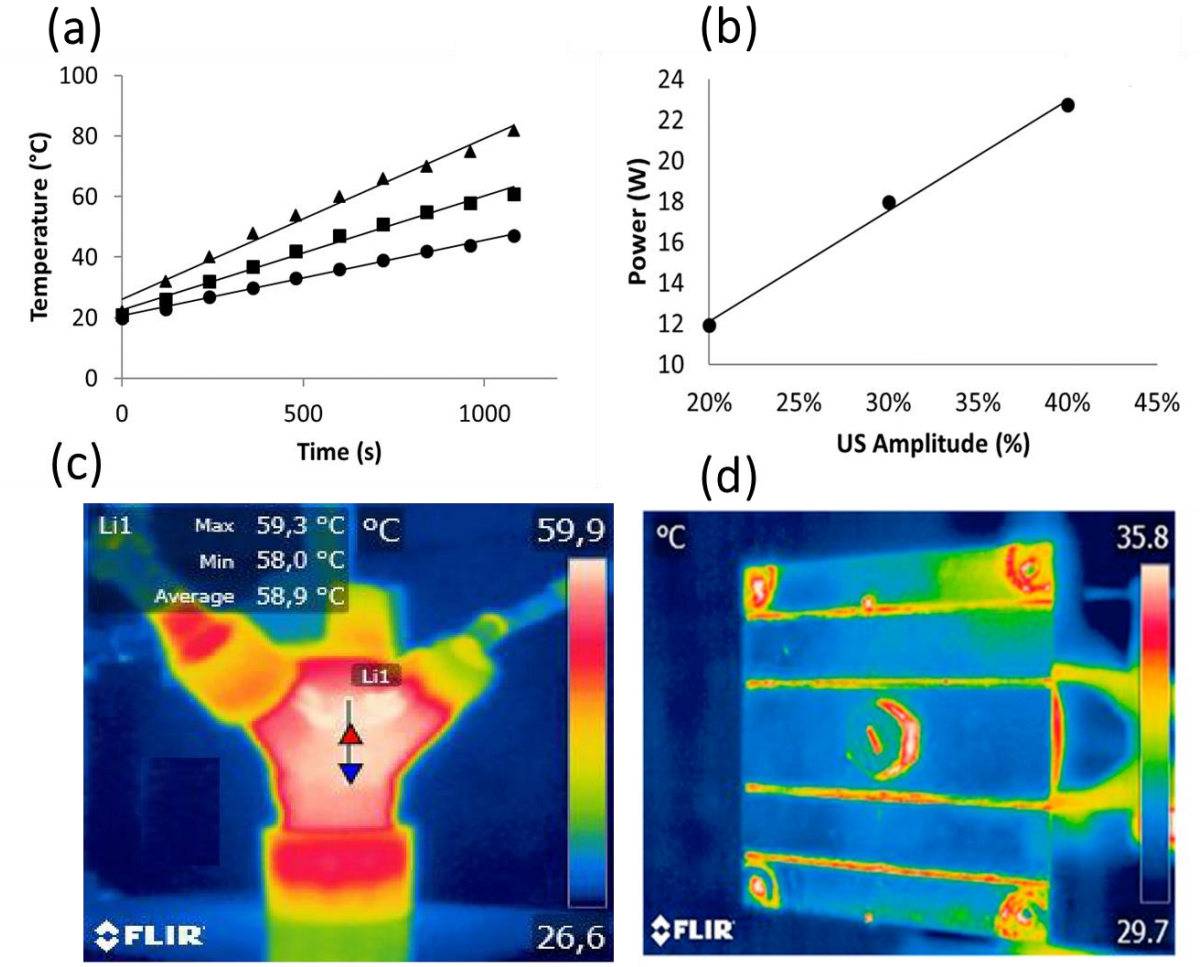

Figure 9. (a) Calorimetric calibration curves at three different amplitudes (20 (circles), 30 (squares), and 40% (triangles)); (b) dependence of the ultrasound calorimetric power on the instrument amplitude; (c,d) thermal mapping by infrared camera of a four-way-type reactor (c) and of a microchannel reactor (d). Images reproduced with permission from [105] (a,b), from [149] (c) and [150] (d).

3.1.2 Temperature mapping

Bubble collapse generates very high temperatures, which cause local heating. As a result, measuring the local temperature in the liquid provides quantitative information about the local

cavitation activity. Temperature mapping allows to determine the location of cavitation zones (hot spots), as well as dead zones [151].

Temperature mapping can be carried out by thermocouples/thermisters, but this approach has several disadvantages as the probe can be damaged by cavitation, its size prevents mapping of small channels, and the probe surface can affect cavitation activity distribution [152]. Recently, thermal cameras have been proposed as non-invasive alternative for real-time, thermal imaging of reactors, also with complex shapes [150] (**Figure 9c,d**).

3.1.3 Hydrophone measurements

Hydrophones enable a quantitative measurement of the acoustic pressure field in a reactor, which can be used to locate cavitation regions via frequency spectral analysis.

The noise emitted by a liquid medium irradiated with ultrasound comes from the oscillation and collapse of cavitation bubbles. In an ideal system, without dissipation, the signal captured by a hydrophone is a sinusoidal sound signal, indicative of bubble oscillation according to the fundamental driving frequency, f (**Figure 10a**). With increasing power input, bubble oscillation departs from this ideal behavior producing convex waveforms. In the acoustic emission spectrum, peaks appear at various frequencies, either subharmonic (f/n), harmonic (nf) and ultra-harmonic ((2n + 1)f/2) of the fundamental driving frequency. While harmonic peaks are generated by bubble oscillation before collapse [94], higher harmonics can be explained in terms of the forced non-linear bubble oscillations and subharmonic frequencies have been related to bubbles with an equilibrium radius greater than the resonance value [153]. Physical effects due to bubble collapse (shock waves, micro-jets, and micro-streaming) increase the degree of irregularity of acoustic waveforms, generating a broadband signal (i.e., an elevated baseline), which is indicative of transient cavitation.

Therefore, by repeated hydrophone measurements at different locations within the sonoreactor, a mapping of the acoustic pressure can be obtained (**Figure 10b**) and cavitation zones can be identified by analyzing the features of the broadband signal. When the ultrasonic horn is placed at positive values in the Z plane, a region of broad acoustic pressure is observed, with the

highest intensity below the tip (Z = +4 cm in Figure 9b). For negative values of Z the intensity is more uniform with a discrete distribution [154].

There are different types of hydrophones: the most common type is based on a piezoelectric transducer, which generates an electric potential upon exposure to a pressure change, such as a sound wave. A less common alternative is represented by fiber-optic probe hydrophones, in which detection is based on a change in refraction index modulated by the acoustic pressure field [155].

The main disadvantages of hydrophones derive from their being immersed into the sonoreactor: they can be damaged by the cavitation activity as well as affect the cavitation activity distribution (for instance, by acting as nucleation sites for cavitation bubbles). Finally, the probe size limits the hydrophone applicability to the mapping of reactors with complex shapes, such as microchannels.

Despite these limitations, hydrophones can be adopted to probe the acoustic field distribution of sonoreactors at both the laboratory scale and at large scale (see e.g. **Figure 27**). For instance, Wang et al.[156] adopted a miniaturized hydrophone to determine the acoustic field distribution along the radial and depth directions within a multi-frequency, cylindrical sonoreactor with capacity of 17 L.

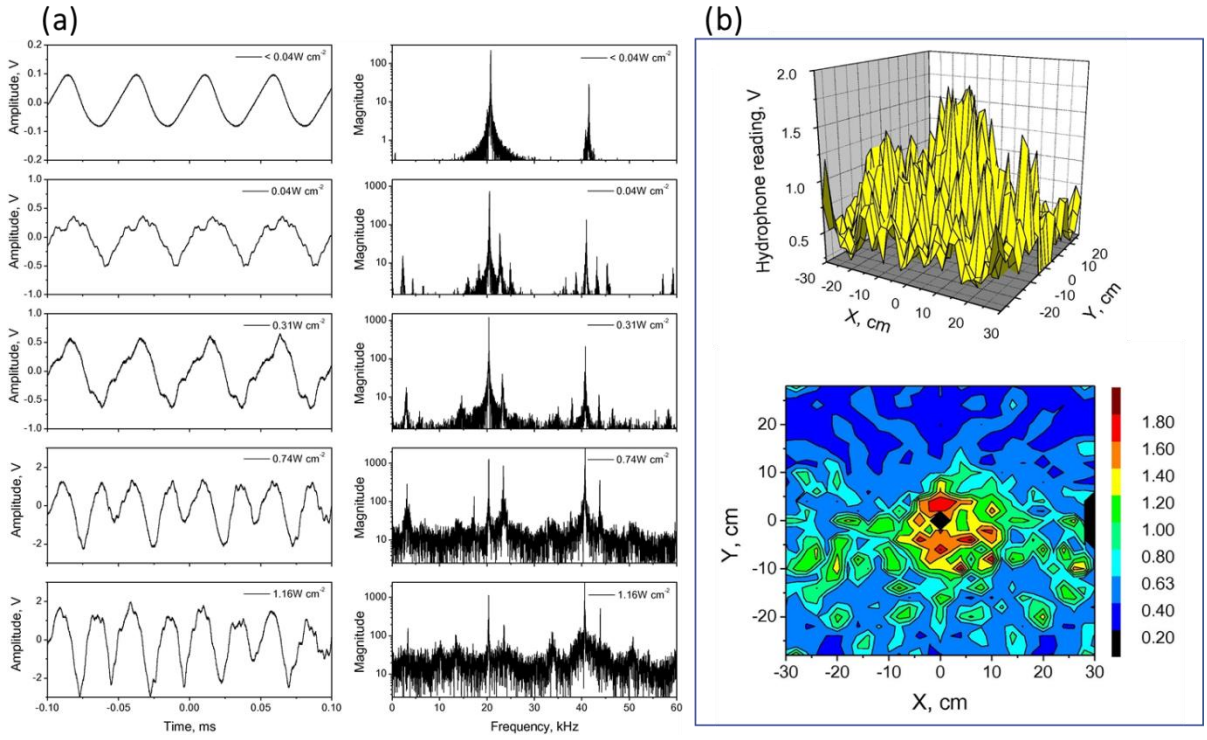

Figure 10. (a) Ultrasonic waveforms (left) and relative frequency spectra (right) observed in water under ultrasound irradiation at different power intensities; (b) 3D (top) and contour (bottom) mapping of hydrophone measurements in a sonochemical reactor. The probe is located in the Z plane at Z = +4 cm; reprinted with permission from [154].

3.1.4 Aluminum foil erosion

The observation of the erosion patterns of an aluminum foil immersed into the sonochemical reactor can be used to qualitatively estimate the distribution of the acoustic pressure. The indentations/erosions observed in the aluminum foil indicate active zones of cavitation. The active zones of cavitation can be compared with numerical modeling that calculates the overall volume fraction of cavitation bubbles as in **Figure 11**. While the aluminum foil method is really easy and inexpensive, it is a qualitative technique, although some attempts of semi-quantitative comparisons have been reported based on the aluminum foil weight loss [155]. Moreover, owing to its reliance on physical effects due to micro-jets, this approach can be used only at low frequency operation, where physical effects are significant. Another

drawback of this method is the possible alteration of the cavitation activity due to the presence of the aluminum foil in the liquid medium.

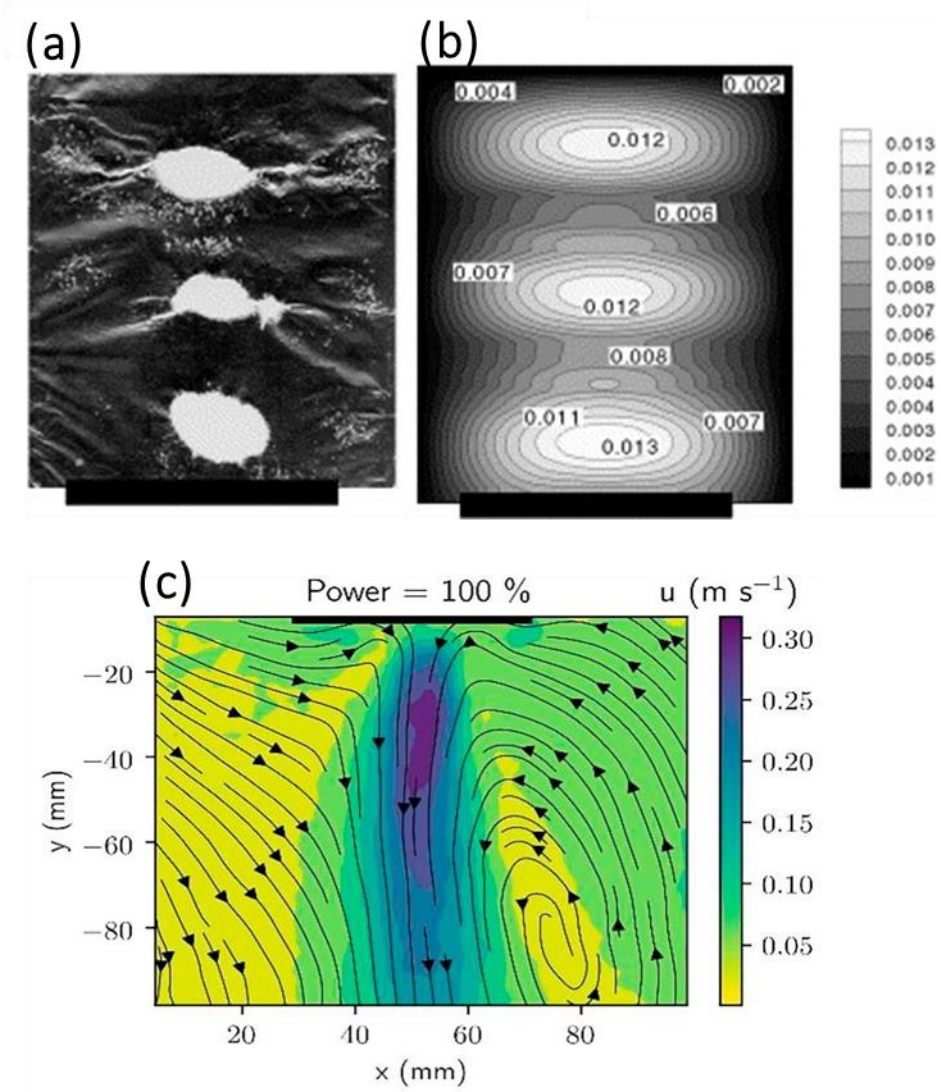

Figure 11. Aluminum foil erosion (a) and relative modeled active areas of cavitation (b); (c) time-averaged particle image velocimetry images showing the spatial distribution of average acoustic flow structures right below the transducer tip; reprinted with permission from [157] (a,b) and [158] (c).

3.1.5 Particle image velocimetry

Particle image velocimetry is a non-intrusive, optical method used to study fluid dynamics. In particular, particle image velocimetry measures flow velocity vector fields in a plane, providing information on the uniformity of the cavitation activity in the reactor [159,160] .

This method is based on the determination of particle displacement in time using a double-pulse laser technique [159]. Before the measurement, the liquid medium needs to be seeded with luminescent tracer microparticles, which can be excited by the laser and monitored with a CCD camera. As a matter of fact, cavitation bubbles cannot act as reliable tracers due to their different size. During the measurement, a laser light sheet illuminates a plane in the flow and a digital camera records the luminescent particle positions in that plane. After a fraction of a second, a second laser pulse illuminates the same plane, producing a second image of the particle positions. The couple of images using data analysis technique can determine the particle displacements in the entire flow region. Knowing the delay time between the two images and the spatial calibration, a velocity vector field can be determined, thus quantifying the local liquid circulation currents. **Figure 11c** displays a typical time averaged plot of particle image velocimetry. The time averaged distribution changes with changing operating condition, among which applied power (amplitude). In particle image velocimetry images, different colors represent different velocity magnitude, in m s^{-1}, while the arrows indicate the flows [157].

3.1.6 Electrodiffusional method

Changes in the mass transfer coefficients due to cavitation activity can be determined by voltammetry using a sonoelectrochemical cell with a stationary working electrode [161]. A quasi-reversible redox couple, $Fe(CN)_6^{3-}$/ $Fe(CN)_6^{4-}$, is generally used to this purpose due to its fast quasi-reversible electron transfer, which allows to consider the electrode kinetics under mass transfer control. Hihn and Pollet [161] have proposed an equation to convert the electrochemical values obtained by this method into so-called equivalent velocities, corresponding to normal flows directed toward the electrode surface resulting in the same electrochemical signal than in the presence of ultrasound. Using this method, the acoustic activity can be mapped by systematically moving an electrode in an ultrasonic field [41].

3.1.7 Sonochemiluminescence

Sonochemiluminescence is a widely used technique for the visualization of active cavitation zones in a reactor.

The most common sonochemiluminescence reagent is Luminol (3-aminophthalhydrazide) [162] in alkaline conditions. Upon ultrasound irradiation, oxidizing species, such as $^{\bullet}OH$ radicals, generated from sonolysis of water molecules, transform luminol to excited-state 3-aminophthalate (3-APA), which emits fluorescence light in the blue region (**Figures 5 and 7**) (Equation 6):

$$\text{Luminol} + {}^{\bullet}OH \rightarrow \text{3-APA}^{*} \rightarrow \text{3-APA} + \text{light} \qquad (6)$$

As this reaction is activated by hydroxyl radicals or other oxidizing radical species generated by cavitation, the brighter regions indicate the active cavitation zones and the luminescence intensity is proportional to cavitation intensity (i.e., the number of collapses) [151].

3.2 Chemical methods

3.2.1 Chemical dosimeters

Chemical dosimetry measures cavitation activity in terms of radical species formed upon collapse of transient cavitation bubbles. These reactive species are used to activate chemical reactions that can be monitored via a change in either light absorption, fluorescence emission or HPLC measurements. From chemical dosimetry measurements, the sonochemical efficiency can be obtained as the ratio of the number of reacted molecules to the ultrasound energy.

These techniques, while broadly adopted in the literature, have some limitations: they provide only a global quantification of the cavitation activity of the system (no local activity), have a relatively large experimental error, and are not sensitive to the contribution of oscillating bubbles to the cavitation activity (which can be significant for physical processing).

The most commonly employed techniques are:

- **Weissler reaction or KI dosimetry**: when KI solution is irradiated by ultrasound, I^- ions are oxidized to I_2 by highly reactive species generated by acoustic cavitation, such as $^{\bullet}OH$ radicals and H_2O_2. The produced I_2 reacts spontaneously with excess I^- ions to

form the triiodide ion complex, I_3^-. The latter can be quantified by UV spectrophotometry at 353 nm.

In the present method, the sonochemical efficiency value corresponds to the average I_3^- liberated per unit amount of utilized energy, which is given by Equation 7:

$$SE = \frac{C_I V_I}{P_{cal} t} \qquad (7)$$

where SE is the sonochemical efficiency, C_I is the measured I_3^- ion concentration, V_I is the KI solution volume, P_{cal} is the calorimetric power and t is the irradiation time [87]. This method is very popular as it is simple, fast and requires no expensive equipment. However, it should be noted that KI dosimetry lacks specificity, as various radicals can readily oxidize I^- ions: for instance, sonolysis of water in the presence of N_2 forms HNO_2, which can oxidize iodide ions, catalyzed by dissolved O_2 [163].

- **Fricke dosimetry** is based on the oxidation of Fe^{2+} to Fe^{3+} under ultrasound irradiation [164], activated by oxidizing species formed by acoustic cavitation ($^{\bullet}OH$ radicals and H_2O_2):

$$Fe^{2+} + OH^{\bullet} \rightarrow Fe^{3+} + OH^- \qquad (8)$$

$$Fe^{2+} + OH^{\bullet} + H^+ \rightarrow Fe^{3+} + H_2O \qquad (9)$$

$$Fe^{2+} + H_2O_2 + H^+ \rightarrow Fe^{3+} + H_2O + OH^{\bullet} \qquad (10)$$

The amount of Fe^{3+} ions can be measured by UV-vis spectrophotometry at 304 nm.

- **Terephthalate dosimetry:** terephtalic acid reacts with hydroxyl radicals to form highly fluorescent 2-hydroxyterephthalic acid according to the reaction:

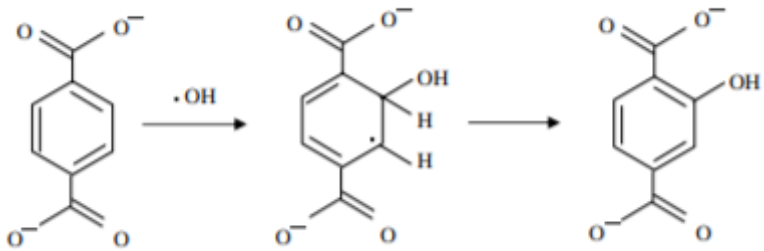

The method is quite time consuming (**Table 1**), but highly specific to $^{\bullet}OH$ radicals and more sensitive that spectroscopic dosimetries [165,166].

Other dosimetry methods are based on salicylic acid [167,168], nitrite and nitrate dosimetry [70]. Direct quantification of produced H_2O_2 is also performed [125].

Recently, electron paramagnetic resonance (EPR) spectroscopy together with spin trapping agents has been adopted to identify and quantify acoustically generated radicals in organic solvents, including mixtures containing suspended solids. This technique appear reliable, however, the main limitation is the need to perform ultrasound experiments in the vicinity of the EPR equipment, as radicals require to be spin-trapped and analyzed by EPR instantaneously[131].

Table 1. Experimental methods for the characterization of cavitation activity in ultrasonic reactors, with examples of experimental procedures.

Method	Information	Experimental conditions	Refs.
Calorimetry	quantification of effective calorimetric power	reactor filled with a weighted amount of pure solvent; temperature measurements at several spots in the reactor using thermocouple/thermometer	60,105
Thermal mapping	location of cavitation zones	infrared thermometer camera	149,150
Hydrophone measurements	quantitative measurement of the distribution of the acoustic pressure field	for accurate measurements, signals need to be converted by oscilloscope, fast Fourier transform (FFT) or data acquisition software	94,153
Aluminum foil erosion	qualitative estimate of acoustic pressure distribution	aluminum foil kept perpendicular to the transducer surface (i.e., parallel to the direction of sound propagation)	139,153
Particle image velocimetry	measurement of flow velocity: description and quantification of the acoustic flow field	light from a pulsed Nd:YAG laser (λ_{em} = 532 nm) is transformed to a flat light sheet using a cylindrical lens; detection by a CCD camera placed orthogonally to the laser sheet; liquid is seeded with fluorescent microparticles absorbing at 532 nm; immediate velocity vector fields and average velocity vector fields are determined by analysis algorithms	140,159,160

Sonochemiluminescence	visual representation of cavitation zones	reagents: 0.1 g/L 3-aminophtalhydrazide and 1 g/L NaOH; light emission measured by an exposure-controlled camera (2-5 min exposure) or a CCD camera in a dark room; relative sonochemiluminescence intensity profiles can be analyzed via image-processing software	75,97
Weissler dosimetry	sonochemical efficiency in the whole reaction solution	reagent: 0.1 M KI solution; I_3^- absorbance at 353 nm is measured by UV-vis spectrophotometer	60
Fricke dosimetry	sonochemical efficiency in the whole reaction solution	reagents: 0.001 M $(NH_4)_2Fe(SO_4)_2(H_2O)_6$, 0.4 M H_2SO_4, and 0.001 M NaCl; Fe^{3+} absorbance at 304 nm is measured by UV-vis spectrophotometer	60
Terephthalic acid fluorescence	sonochemical efficiency in the whole reaction solution	reagents: 0.2 mM terephthalic acid solution; irradiated solutions must be kept in the dark; measurement of fluorescence intensities 2–4 h after sonication by spectrofluorimeter (λ_{exc} = 310 nm, λ_{em} =426 nm)	61
Electrodiffusion method	quantification of the fluid convective motion in sonoreactors	three-electrode cell connected to a potenziostat (working electrode: Pt disk opposite and parallel to horn; reference electrode: Pt wire; counter electrode: Pt plate outside the ultrasound field); 0.005 M $Fe(CN)_6^{3-}$/ $Fe(CN)_6^{4-}$ in 0.2 M NaOH	159,169

3.3 Computational methods

The ultrasonic emitter geometry and its position, its frequency and power (amplitude), as well as the reactor geometry, determine the distribution of acoustic pressure in the medium. As discussed in Section 3.1.3, hydrophones can provide a local measurement of the acoustic pressure. Even when hydrophones are either integrated at multiple locations in a reactor, or delocalized inside the reactor to acquire multiple data points, the measurements are discontinuous and the resulting acoustic pressure "mapping" is incomplete.

Numerical modeling is the only way to obtain acoustic pressure as a function of time at any point of distance from the emitting surface, which varies according to the wave equation (Equation 10):

$$\nabla^2 P \frac{1}{\rho} - \frac{1}{\rho c^2}\frac{\partial^2 P}{\partial t^2} = 0 \qquad (10)$$

where P is the acoustic pressure, c is the speed of sound in the liquid medium, t is the time, ρ is the fluid density and $\nabla^2 P$ the Laplacian of P to identify space of the sound field:

$$\nabla^2 = \frac{\partial^2 p}{\partial x^2} + \frac{\partial^2 p}{\partial y^2} + \frac{\partial^2 p}{\partial z^2} \qquad (11)$$

In the simplest case, an incompressible fluid medium of finite volume, limited by a surface, points outward with respect to a central ultrasonic probe of a given frequency and power. Assuming the ultrasound waves to propagate linearly and in a stationary way, and neglecting shear stresses, the equation to solve to find the local pressure at varying distance from the probe is the Helmholtz equation (Equation 12):

$$\frac{\nabla^2 P}{\rho} - \frac{\omega^2}{\rho c^2} P = 0 \qquad (12)$$

where P is the acoustic pressure, $\nabla^2 P$ the Laplacian of P, c is the speed of sound in the liquid medium and ω is the angular frequency.

To find acoustic pressure in an ultrasonic cell, the Helmholtz equation must be solved in the frequency domain[170]. The Helmholtz equation can be solved using a variety of numerical methods by setting appropriate boundary conditions:

- At the tip of transducer, $P = P_0$, where P_0 is the wave amplitude, *i.e.* we consider that the whole ultrasound energy is entering into the reactor via the transducer tip.
- $P = 0$ ('infinitely soft' boundaries), *i.e.* the pressure amplitude vanishes at the reactor wall (total reflection of ultrasound). This is true only when the wall thickness is negligible with respect to the ultrasound wavelength (*e.g.*, for reactors operating at 20 kHz or 36 kHz[171]). Alternatively, 'infinitely hard' boundaries can be considered using the condition:

  $$\nabla P \cdot \mathbf{n} = 0 \qquad (13)$$

  where **n** is the normal vector pointing outward the liquid. While broadly used, the simple approximations of infinitely soft/rigid boundaries cannot properly describe interfaces between liquid and the solid walls (see e.g. **Figure 7**). Some modeling studies have taken into account the effect of the vibration of the reactor wall [85,172].

To this purpose, numerical modeling integrated by either finite elements software or multiphysics simulation software, such as PAFEC-vibroacoustics [172], ATILA code[173], ANSYS acoustics [174], PZflex code [175]and COMSOL Multiphysics [176](previously known as FEMLAB[86]), is generally adopted. These software display a continuous virtual mapping of the acoustic pressure and visualize its distribution inside a sound cell or reactor[176]. To validate numerical modeling, discontinue measurements with hydrophones can confirm locally the output of the numerical modeling [154].

Multiphysics software rely on the finite element method (FEM) to solve partial differential equations. From a visual perspective, the finite element method corresponds to the creation of meshes throughout the surface and the volume of the system under study for 2D and 3D simulations, respectively. Every micro-environment defined by the meshes, corresponds to a computational domain. Potentially, every domain may have its own defined physicochemical properties.

2D simulations are usually run in preparation of lengthier and more complex 3D simulations. In the case of a simple cylindrical vessel with sonication through a 20 kHz,

2D and 3D simulated acoustic pressure was the same at every axial distance from the probe [177].

As discussed in Section 2.2.3, during the propagation of ultrasound waves through a liquid medium, attenuation occurs resulting in a decrease in intensity as a function of the distance from the emitter. The attenuation by the incompressible fluid is either linear or non-linear and is affected by the presence of cavitation bubbles in the medium. Among the proposed models to describe attenuation effects, the acoustic pressure equation can be modified as follows [171]:

$$\nabla^2 P \frac{1}{\rho_c} - \frac{1}{\rho_c {c_c}^2} \frac{\partial^2 P}{\partial t^2} + d_a \frac{\partial P}{\partial t} = 0 \quad (14)$$

where ρ_c is the complex density and c_c is the complex speed, which become equal to ρ and c in the absence of attenuation phenomena. These two parameters depend on the complex wave number and complex impedance, which have been defined in different ways in the literature, as discussed extensively in ref [85].

The most commonly employed finite element modeling software, COMSOL Multiphysics, offers an Acoustic Module as an add-on, which is key to model ultrasound-related fluid dynamics. Multiphysics simulation software return ultrasound mapping images as the ones in **Figure 12**. In the latter, the maximum acoustic pressure is located very much in proximity of the ultrasonic probe tip and then attenuates within a space <10 mm because of the sound attenuation in water. In the work by Rashwan et al.[177], the acoustic pressure calculated in the 2D and 3D models was the same, which was ascribed to the coupling between the flow and sound fields. It also appeared that the 20 kHz frequency fell at the 3rd mode, thus generating resonance, thus eliminating three-dimensional effects.

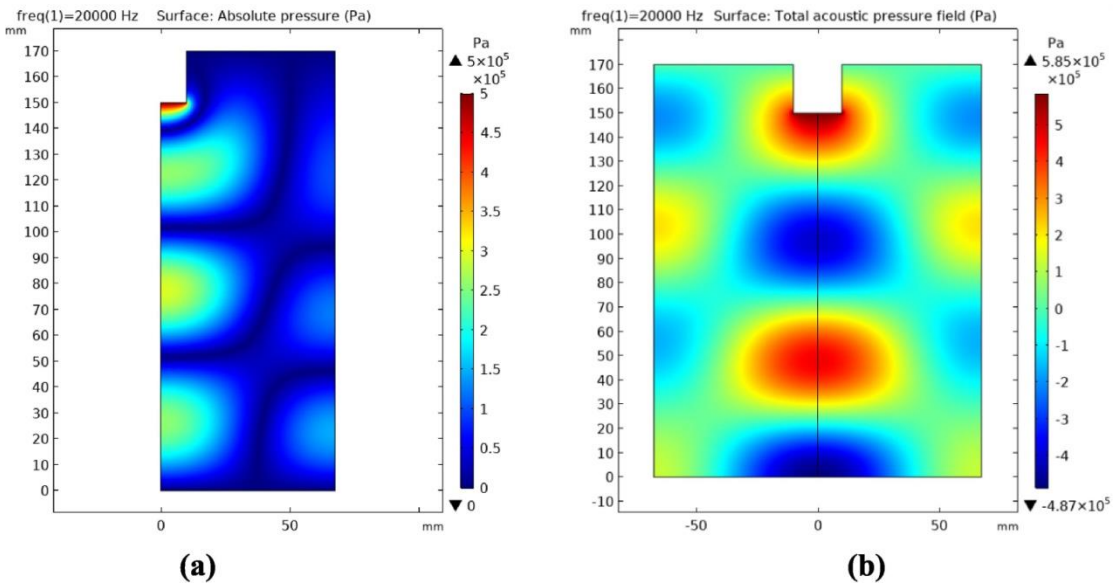

Figure 12. (a) Absolute pressure and (b) actual acoustic pressure distribution contours of a 20 kHz ultrasonic probe in water, 36 W, from [177], with permissions.

The finite element mesh is always bounded, which means that it is inadequate to model unbounded media (e.g. far-field radiation). In the presence of far-field radiation, i.e., a field whose intensity decreases with distance from the sources, unbounded methods, such as the boundary element method (BEM) [172] shall be coupled with the finite element method. The boundary element method (as well as the Dirichlet to Newman method), bases on non-local boundary conditions, while acoustic dampers and perfectly matched layers (PML) base on approximate local boundary conditions[178]. The interested readers can find a detailed description of these methods in ref. [178].

Acoustic pressure mapping is a key to determine the optimal position of the ultrasonic probes in reactors, as well as to scale up sonochemical reactors. An example of optimization of acoustic pressure mapping of ultrasonic emitters and their geometry via COMSOL modeling was reported by Lais et al. [179], who modeled acoustic pressure fields by finite element analysis to optimize the ultrasonic cleaning of large cylindrical pipes.

4. Ultrasonic reactor configurations

Several ultrasonic reactor designs have been reported, mirroring the large number of applications of acoustic cavitation. Sonoreactors can be divided into two broad categories: batch and continuous reactors. Within each family, large differences exist in terms of the type and number of transducers, reactor geometry, direct or indirect sonication mode, and flow characteristics. The main reactor designs are discussed in the following sections.

4.1 Ultrasonic batch reactors

4.1.1 Ultrasonic bath reactors

Ultrasonic baths are ubiquitous equipment in laboratories due to low-cost and simplicity. They usually consist of a container, generally a stainless-steel tank of rectangular cross-section, equipped with ultrasonic transducers (mostly piezoelectric) attached at the bottom or/and on the walls. In traditional ultrasonic baths, the transducers are usually mounted in an external enclosure to the tank, to which they tightly adhere through epoxy resins; they are not therefore visible from outside (**Figure 13**). The enclosure also contains the electronic board(s) connected to the transducer. Generally, bath reactors can be equipped with a heating/cooling system and adjustable power. The sample can be either directly or indirectly sonicated.

For most commercial bath reactors with fixed transducers, the operating frequency is usually fixed depending upon the device application. In early times, ultrasonic baths were designed to provide frequencies from 20 to 40 kHz to ensure a good cleaning via the physical effects generated by the implosion of larger bubbles. Nowadays, most ultrasonic baths operate at a frequency around 40 kHz for the purpose of human safety[180]. Indeed, since ultrasonic baths are usually operated for several hours, low ultrasound frequencies close to the human audible limit (20 kHz) represent a higher noise exposure risk compared to higher frequencies. Regardless, from the authors' experience, wearing ear protection devices and, when possible, enclosing the bath in

sound abating cases, is recommended also when operating at frequencies beyond 40 kHz.

Ultrasonic bath reactors operating beyond these frequencies can be manufactured *ad hoc* for specific sonochemistry studies. Henglein at Hahn-Meitner-Institut, Berlin, fabricated one of the oldest ultrasonic high-frequency bath configurations using quartz or piezo-ceramic transducers as an ultrasound source, wherein the emitting surface of the transducer attached was about 25 cm^2 [181].

Ultrasonic baths with an immersed transducer in direct contact with the mixture to sonicate have been also constructed with varying frequency. Ultrasonic submersible transducers can be installed in a cleaning bath reactor in different ways, at the bottom, side or top (**Figure 14**). KLN Ultrasonic Company developed submersible transducers of different size for industrial cleaning, with the name of "TSP-P". These devices consist of piezoceramic transducers ("Powersonic") fixed inside hermetically welded metal box (**Figure 14d**). The frequencies of such submersible transducers depend on the application and range from 20 to 132 kHz. This configuration offers advantages compared to the traditional ultrasonic cleaning bath such as: (i) exchangeability of the mobile submersible transducers, which can be customized in different number, size and shape; (ii) the position and orientation of the transducers can be also controlled to maximize cavitation; (iii) the transducer frequency can be changed based on the application; iv) higher cleaning efficiency because of the direct contact with medium rather than through the wall of the bath [182]. On the other hand, ultrasonic transducers directly in contact with a liquid, are prone to both chemical and mechanical corrosion, which intensifies with operation time, power, and pH (either basic or acid) [78].

Ultrasonic bath reactors are widely used for cleaning [182,183] , synthesis [184-186], extraction [187,188], cracking [189], electrodeposition [190] and water treatment [191,192]. Bath reactors are mostly suitable for the homogenization, cleaning and synthesis of small quantities, which need a relatively low energy density to avoid any damage to the sample or the equipment [193].

At industrial scale, large-volume and high-power ultrasonic baths are also adopted for cleaning surfaces, for instance in the food, automotive, electroplating and plastic

(moulds) industries, and for coating removal during stripping [194]. TierraTech supplies both automated modular systems of ultrasonic cleaning with a useful capacity up to 600 L, which can be programmed for degreasing of 32.000 parts in 120 h, and large-equipment cleaning tanks with capacity up to ca. 17.000 L [195]: for instance, the TT-8000 equipment for special cleaning, suitable for cleaning of marine engines, has a 8000 L capacity and is equipped with 20 1,700 W emitters, for a total power of 51 kW, and of an auxiliary tank for the extraction of oils and fats to avoid contamination in the cleaning tank [196].

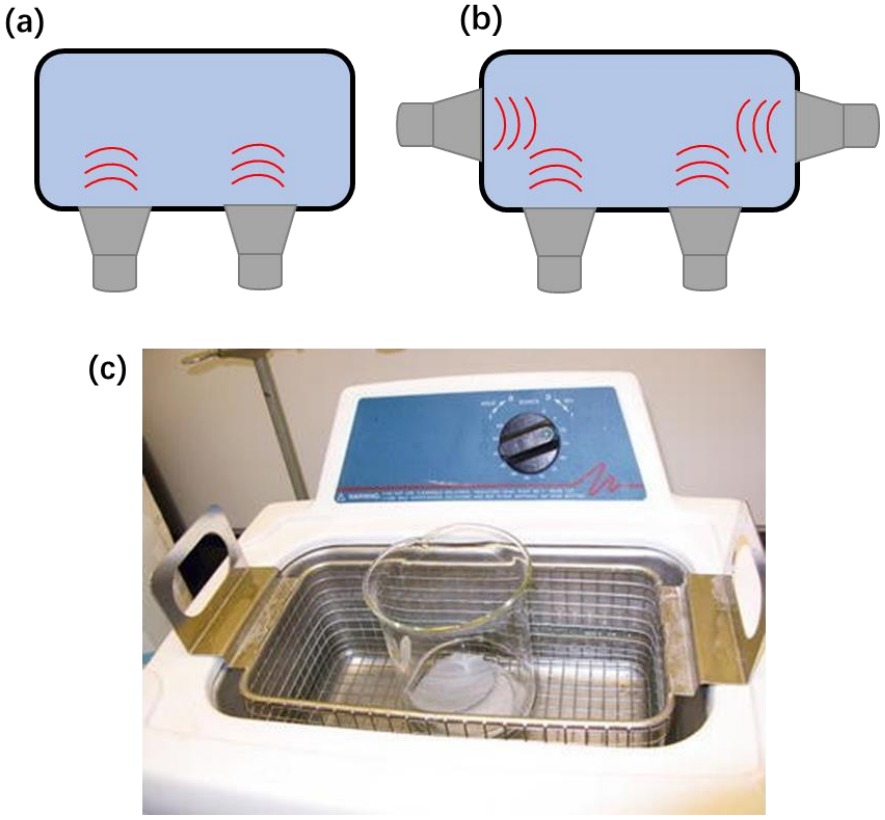

Figure 13. (a): Ultrasonic bath with transducers attached outside at the bottom of the bath, and (a): at the bottom and sides. (c) Laboratory-scale ultrasonic bath, reproduced with permission from [196].

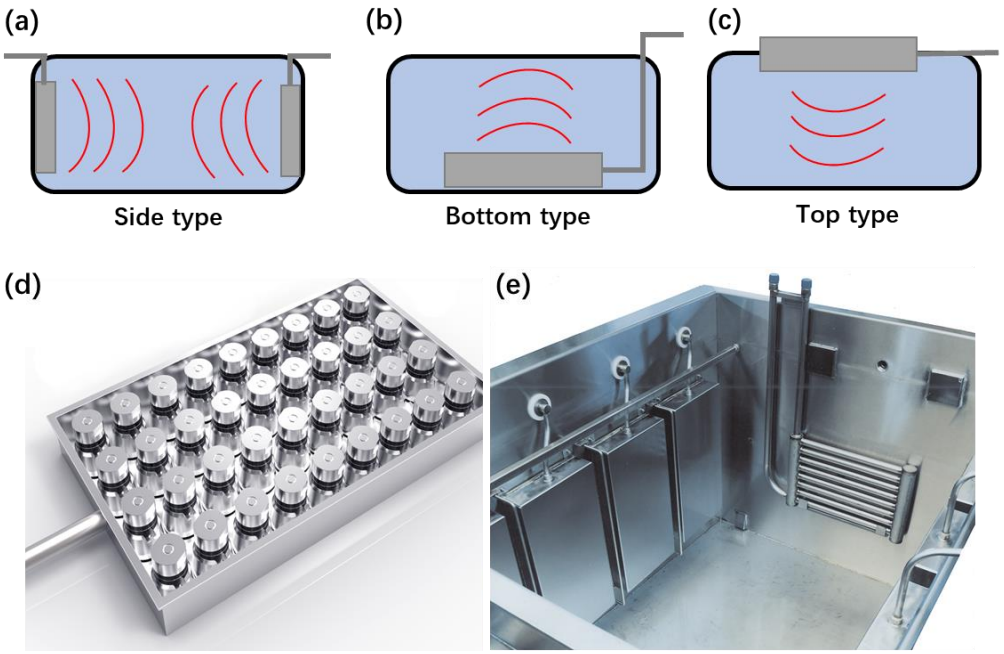

Figure 14. (a-c) Possible positions of submersible transducers in a bath reactor. (d): Submersible transducer stack. (e) Industrial ultrasonic bath with submersible transducers on the side walls, adapted from ctgclean website [197].

4.1.2 Ultrasonic sonotrode-based batch reactors

Ultrasonic immersed horn reactors leverage high intensity ultrasonic power in direct contact with the mixture. They are mostly adopted for sonochemical studies and industrial applications that require high intensity cavitation [198]. The local ultrasonic energy intensity (W cm^{-2}) is up to 100 times higher than in ultrasonic baths, because the area of ultrasound emission is lower. Typical applications of ultrasonic probe systems are disintegration [199,200], food processing [201-203], synthesis of nanomaterials/catalysts [204-207], liquid degassing [208], degradation of organic pollutants [209,210], extraction [211] ultrasonic welding [212-214], molding [215] bonding [216] and consolidation [217].

In sonotrodes, a metal rod is attached to the end of the transducer. The metal rod is also known as a sonic horn or velocity transformer, which magnifies the acoustic energy of the transducer, while the transducer device is kept clear, and out of the reaction medium (only the metal rod is immersed in the reaction vessel) as in **Figure 15a-b**. Most of the

probe devices are designed to work with a range of detachable horns providing the required energy. The shape and dimensions of the horn and the vessel volume, as well as the liquid height, determine the areas of acoustic activity and thus the reaction conditions of such a system [218-222], as discussed in detail in **Section 2.2**.

One of the major drawbacks of this system is horn erosion, which not only involves additional cost when it needs to be replaced, but can contaminate the processing liquids leading to biased results [78]. The fabrication of horns is not trivial: it includes selecting a metal or alloy to manufacture them (as discussed in detail in **Section 2.2**), designing the geometry for the required amplitude, and be meticulously tuned to the working frequency [223-227] . After a period of operation, depending on pH, temperature and amplitude, every horn degrades and eventually needs to be replaced [227-229]. For this reason, some horns have replaceable tips to avoid the costly replacement of the whole horn. However, there is a consensus about not using replaceable tips with organic solvents or low surface tension liquids, as these latter can interpose between the probe and the replaceable tip, thus isolating the tip from the probe and preventing it from vibrating at the resonant frequency and damaging it. When processing organic solvents or low surface tension liquids, a solid probe should always be used. Moreover, some studies reported that, after a quite long usage, the degradation of sonotrodes can take place in positions other than the tip. For example, Tian et al. [230] studied the cavitation erosion mechanism of Al_3Ti sonotrodes in industrial metal casting and followed the microstructural changes in the horn and the locations of the cavitation erosion over 36 h. The authors reported that at 25°C, three cavitation erosion areas appeared on the sonotrodes at positions 42, 134 and 221 mm from the tip (**Figure 15e**).

One of the known drawbacks in batch reactors equipped with ultrasonic horns is the uncontrolled temperature rise of the medium due to heat dissipation of the ultrasound energy. The raise in the temperature depends on the volume of the liquid and its physicochemical properties. A cooling bath or a cryogenic fluid circulating in a jacket external to the reactor are possible solutions.

A Rosett cooling cell is a reaction vessel meant to be immersed in an ice bath or a cryogenic liquid. It is manufactured with loops at the bottom to circulate the

ultrasonically propelled liquid, with the double purpose of mixing it and providing a higher surface area for the heat transfer contact with the cooling medium (**Figure 15f**). The Rosett cell has been designed by Theodore Rosett in 1960s [231], to maintain the cell temperature during for the release of proteins and enzymes from Saccharomyces cerevisiae in extended sonication treatment. A few years later, the Rosett device was patented and commercialized to treat heat sensitive materials by sonication [232]. Nowadays, Rosett cells are used for many ultrasonic applications such as solubilization [233], synthesis of nanomaterials [234,235], esterification [47] and particle dissolution and size reduction [236], etc.

Different shapes of horns are available such as uniform cylinder, linear taper or cone, exponential taper and stepped. More recently, horns with special shapes have been made available on the market. For example, Hielscher developed the so-called Cascatrode (**Figure 15c**) for industrial processing that require high cavitation power [237]. The configuration of such cascatrode system relies on the attachment of disc-shaped segments along with the neck of the sonotrode, wherein, each disc is placed in correspondence of the oscillation maxima of the rod, resulting in large sonication surface area all along the sonotrode. Cascatrode devices with different lengths or number of rings can be fabricated. Unlike traditional sonotrodes, cascatrode offer radial transmission of ultrasonic waves in the medium rather than longitudinal.

Wei et al. [225] fabricated a multi-stepped ultrasonic horn with a cone-shaped tip for wider cavitation distribution based on the principles of the dynamic wave equation. The authors reported that, unlike the common ultrasonic horns that produce localized cavitation below its converging tip, the results of sonochemiluminescence experiments showed that the multi-stepped ultrasonic horn create multiple ultrasonic reactive zones along the length of the horn (**Figure 15d**).

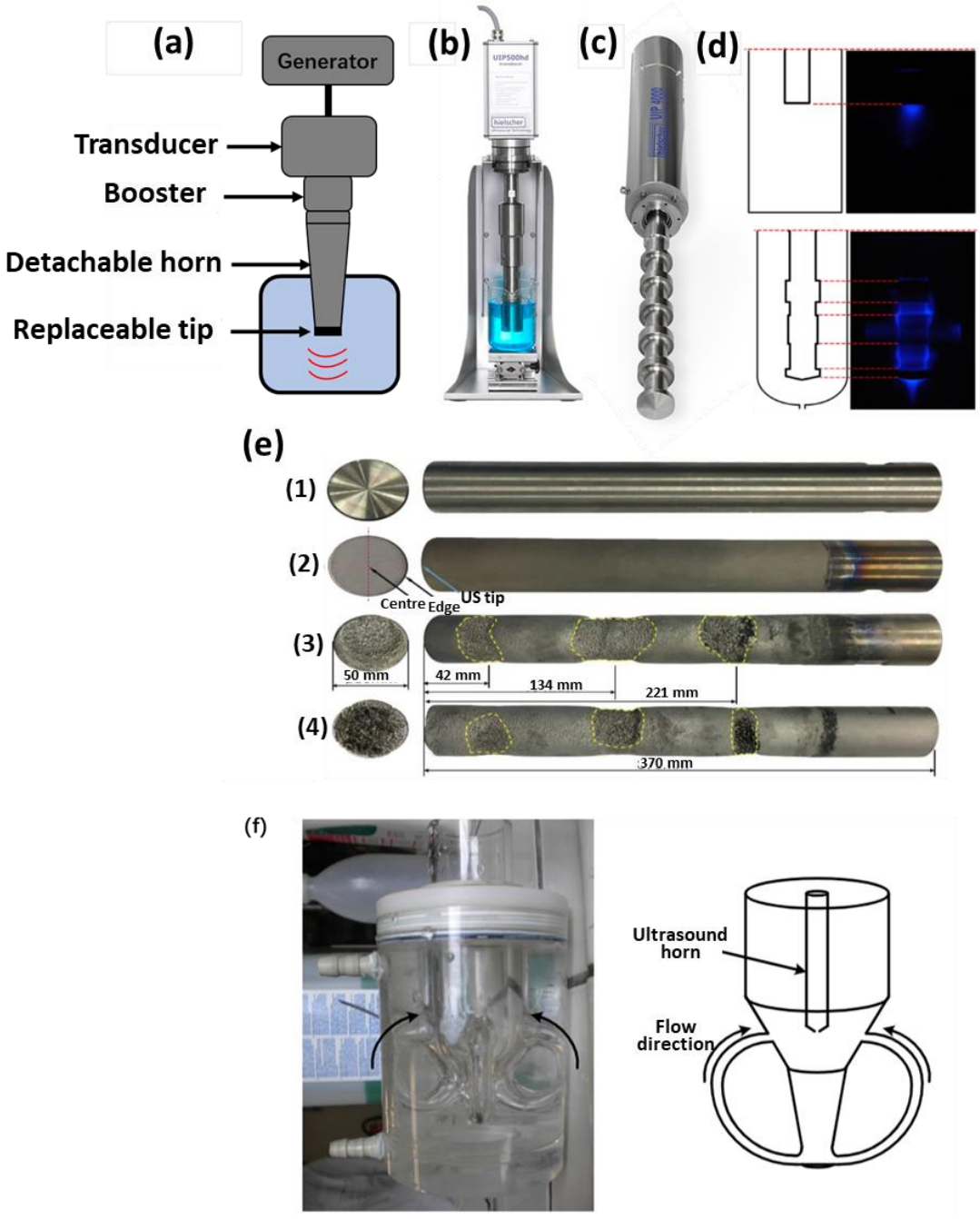

Figure 15. (a) Simple diagram of a ultrasonic sonotrode batch reactor, (b) Hielscher ultrasonic processor UIP500hd (20kHz, 500W), image adapted from Hielscher website [238], (c) Hielscher Cascatrode with 5 rings (Hielscher Ultrasonics GmbH) [239]. (d) Distribution of cavitation on the surface of a normal horn and on the surface of multi-stepped ultrasonic horn with a cone-shaped tip, reproduced with permission from [225]. (e) Effect of cavitation on sonotrodes erosion: (1) a brand new sonotrode, (2) a used sonotrode with erosion invisible to the naked eye (short term use), (3) and (4)

sonotrodes displaying with severe erosion, reproduced with permission from [228]. (f) Rosett cell ultrasonic reactor, reproduced with permission from [20].

Applications of ultrasound in drying [240,241], microbial inactivation [242], supercritical CO_2 extraction [243-245], aerosol agglomeration processes [246,247] and defoaming [248], require airborne ultrasonic transducers. Several transducer geometries have been developed specifically for the ultrasonic treatment of gases or multiphase media [249,250]. Airborne transducers consist principally of a piezoelectrically activated vibrator, which provides ultrasonic radiation. The vibrating flat plate radiator driven by the mechanical amplifiers (horn) offers a powerful radiation. Eskin et al. [208] used plate sonotrode for the ultrasonic degassing of aluminum melts and the results showed that the effectiveness of degassing in batch system with a plate sonotrode was significantly higher (70–80%) than with a conventional cylindrical sonotrode (45–50%). The plate radiator can be designed in different shapes such as circular, rectangular or cylindrical, and it can incorporate a stepped, grooved or stepped-grooved profile (**Figure 16**) [251-253] . The interested reader can find more information on the design of plate radiator geometry and profile on the review by Gallego-Juárez et al. [254].

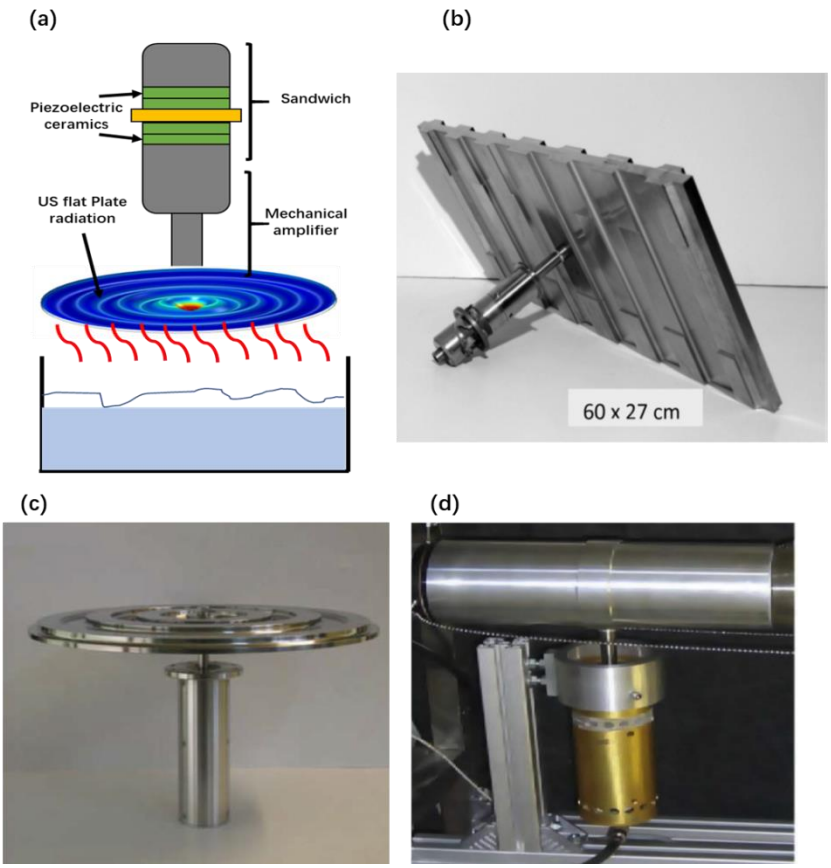

Figure 16. (a) Simple diagram of an airborne sonotrode system for liquid degassing. (b-d) Images of rectangular, circular or cylindrical transducers, (b) Reproduced with permission from [242], and (c)-(d) from [254].

4.1.3 Ultrasonic cup-horn reactors

Ultrasonic cup-horn systems consist of a reaction vessel with an ultrasonic horn glued inside it. The ultrasonic emitter is a sonotrode that transmits the ultrasonic waves in the medium from the bottom to the top, often used for indirect sonication (Figure 17). Commercial cup-horn systems can provide 50-times higher energy intensity compared to cleaning baths. Conversely, compared to ultrasonic horns, their energy intensity is lower because of the larger emission area.

Ultrasonic cup-horn reactors have been applied to the extraction of trace metals from troublesome matrices [255,256] cup-horn setups enable the use of concentrated acids and even of HF, needed for a fast and efficient extraction from silicon-containing matrices,

that would instead quickly degrade an immersed horn. De La Calle et al. [255] reported that cup-horn systems are less prone to corrosion than ultrasonic probes when applied in the acid leaching of noble metals, such as gold and silver, from environmental samples. Teixeira et al. [257] studied the ultrasound-assisted extraction of heavy metals from organic fertilizers using a cup-horn system (VCX 505) working at 500 W and 20 kHz. The authors reported a quantitative extraction of eight metals at room temperature and pressure; with respect to standard microwave-based extraction, the ultrasound-assisted procedure required less chemicals, reducing costs and waste, and used milder conditions, thus reducing sample losses due to volatilization.

Other applications of cup-horn setup have been reported in organic [258] and nanoparticles synthesis [259]. For instance, Santos et al. [258] compared bath, cup-horn and immersed horn systems for the ultrasound-assisted acid hydrolysis of cellulose to produce furanic platforms and the synthesis of furfural; the authors reported that the cup-horn system was the most efficient with a furfural yield of 78%. Cappelletti et al. [260] compared cup-horn systems operating at 19.9 kHz (75 W) and 300.5 kHz (70 W) with a high power ultrasound bath (20.3 kHz, 60 W) for the ultrasonic synthesis of ferrocenyl derivatives in aqueous media: The cup-horn setup working at 19.9 kHz gave rise to an almost double reaction yield with respect to the ultrasound bath (85 vs. 48%).

Cup-horn systems have also been adopted for the ultrasound-assisted degradation of pollutants [261]. Giannakoudakis et al. [262], designed a sonophotocatalytic batch reactor for pollutant oxidation adopting an ultrasonic cup-horn sonicator (Qsonica, 20 kHz) and LED lamps placed on top of the reactor. Besides generating ˙OH radicals from the implosion of the acoustically generate bubbles, ultrasound coming from the bottom also ensured the mixing of the TiO_2 suspension replacing traditional magnetic stirring, thus promoting mass transfer. The authors reported that an increase of the ultrasonic power, produce more radical species and dispersed them better in the reactor.

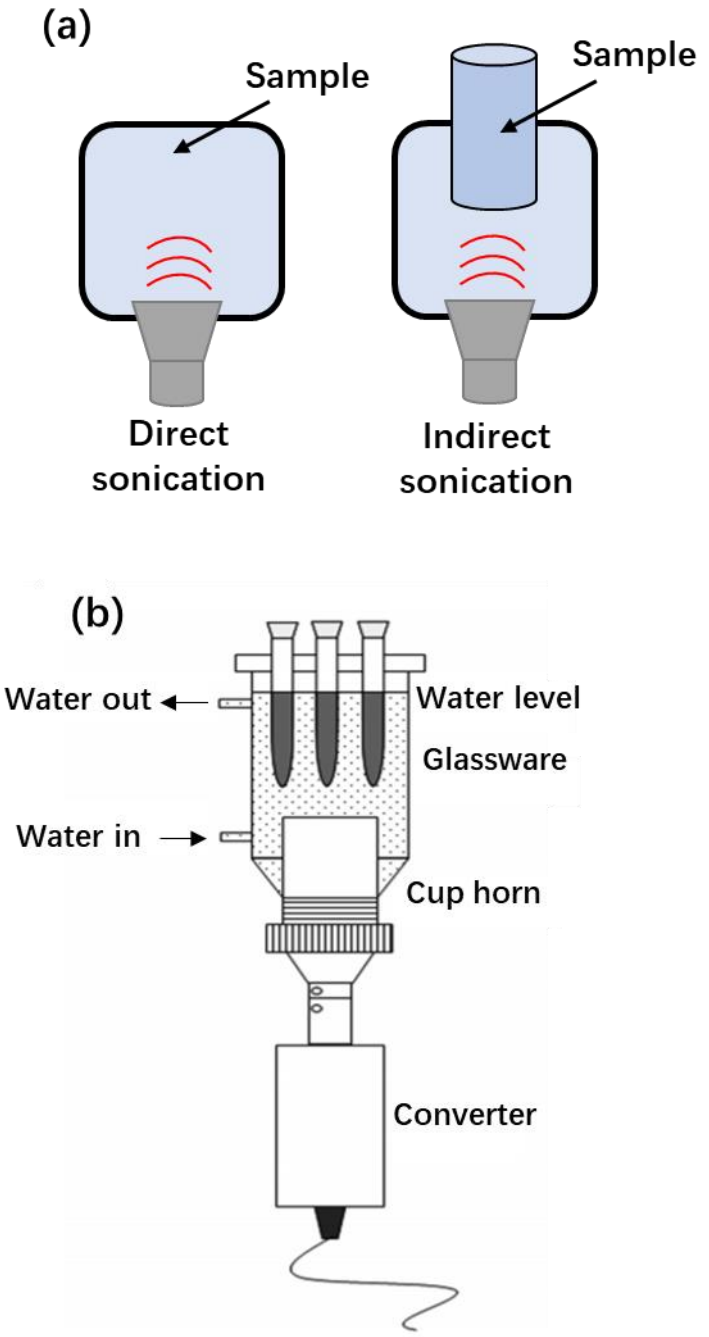

Figure 17. (a) Schematic of cup-horns for direct and indirect sonication, (b) Scheme of the cup-horn sonoreactor system with multi-position support, reproduced with permission from [257].

4.2 Continuous (flowthrough) ultrasonic reactors

In large-scale operations, flow arrangements offer greater flexibility in terms of reactor design and reagent concentration. Continuous reactors should always be preferred over batch reactors if the process allows.

4.2.1 Continuous with emitting walls

Polygonal reactors, such as the hexagonal reactor reported in **Figure 18**, feature transducer arrays that surround the polygonal vessel containing the liquid medium. By using multiple transducers, a more uniform cavitational activity can be obtained. Moreover, multiple frequency irradiations can be performed. Gogate et al. [192] reported a hexagonal flow cell with a total capacity of 7.5 L working at triple frequency; three transducers were placed on each face of the hexagon, leading to seven different operating combinations of operating frequencies. They reported a uniform distribution of cavitational activity in the bulk of liquid (10–30% variation with respect to 80–400% in a horn reactor configuration).

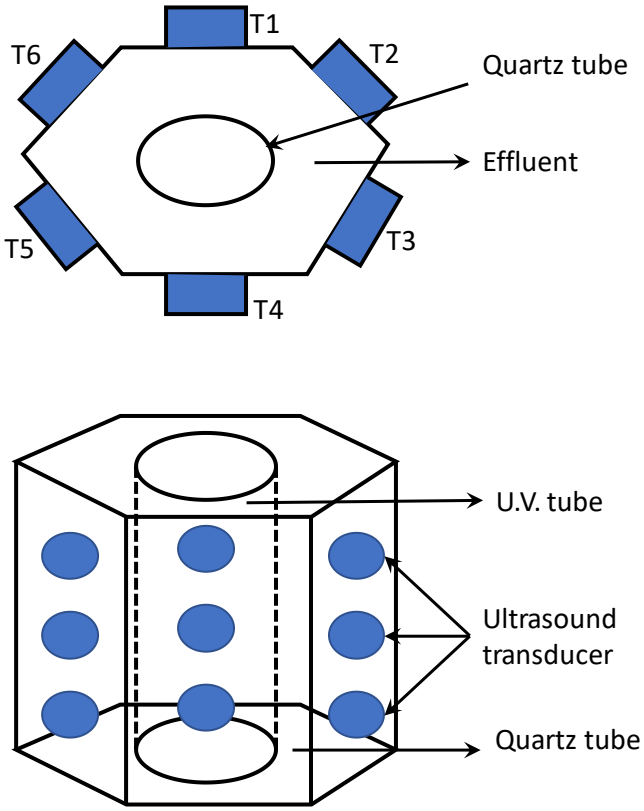

Figure 18. Scheme of a hexagonal flow cell with multiple transducers; adapted from ref [192].

In the tubular flow configuration, the transducers are attached to the walls of cylindrical reactors **Figure 19a-c**. The emitting ultrasonic field is concentrated and focused on the middle of the tube rather than nearby the inner surface of the walls, which reduces significantly the cavitational degradation of the reactor walls [173]. It is important to

mention that the cylindrical geometry in flow reactors is more recommended because it provides a better reflection of ultrasonic field compared to hexagonal flow reactors [146].

Additionally, one of the main advantages of tubular systems is that the devices available in the market can be easily integrated to any existing system. Tubular flow reactor can be equipped with cooling system to control the temperature of the medium.

Lippert et al. [263] used a flatbed reactor with a rectangular cross-section equipped with six ultrasonic transducers fixed on the outer wall (BANDELIN electronic GmbH & Co. KG, Berlin, Germany) as displayed in **Figure 19d**. This structure is characterized with enhanced ratio between oscillating surfaces and sonicated volume. The distance between transducer plates is a key parameter to warrant homogeneity of the ultrasound field in the chamber [264]. Lippert et al. [265] studied the dynamics of water, activated sludge, and digested sludge within this flatbed reactor (**Figure 20**) through visualization via the injection of dye streams. The ultrasound caused the flow to be turbulent in water, while in the sludge the flow remained mostly laminar.

Bandelin et al. [266] tested sonotrode and flat reactors in the treatment of different types of sludge to produce biogas. They concluded that the sonotrode reactor was more efficient to process highly viscous waste activated sludge with high total solid content, while the tubular reactor was more suitable to promote methane production in less viscous waste activated sludge, energy input being the same. Koch et al. [267] employed a tubular reactor for the release of soluble chemical oxygen demand (COD) and anaerobic digestibility of different sludges (raw, digested and agricultural). They suggested that the application of tubular reactors for sludge treatment is recommended vs. direct sonotrodes, since a tubular reactor ensures similar performance with low maintenance and cost.

In flow tubular systems, the number of transducers is a key parameter to achieve uniform strong cavitation field (**Figure 19e**). It also allows to integrate transducers with varying frequency irradiations, which permits to apply high intensity cavitation zones at the same levels of power dissipation [268].

SYNETUDE (France) fabricated a continuous flow ultrasonic reactor so-called

SONITUBE® with standard frequency of 20 and 35 kHz, with power of 1200 and 400 W (power density 0.8-1.7 kW/L and 2.8-5.7 kW/L) for different physical and chemical processing applications at the laboratory and commercial scale [269]. The diagram and the picture of the standard *SONITUBE*® reactor are shown in **Figure 19f-g**. The inner diameter of the capillary can be either 20 or 50 mm, resulting in a useful volume of 0.07 and 0.7 L. The ultrasonic transducer excites the tube (sonotrode) wall at the resonant frequency. Such a system exhibits a treatment capacity ranging from a few liters up to several cubic meters per hour depending upon the application.

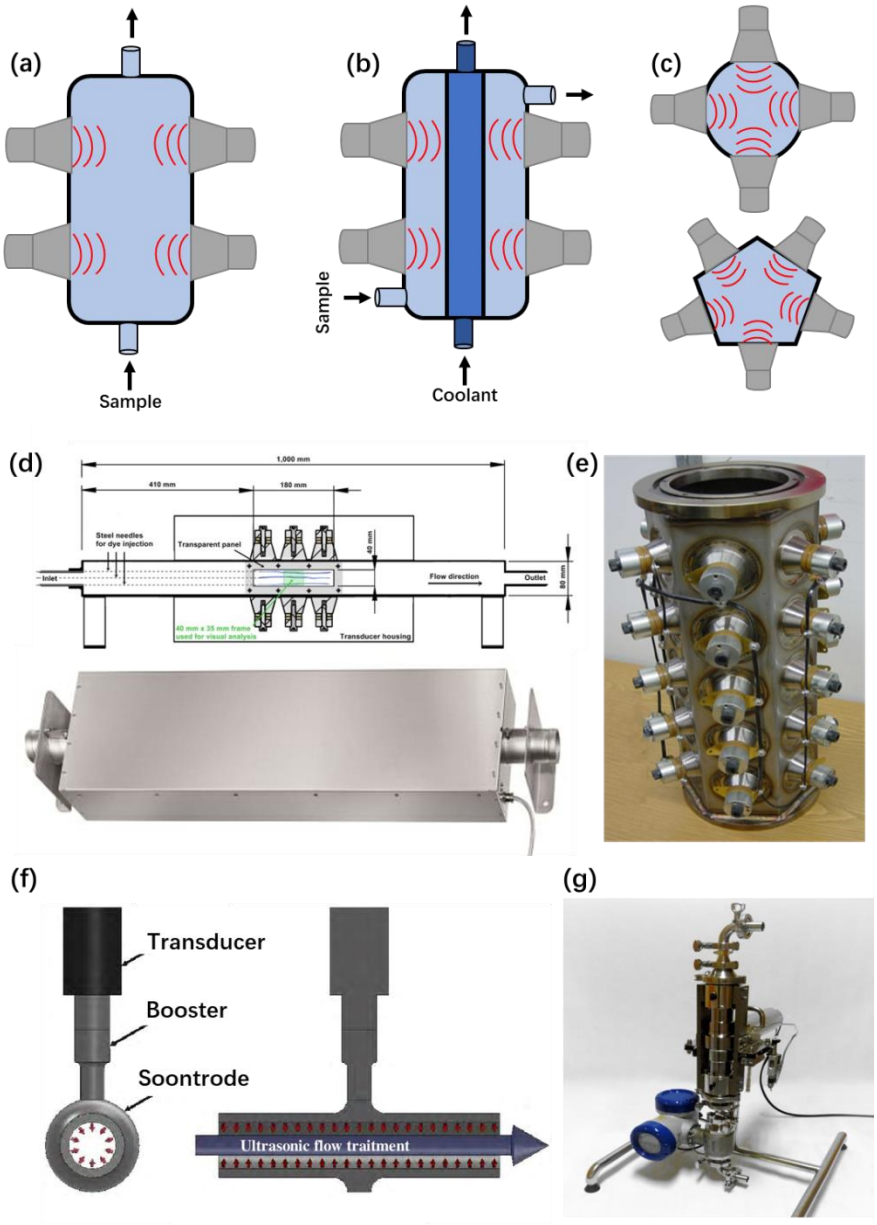

Figure 19. (a) and (b): Diagrams of tubular continuous reactors without and with a cooling system, respectively. (c) Cross section of flow continuous reactors. (d)

Longitudinal section plot and image of tubular reactor (BANDELIN electronic GmbH & Co. KG, Berlin, Germany), reproduced with permission from [265]. (e) Image of tubular transducers with frequencies of 20 - 40 kHz for industrial application (KLN Ultraschall AG, Germany). (f) and (g): Diagram and image of SONITUBE® flow reactor (SYNETUDE, France), adapted from [269].

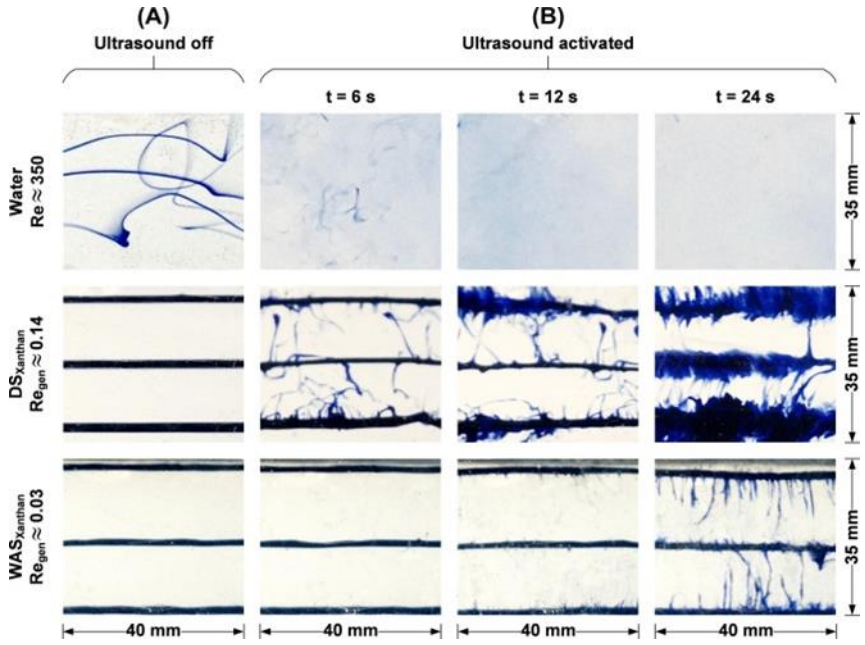

Figure 20. Images showing flow dynamics behavior of water and sludges in ultrasonic flatbed reactor, reproduced with permission from [265].

4.2.2 Continuous reactor with incorporated sonotrodes

Continuous reactors with incorporated sonotrodes combine high intensity, focused ultrasound and the advantages of continuous flow systems. Such a system can be used in a wide range of applications [270-272]. Servili et al. [273] used a continuous reactor equipped with cascatrodes for the extraction of oil from olive paste. The ultrasonic device, manufactured by Hielscher Gmbh (Teltow, Germany), consists of an ultrasonic generator (20 kHz), a power supply (4 kW) and cascatrodes placed in a vertical stainlesssteel tube (**Figure 21a**). Vernès et al. [274] have used a continuous ultrasonic reactor with horns (UIP1000hd, Hielscher Ultrasonics, GmbH, Germany) for the ultrasonic extraction of proteins from spirulina. The system consists of an ultrasonic treatment chamber equipped with a sonication horn connected to a stainless-steel

cylindrical feed reactor. **Figure 21b** shows the image of full-scale flow reactor equipped with seven ultrasonic sonotrode (1500 W, 20 kHz), the sample runs continuously in the tube upward direction and it is subjected to a high intensity ultrasonic field. Such a system can operate 24h/7day and it can process up to 5m^3 per day. Depending on the application and type treatment required, multiple sonotrodes can be used, wherein the energy applied of sonotrodes ranges from 1000 W to 16000 W. This system can be used for water or solid ultrasonic treatment at the industrial scale.

ULTRAWAVES company (Germany) in collaboration with SONOTRONIC Nagel GmbH (Germany) have developed a pilot scale continuous reactor with a sonotrode for disintegration and enhanced biodegradation of solids (**Figure 21c-d**) This commercial reactor, designed in a research laboratory at the Technical University of Hamburg–Harburg [275-279], has the largest number of full scale industrial applications for sludge disintegration in wastewater stations [280]. The compact reactor is equipped with five sonotrodes (2 kW, intensity range: 25-50 W/cm^2) installed in different chambers. The sample is subjected continuously to the highly focused cavitational power when it is pumped upwards through the reactor channels. **Figure 21e-f** shows the configuration of the novel ULTRAWAVES high-power ultrasonic system (ULTRAWAVES Water and Environmental Technologies, Hamburg, Germany) which prevents the deposition of sludge mass within the individual chambers as compared to standard ULTRAWAVES design, suggesting less maintenance.

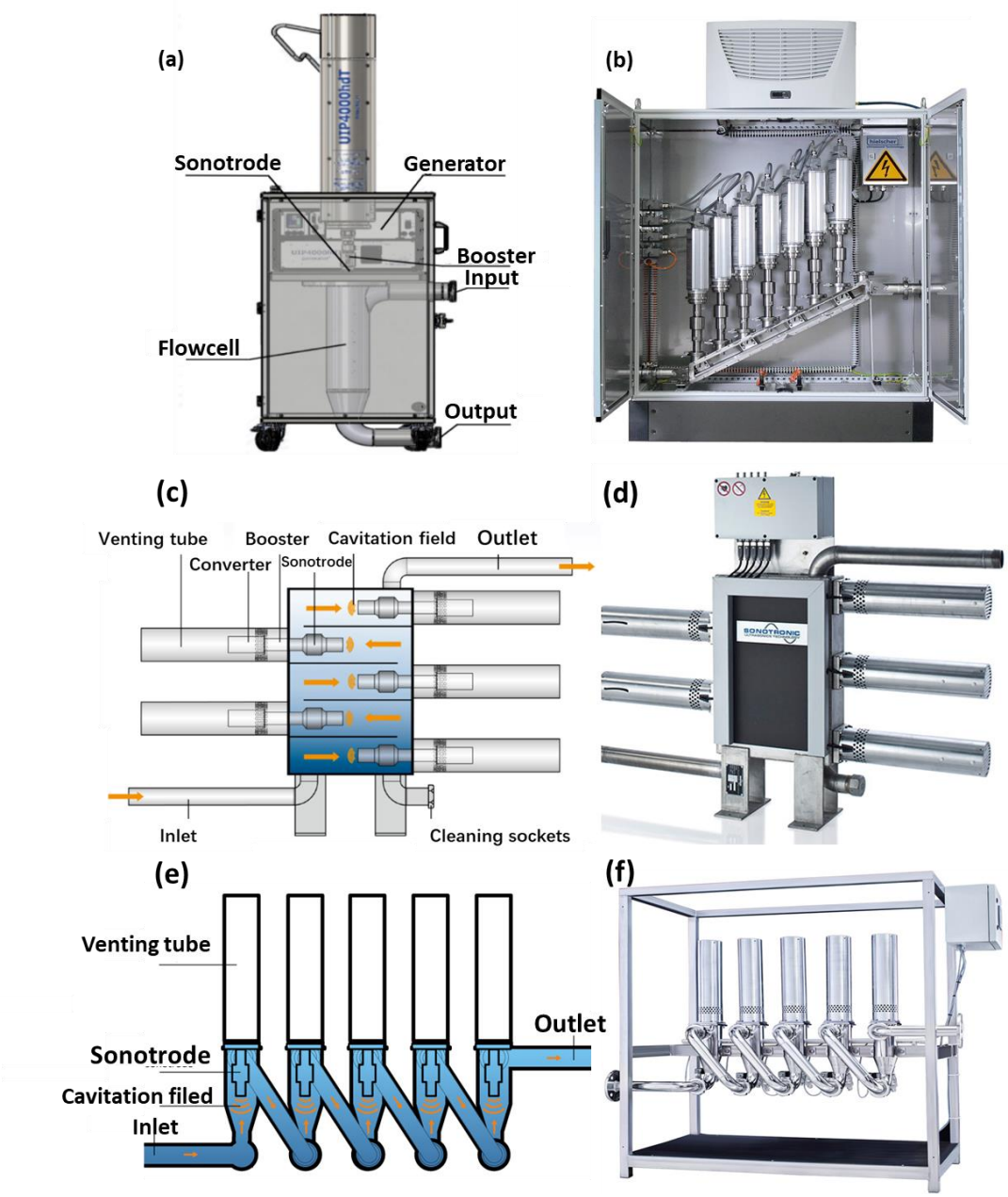

Figure 21. (a) Continuous sonoreactor with highly focused ultrasound incorporated inside, reproduced with permission from [274]. (b) Industrial continuous ultrasound flow reactor equipped with 7 sonotrodes. (c) and (d): Diagram and image of full-scale continuous sonoreactor (ULTRAWAVES Water and Environmental Technologies, Hamburg, Germany). (e) and (f): Scheme and photograph of ULTRAWAVES high-power ultrasonic system.

Flow reactors can also be applied to combined MW/ultrasound irradiation. Such a combination has powerful synergistic effects in organic synthesis and catalysis. Due to the rapidity, lower energy applied and selective transformations, the hybrid microwaves/ultrasound technology has received afterwards much attention from both the scientific and industrial communities [77,281-283]. **Figure 22** reports combined MW/ultrasound reactors for sequential irradiation: a pump circulates the reacting mixture through two separate reaction cells, one placed inside the MW oven and the other (fitted with an ultrasound probe) outside it. In this way, commercially available metallic horns can be used. The set-up reported in **Figure 22b** is based on a ultrasound horn and a 750 W MW oven, and it is equipped with a heat exchanger using refrigerated silicone oil) and uses 150-200 mL min^{-1} flow rates [284].

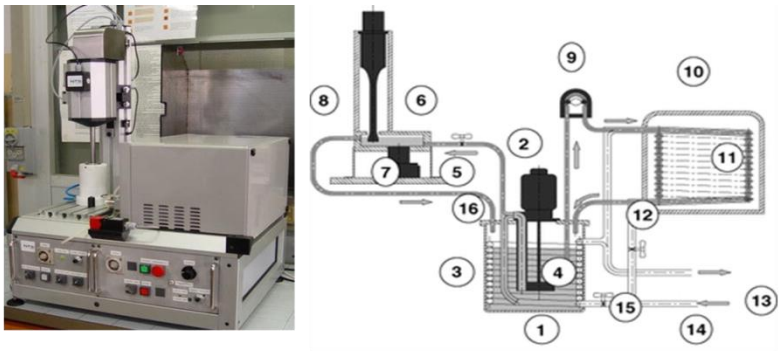

(1) Tank (5L)
(2): Centrifugal pump
(3): Recirculation
(4): Cooling coil
(5): Regulation of inlet to US cell
(6): US reaction cell (150 mL)
(7/8): 300 kHz/20 kHz probes)
(9): peristatic pump
(10/11): MW oven/reaction compartment (170 mL)
(12): refrigeration oil from coaxial hose
(13): cooling oil
(14/15): valves that regulate the flow of cooling oil
(16): samples outlet

Figure 22. (a): Combined Microwaves/ultrasound reactor, reproduced with permission from [285], (b): scheme of a loop reactor for sequential MW/ultrasound irradiation, reproduced with permission from [284].

4.2.3 Continuous ultrasonic microreactors

Ultrasonic flow microreactors, characterized by channel sizes in the order of few mm or less, are constructed usually for laboratory or small-scale applications, and they offer the same advantages of industrial scale reactors, such as better control of reactions

conditions, better heat and mass transfer, as well as flexibility compared to batch reactors [152,286-289].

One of the limitations of the use of ultrasonic systems in food and pharmaceutical industries or for the synthesis of other applications requiring highly pure products is the fact that the continuous cavitation on the surface of the sonotrodes leads to severe erosion, which contaminates the products by metallic species such as titanium, thus barring the use of ultrasonication process to food and fine chemicals processes [290]. Solutions in terms of reactors design to overcome such issue have been addressed. Hielscher Ultrasonics in co-operation with the ETH Zürich developed a special ultrasonic flow cell to sonicate indirectly the medium with high intensity in closed system without being contaminated [291]. As shown in **Figure 23a**, the flow-through microreactor consists of a cylindrical steel jacket, which involves a 2 mm inner diameter glass tube. The reaction tube has no contact with the atmosphere nor with the ultrasonic sonotrode. To fix the temperature of the medium during the ultrasonic reaction, the water surrounds constantly the tube in circulation. The sonotrode is placed at outside of the steel jacket. This ultrasonic microreactor can be used for the production of highly pure products at laboratory or large scale [292].

Hielscher Ultrasonics developed an insert for flow cell reactors called MultiPhaseCavitator (InsertMPC48, **Figure 23b**). The InsertMPC48 system can be used to enhancing phase-transfer process kinetics or combination/dissolving effectiveness in liquid-liquid or liquid/gas phases. In InsertMPC48 system, the injection of liquid or gas into a liquid medium is carried out via very fine cannulas with diameters from 0.3 mm to 1.2 mm, wherein, the injection of gas bubble or liquid droplets is done right in the cavitation zone to be mixed immediately with the flowing liquid in the tube. The liquid is injected via the cannulas and it goes to the flow tube/cell in fine in narrow strands. When the liquid phase enters in the flow cell, cavitation generated at 20 kHz converts the incoming liquid strands into fine droplets. This system works in continuous processing or also batch. The InsertMPC48 reactor can be used for different applications such as mass-transfer in chemical reactions. For instance, it has been applied to polymerization of lactide to the polymerization of polylactic acid, PLA [293,294].

Dion et al. [173,295] developed and patented a new contamination-free cylindrical sonoreactor for fine chemical processes (**Figure 23c**). The device consists of many electroacoustic transducers radially placed around the reaction tube. The number of transducers is variable typically from 4 to 16. The heads of these transducers are pressed on the wall of the elongated tube, which made of flexible material (polytetrafluoroethylene, Teflon^{TM}). The heads have a concave surface that ensures an excellent fitting on the outer wall. The liquids sample is treated in circulation in the tube. The transcoders transmit the acoustic waves through the wall, leading to induce an acoustic cavitation in the central zone of the tube, while the produced ultrasonic cavitation can be controlled away from the inner tube wall depending on the applied energizing current. In another operation mode of this ultrasound device, acoustic cavitation can be produced in all points via the management of the vibration of transcoders of the tube to carry out a turbulence behavior or to mix the medium. The whole system is placed in a sealed chamber, where the pressure can be controlled and lubricant and coolant can be circulated.

John et al. [288,296,297] designed a temperature controlled micro-reactor which applied the ultrasound on microchannel for liquid-liquid extraction. As shown in **Figure 23d**, the microchannel tubes undergo an ultrasonic field by direct or indirect contact with the transducer. In direct contact, the tubes are sonicated directly by the transducer without the presence of liquid, while, in terms of indirect contact, the microchannel tubes are placed in temperature-controlled liquid medium. The temperature-controlled medium is flown in a 10 mm thick, 80 × 80 mm hollow-aluminum plate, acting as ultrasonic bath with a configuration fitting the geometrical factor of the flow-tube reactor. The reaction liquid to be treated or mixed is pumped in circulation through a PFA tube of 0.8 mm inner diameter. The authors mentioned that the highest effectiveness of the process was found at 20.3 kHz, 840 mV and flow rate of 0.1mL/min. In addition, the flow system configuration is considered to be more suitable for fine chemical processing compared to conventional horn setups because it avoids the contamination of the medium by horn erosion. Dong et al. have used this system in gas–liquid mass

transfer intensification [288], and the authors reported that the overall mass transfer coefficient was enhanced by 3.3–5.7 times.

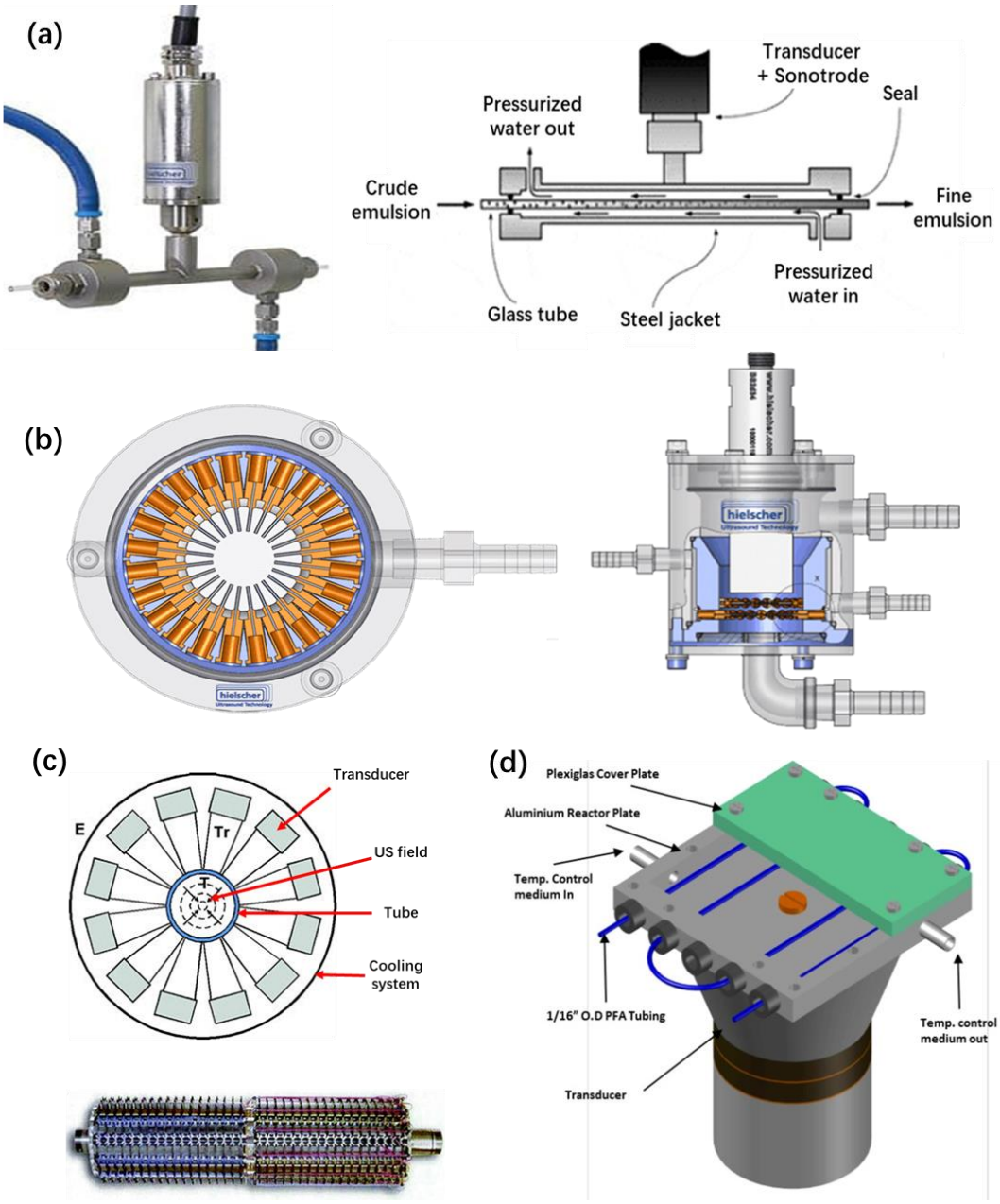

Figure 23. (a): Photograph of UIS250Dmini Ultrasonic Flow Cell, and its corresponding schematic diagram. (b): Diagram of cross-section and full scheme of InsertMPC48 sonoreactor. (c): Cross-section and the core of SonerTec sonoreactor. (d): Temperature controlled reactor for ultrasound-assisted liquid-liquid extraction, reproduced with permission from. [288].

4.3 High frequency sonoreactors

In general, sonoreactors with frequency higher than 100 kHz are less common than the ones in the 20-100 kHz. The ultrasonic parameters should be studied and optimized at high-frequency systems for successful large-scale applications. The ultrasound process efficiency depends strongly on the distributed sound pressure throughout the ultrasonic chamber. The more the penetration of sound is achieved within the reactor, the more ultrasound efficiency could be obtained. Leong et al. [298] have investigated the sound pressure distribution at different distances for two ultrasonic plate transducers at 400 kHz (120 W) and 2 MHz (128 W) in a 2 m long sonoreactor (**Figure 24**). The authors found out that at 2 MHz a strong pressure amplitude was localized nearby the transducer, while a considerable decrease of around 40% of sound pressure was detected at distance ranging from 55 to 155 mm from the transducer. In addition, it was found that the sound pressure can be enhanced via the placement of a reflector plate 500 mm. On the contrary, the transducer with 400 kHz showed a better sound penetration though the fluid without a notable material loss. Unlike 2 MHz system, 400 kHz can produce a better uniform distribution of sound pressure with or without the reflector plate. It was concluded from this study that the use of medium frequency range is recommended for sonoprocessing. While, in the case of systems that require high frequencies, the processing in shorter chambers with the use of reflector plates could give a better sound distribution and excellent ultrasonic performance.

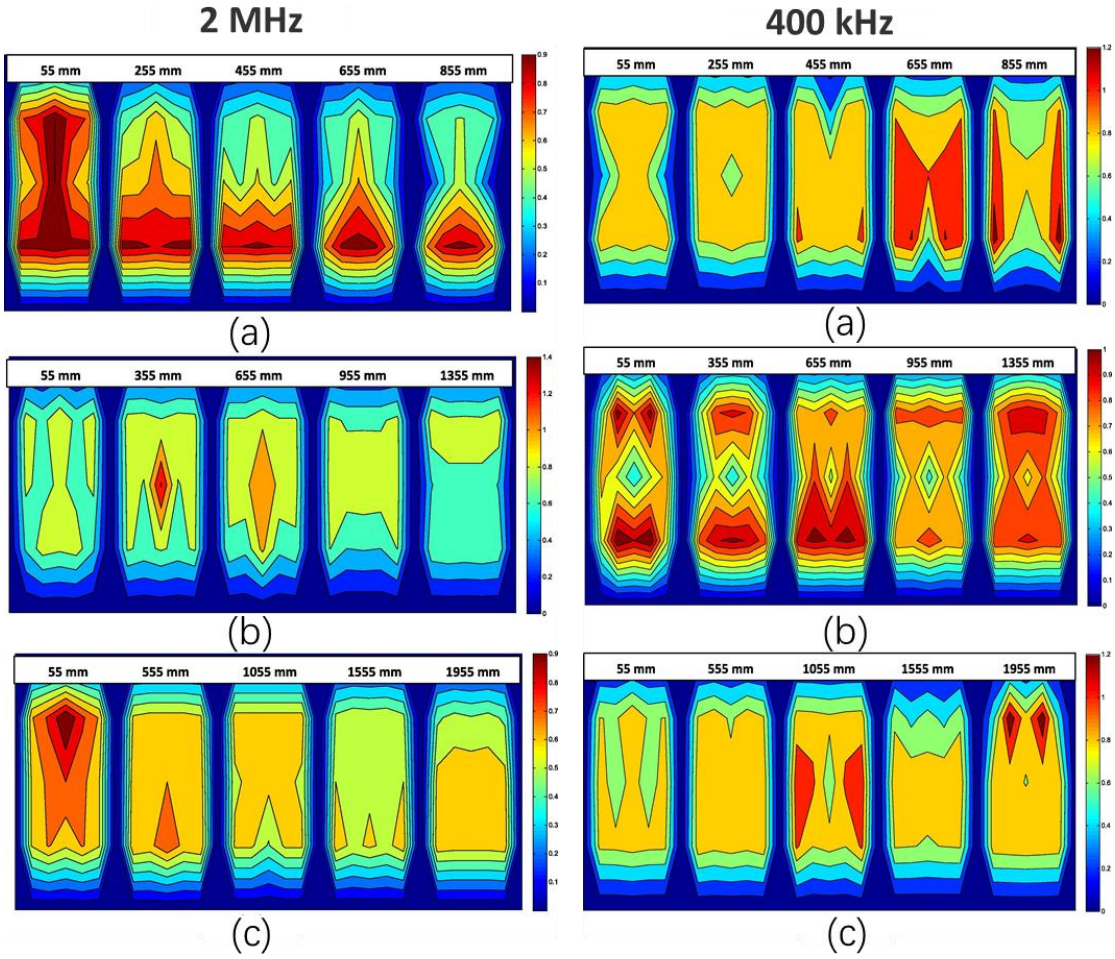

Figure 24. The distribution of sound pressure for transducers with refactor plates of 2 MHz and 400 kHz frequencies located at different positions. Reproduced with permission from [298].

High frequency systems have been widely used for separation processes. The frequency is selected based on the type of materials as well as the biomass structure, wherein, frequencies from 1 to 2 MHz have showed an excellent separation of small sized particles, while in the case of oils separation, frequencies ranging from 400 to 600 kHz are recommended [299]. As shown in **Figure 25**, Juliano et al. [300] have used 200 L-reactor equipped with 400 and 600 kHz transducers for oil extraction from 300 kg of paste. High frequencies are applied also for the sludge anaerobic digestion [301], where, frequencies values from 200 kHz [302] to 1.8 MHz [303] were reported. High frequency ultrasound systems are privilege in the case the synthesis of particles and nanomaterials [304].

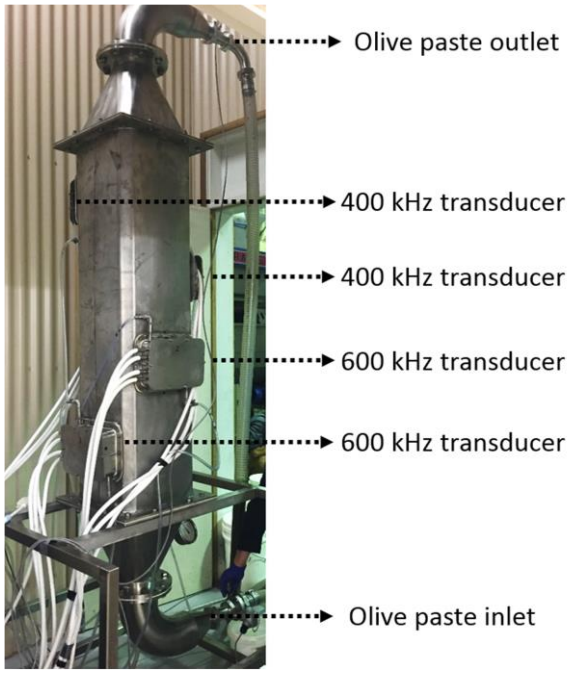

Figure 25. Megasonic sonoreactor Sonosys Ultraschallsysteme GmbH (Neuenbürg, Germany) with 400 and 600 kHz transducers, used for oil extraction; reproduced with permission from [303].

5. Large scale applications

The range of application of sonoprocessing is very wide and diverse that a detailed picture is too vast to be covered in this review. Selected applications will instead be discussed, with a special emphasis on technologies already industrially viable. It should be noted, however, many companies do not disclose their ultrasound-based technologies, hence the present list of large-scale applications is certainly far from complete. The lab-scale and commercial reactors these applications rely on, can be found in **Section 4**.

5.1 Ultrasound in environmental remediation

Over more than two decades, consistent research has been carried out on the application of ultrasound to environmental remediation, including water purification, sludge disintegration, microorganism inactivation, soil treatment, etc.

Among the well-established environmental applications of ultrasonic processing, there is sludge disintegration [108,266,305-309]. Mostly, low frequencies, ranging from 20 to 40 kHz, are used to obtain the physical effects required for the sludge treatment. The ultrasonic disintegration of sludge can offer several advantages including effective sludge dewatering[310,311], reduced foaming[312], detoxification and disinfection[313,314], enhanced biogas production[315,316], and activation of ammonia-oxidizing bacteria (AOB)[317-319]. The application of ultrasonic technology to sludge disintegration has already been successfully transferred to industrial applications, proving an energy-efficient and cost-effective alternative to conventional technologies. In this respect, several ultrasound-based technology systems are currently on the market. The ULTRAWAVES technology (**Figure 26a**) is a 5 kW ultrasonic system equipped with five oscillating units, consisting of a converter, booster and sonotrode, operating at either 20 or 35 kHz. The number of oscillating units can be adjusted depending on the volumetric flow to be treated, which can reach up to 2 m^3/h. Larger flow rates can be treated by increasing the number of ultrasonic modular systems used. Each oscillating unit is operated with a nominal power of 1 kW. In 2005, it was installed in the wastewater treatment plant in Meldorf (Germany) to overcome the issue of foaming formation observed in the wastewater treatment station, which is the result of massive growth of filamentous bacteria (*Microthrix parvicella*) in waste activated sludge [277]. ULTRAWAVES systems are used in many countries including Germany, Denmark, Italy, Austria, Great Britain, Netherlands, Hong Kong, China, Japan, USA, India, Australia, Brazil, etc. The Weber Entec DesiUS company has developed an ultrasonic system for large-scale use, which has been installed in many countries. The DesiUS system can provide a homogeneous cavitation field within a rectangular reactor (BioPush) via 6 surface ultrasonic transducers operating at 22 kHz placed on each side, yielding an overall 2,000 W ultrasound performance per ultrasonic reactor. Such systems can be multiplied and successively connected for enhanced treatment. Numerous wastewater treatment plants have installed DesiUS systems in countries such as Germany, Lithuania (**Figure 26b**), Switzerland (**Figure 26c**), Italy, Thailand, Russia and Singapore. The VTA GSD ultrasonic system was developed and patented by

Austrian *VTA* group (https://vta.cc/en). It is focused on the ultrasonic treatment using ultrasonic oscillators with low energy usage. The device consists of a container having a mechanical agitator and rod-shaped ultrasound transmitters, operating at 25 kHz, which are parallel to the axis of the container. The VTA GSD system has been applied in wastewater treatment plants in Austria, Germany, Italy, Lithuania, France, Swiss, Spain, South Korea (**Figure 26d**), Belgium and Poland. Sonix technology developed by the UK company Sonico has been used worldwide in wastewater treatment stations for sludge disintegration. Unlike block or probe-based horns, the Sonix radial horn is designed specifically to vibrate and form a focused effective zone of cavitation for enhanced cell lysis (**Figure 26e**).

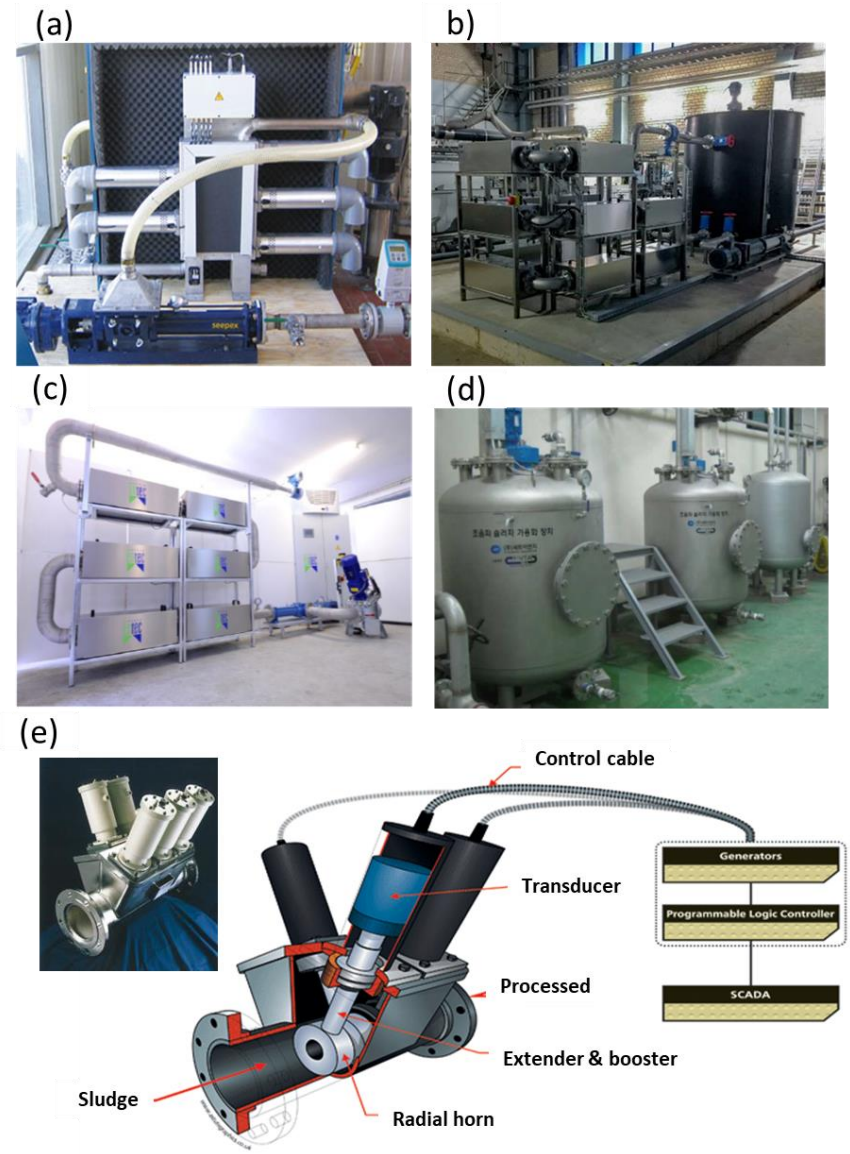

Figure 26. Ultrasound technology at large scale in wastewater treatment plants. (a) Installation of a high-output ULTRAWAVES reactor in a wastewater treatment plant in Germany, (b) Weber Entec DesiUS plan equipped with 14 sonoreactors installed in a wastewater treatment plant in Lithuania. (c) Weber Entec DesiUS with 2 kW U ultrasound power was integrated at a Swiss wastewater treatment plant. (d) VTA GSD plan installed in a wastewater treatment plant in South Korea. (e) Sonix technology developed by the UK company Sonico for large scale ultrasonic sludge treatment.

5.2 Ultrasound in synthesis

Over the last two decades, ultrasound-assisted syntheses of chemical products and (nano)-materials have been widely used in different research topics. The mechanisms and basics of sonochemical materials syntheses and ultrasound-assisted organic syntheses are discussed by Suslick and coworkers [3] and by Banerjee [18], respectively. Some of these approaches have been successfully translated to large-scale applications. For example, sonocrystallization technology has already been applied by leading pharmaceutical companies: for instance, Pfizer Global Manufacturing implemented in 2008 a Prosonix Prosonitron reactor based on sonocrystallization technology at its manufacturing facilities in Ireland. **Figure 27** shows a large-scale setup for the US-assisted antisolvent crystallization of active principal ingredients (DISCUS, Prosonix), used to promote efficient solute / solvent diffusion into the antisolvent and the formation of micro-crystals. The Prosonix technology has also been applied by UCB Pharma (Major Pharma) at pilot scale for sonocrystallization control of shape, size and polymorph, and it has been operated by Alcoa World Alumina and Aughinish Alumina (Glencore) as large-scale continuous sonocrystallizer. In the case of the latter, over 2 years continuous operation in aggressive conditions were reported by the manufacturer. The Prosonix Prosonitron P500 HD and P750 HD are continuous sonoreactors providing radially-focused ultrasound using, respectively, 21 transducers (600 W, with a 4.4 L sonicated volume) and 42 transducers (1200 W, 8.2 L sonicated volume).

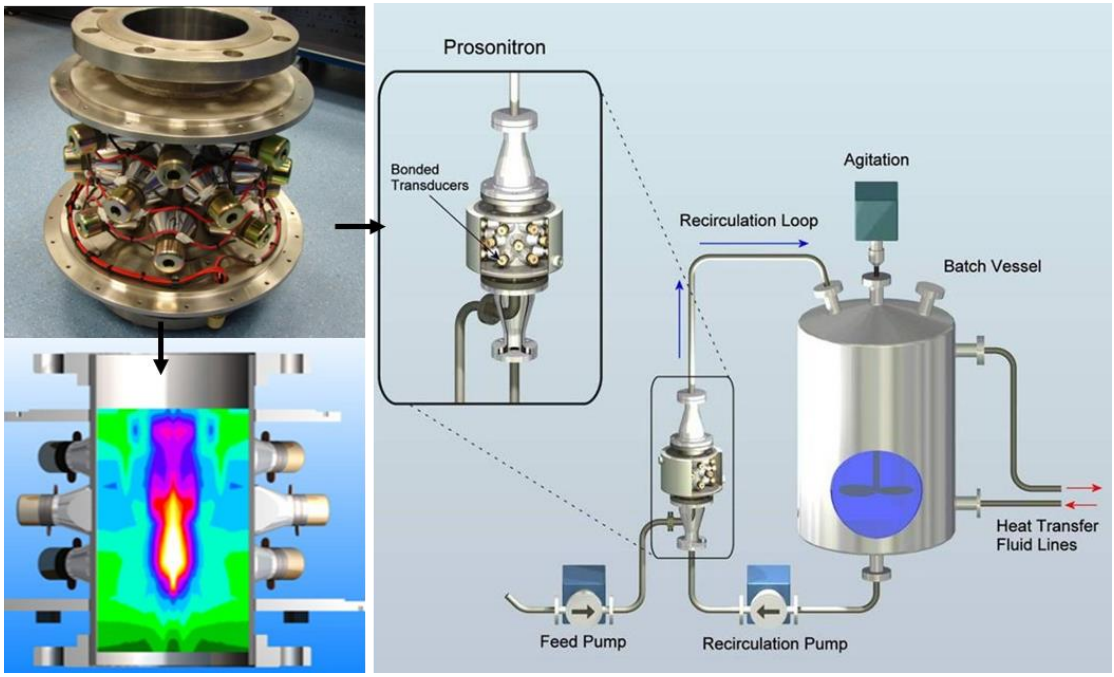

Figure 27. Scheme of the DISCUS antisolvent sonocrystallization process with an image of the Prosonitron P750 HD and cavitation mapping performed by an NPL acoustic sensor.

Another application that was applied commercially was ultrasound-assisted desulfurization, hydrogenation of crude oil and other oil related products by SulphCo, as an alternative to conventional HDS (Hydro-Desulphurization) unit. The first commercial continuous unit for ultrasonic desulfurization of diesel fuel was installed at the IPLOM petroleum refinery (Genoa, Italy), with a capacity of up to 350 barrels per day [320]. Ultrasound enhances mass transfer, also in heterogeneous systems, and can be used to carry out reactions between immiscible reactants, by promoting the formation of extremely fine emulsions, which in turn accelerates the interface reaction. For instance, ultrasound has been used to promote mass transfer in transesterification reactions during biodiesel production [321].

5.3 Ultrasound-assisted extraction

Ultrasound-assisted extraction has shown numerous benefits in terms of efficiency, ease of operation, short time, lower solvent consumption, and use of ambient temperature allowing the extraction of heat-sensitive molecules [322-326].

Several mechanistic pathways could take place in ultrasound-assisted extraction such as fragmentation, erosion, sonocapillary effect, sonoporation, local shear stress and detexturation, as discussed in detail by Chemat et al. [45]. To achieve more violent bubble implosions for enhanced extraction, most studies have employed low frequencies in extraction systems (in the 20-60 kHz range). The size of bubbles can significantly affect the extraction yield. However, not only bubble size should be controlled but also the surface and internal mass transfer processes, which depend on operating conditions such as ultrasound frequency, time, temperature, solvent, nature/morphology of the materials, etc [327].

Commercial solutions are already present for ultrasound-assisted extraction at both the lab-scale and large-scale. In this respect, Hielscher company commercializes ultrasonic processors coupled with flow cells that have a stated processing capacity for cell extraction up to a 12 m^3/hr flow rate. Giotti, an Italian company, prepares spices extract by ultrasound-assisted cold extraction. Traditional herb extracts are also obtained by ultrasound-assisted extraction at Italian based companies G. Mariani & C. Spa and Euphytos, the latter using REUS apparatus. Le Herbe company uses Qsonica sonicators during extraction for the preparation of Cannabis beverages.

Recently, a combined approach coupling an ultrasonic pretreatment to traditional enzymolysis has shown promise to enhance the bioactivity, enzyme hydrolysis and protein conversion during the extraction of active ingredients (such as phytochemical, antioxidants) from agro-food residues and waste [328]. Enzymolysis is a general term that covers extraction, separation and purification processes involving biological compounds. Enzymolysis suffers from low substrate conversion rates, minimal utilization of enzyme, and long reaction time. Ultrasonic-assisted enzymolysis takes advantage of the thermal and mechanical effects of acoustic cavitation to improve mass transfer efficiency and enhance substrate and enzyme diffusion. Furthermore, the

physical and chemical effects of cavitation lead to protein denaturation, facilitating the binding of enzymes to the substrate, thereby enhancing the enzymolysis efficiency. This technique has been applied to the modification and extraction of proteins [329-331] , starch [332], carbohydrate[333] soybean isoflavones [334] and other plant materials [335,336].

5.4 Ultrasound in food industry

In food industry, the application of ultrasonic process has been considered as alternative to conventional food processing systems or to boost/assist the conventional systems for enhanced and rapid food possessing technologies[337]. High intensity ultrasound at frequencies between 20 and 500 kHz have been instead used to induce effects on the physical, mechanical or chemical/biochemical properties of foods, including extraction of functional ingredients (e.g., aroma), controlling the crystallization of sugars, ice and fats [338], enzyme and microbial inactivation [339], mixing [340], antifoaming [252], fermentation [341], encapsulation [342], biosynthesis [343], cutting [344], drying [345], meat processing [346], liquid foods processing [347], sterilization [348] and so on. In general, the application of ultrasonic systems in food industry can lead to fast reproducibility, high purity and safety, lower cost, and avoiding the long treatment and washing of food products [349-351]. The interested reader can find more information about the mechanisms involved in these processes and applications to the food industry in the reviews by Chemat et al. [352] and Awad et. [353].

As discussed in Sections 2.2.5 and 2.3.4, ultrasound irradiation can cause degassing when bubbles growth continues until a size sufficiently large is reached to allow them to rise up through the liquid, against gravity. Foam control and deaeration commercial solutions for industrial scale operation are provided by Cavitus (Switzerland) and Pusonics (Spain). Pusonics defoaming technologies are based on airborne stepped-plate transducers: they can be fitted for defoaming at canning lines operating at speeds as high as 20 cans/s, or as rotating defoaming systems based on a single 300 W plate-transducer suitable for 6-m cylindrical reactors, resulting in defoaming rates of 10-40 m^3/h with an energy consumption lower than $30W \cdot h/m^3$. The Gen2T self-cooled foam

control system by Cavitus is made of aluminum with chemical resistant surface coating (ALTEF®) and high grade stainless steel, and it is equipped with a solid titanium sonotrode operating at 20 kHz and 1.2 kW; the unit is suitable for carbonated soft drink lines up to 96,000 units per hour and beer can lines up to 120,000 (**Figure 28**).

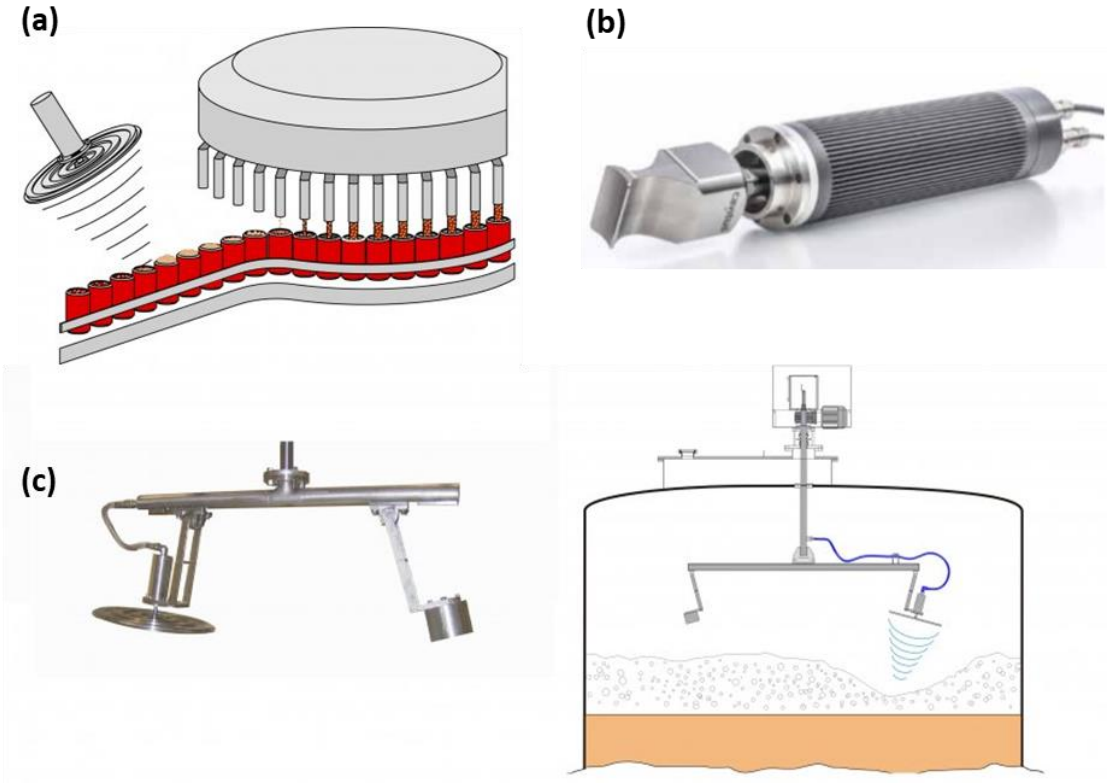

Figure 28. a) Ultrasonic defoaming of canning line by Pusonics; b) Cavitus Gen2T self-cooled foam control; c) UDS driven by a rotary system and scheme of a reactor with rotating defoaming system.

Another area of application of ultrasound is the preparation of food emulsions. Emulsification requires the dispersion of two immiscible liquids, which generally requires the use of large amounts of energy and the addition of stabilizers (such as surfactants) to increase the emulsion shelf life. During ultrasonic emulsification, the physical effects induced by cavitation provide sufficient mixing between the two immiscible phases, resulting in very fine and highly stable emulsions, with a relatively low energy input.

In the classical works by Li and Fogler, [354,355] acoustic emulsification was described as a two-stage phenomenon. Acoustic waves disrupt the stability of the oil-water interface

(Rayleigh-Taylor instability), causing the formation of dispersed phase droplets into the continuous medium. In the second phase, shockwaves created by imploding cavitation bubbles, break-up the dispersed drops into smaller droplets. The final mean droplet size and the distribution depend on combined effect of shear rate, due to acoustic cavitation, and of emulsion rheology, which is related to the physicochemical properties of the emulsion components [356].

Ultrasound-based emulsification has a series of advantages with respect to mechanical methods: emulsions prepared by sonication are characterized by a smaller droplet size and narrower size distribution, they are more stable [357] and lower amounts of stabilizers are needed. By a careful selection of the emulsion components and ultrasound power, transparent edible nanoemulsions with 40 nm droplets have been reported [358]. Recently, Li et al. compared the emulsification effectiveness and energy efficiency of ultrasonic emulsification and high-pressure homogenization, showing that the ultrasonic system uses less electrical energy in lab-scale equipment and remains competitive also taking up-scaling factors into consideration [359]. Studies at pilot scale operation have been reported [360,361], showing better emulsification efficiency of low volume batch systems over continuous flow systems.

Ultrasonic emulsification has been applied to produce food-grade emulsions for the delivery of active components [362,363] and as a homogenization step to improve the quality of emulsified products, such as milk [364]. During ultrasonic emulsification, the chemical effects of cavitation can give rise to lipid oxidation, resulting in metallic and rancid odor [365,366], and deterioration of the milk product. This issue can be limited by properly addressing the oxidation initiation factors: the degradation extent can be reduced by using low frequencies and the lowest possible energy and irradiation time, avoiding prolonged exposure of the emulsion to high temperature and light, selecting starting materials (e.g., oils) with minimum radicals and impurity concentrations, and limiting the horn erosion, as release particles may trigger oxidation reactions. On the other hand, the combination of physical and chemical effects offered by ultrasound can be usefully applied to emulsification processes where radical formation is an added-value, such as emulsion polymerization and nutrient encapsulation.

6. Sustainability and energy challenges

Sonoprocessing technology offers significant advantages over selected conventional processes. The advantages include the use of less or no toxic solvents (greener processing), less or no heat (non-thermal processing), low energy consumption (sustainable processing) and easy scalability (viability). There are still significant challenges remaining when considering the scalability and commercialization of the technology.

For instance, the application of ultrasound to the synthesis of compounds and materials provides increased selectivity, often with the use of less hazardous solvents and in catalyst-free conditions, reducing reaction time and associated energy costs [19]. In sonocrystallisation processes, the addition of antisolvents can be avoided. In pharmaceutical processes, more active polymorphs are generated by ultrasound-assisted crystallization process. Another example is ultrasound-assisted extraction (UAE): Ultrasound-based extraction represents a greener alternative to solvent-extraction and maceration, both in terms of volumes of toxic chemicals, time and energy costs. Chemat et al. [45] compared the energy costs for the extraction of fat and oil from 50 g of oleaginous seeds using maceration at hexane boiling point (6 kWh), Soxhlet (8 kWh) and ultrasound-assisted extraction (0.25 kWh); the advantage of sonoprocessing is clear also in terms of the relative CO_2 emission, accounting for 6400, 3600 and 200 g of emitted CO_2 per 100 g of extracted solid material for maceration, Soxhlet and ultrasound-assisted extraction, respectively.

The successful implementation of sonoprocessing for various large scale processes strongly depends on the economical aspect, which is closely related to the process efficiency. The cost of sonoprocessing includes both capital expenses, for instance cost of the reactor, acoustic insulation of the reactors for noise protection[36], durability of the reactor, etc. and operational costs that are largely dependent on energy consumption. Costs associated with the periodic replacement of the transducers should also be considered. In some cases (*e.g.*, extraction, cell disintegration systems), ultrasound-based techniques have proven very competitive with established technologies, with

return on investment period in the order of few months to years. Ultrasound-based technology has also provided a strong economic business case in a number of food processing applications, with return on investment that can take less than 1 year [349]. For instance, ultrasound-induced defoaming by rotary transducers in large-scale fermenters was reported to reduce by 25% the amount of antifoam agents, corresponding to a daily saving of ca. 375 L of antifoam chemical, leading to a cost saving of about 3000 $/day [342].

On the contrary, in some applications, uncompetitive or mixed results have been reported. For instance, Li et al. [359] recently compared the energy costs of high-pressure homogenization and of ultrasound-assisted emulsification for the preparation of nanoemulsions: sonoprocessing showed higher energy efficiency than high-pressure homogenization at laboratory-scale, and it remained competitive also when scale-up was taken into consideration. On the contrary, wastewater treatment by sonolysis has so far proven uncompetitive, due to the low efficiency of conversion of electrical energy into cavitation energy particularly in large-scale reactors [367]. The highest pollutant degradation efficiencies are generally observed for solution volumes from 0.1 L to 10 L [368], while a further increase of the reactor volume rapidly decreases the process efficiency, due to acoustic wave attenuation by the bulk of the liquid. In order to retain the effectiveness of the treatment in large reactors, the number of transducers must be increased, increasing the investment and operating costs. Mahamuni and Adewuyi[10] estimated a capital cost of 40 million USD for the sole ultrasonic equipment required for a unit able to treat 1000 L min^{-1} of phenol-containing effluent with a 90% oxidation efficiency. These considerations highlight the need, for industrial operation, of further studies on the optimization of the distribution of cavitation areas within large-scale sonochemical reactors through the design of sonotrodes/transducers as well as of the reactor configurations. Particularly promising for scale-up are continuous flow configurations that enable to treat large volumes in time.

For some applications, the use hydrodynamic cavitation instead of acoustic cavitation or the combination of sonoprocessing with other technologies (hybrid processes) may be beneficial. For instance, the combination of sonochemistry with other advanced

oxidative processes for purification of water and wastewaters has shown promising results. Mahamuni and Adewuyi[10] compared the cost of treatment of 1000 L of phenol-containing wastewater, calculated by dividing the total annual operating cost (i.e., the sum of the annual operating and maintenance cost and annual capital cost) with the amount of liters of wastewater treated in a year, assuming that the plant was running throughout the year continuously: they showed up to 100-fold decrease in costs (4100 USD and 37 USD for sonolysis and sono-Fenton process, respectively) and an over 70-fold decrease in the treatment time when combined processes were employed instead of simple sonolysis. In this respect, further investigations are needed to develop new hybrid processes to overcome the hurdles associated with the reactor design, energy efficiency and economic/social benefits.

7. Conclusions and future perspective

Ultrasound-induced cavitation can result in significant benefits for both lab-scale processes and industrial operations. Cavitation is a complex phenomenon, influenced by numerous operating, environmental and geometrical parameters, resulting in non-uniform acoustic fields and complex flow patterns within sonochemical reactors. In order to achieve reproducibility in laboratory-scale set-ups and scalability and cost-effectiveness in industrial-scale operations, it is of pivotal importance to understand the role of each individual parameter and characterize the cavitation activity within the reactor. Fundamental research on laboratory-scale systems has provided useful guidelines to understand and optimize larger and more complex configurations. The available sonotrodes and reactor systems have greatly expanded and tailored solutions for different applications can be found.

Although there are now numerous examples of successful ultrasound-based technologies that have been transferred to real applications, further investigations must be considered from both the scientific and industrial communities for further expanding ultrasound usage, especially at large scale. Ultrasound is indeed a relatively recent technology when it comes to its application for chemical and physical processing.

In terms of fundamental studies at laboratory scale, the geometrical aspects of the used sonochemical reactor should always be reported, as well as a characterization of cavitational activity within the reactor. Unfortunately, these aspects are often missing in literature studies, especially on non-specialist journals, limiting the comparability between different set-ups.

Despite we gathered the available information and provide recommendations on how to use analytical tools to harness ultrasound potential, the state-of-the-art to characterize the full range of ultrasound chemical and physical effects is limited as it is being developed.

We therefore anticipate and encourage the following techniques to be incorporated in the study and optimization of the design of both laboratory- and industrial scale reactors:

- Consider applying ultrasound emitters with frequencies other than the commercially available 20-40 kHz for selected applications such as chemical synthesis and pollutant degradation in wastewater treatment. The recommended ones are from few hundreds of kHz to 1 MHz for these applications. Indeed, both chemical (radicals) and physical effects (mass transfer) enacted by ultrasound seem to have a beneficial role in the applications mentioned above, and localized effects rather than macroscopically distributed elevated acoustic pressure leads to best results. We recommend frequencies for different applications in section 2.2.1. This requires interfacing with companies specialized in manufacturing acoustic emitters to machine piezoelectric components emitting at specific frequencies as equipment operating from hundreds of kHz to 1 MHz is not usually available over the counter.
- Identify the resonance frequency(ies) of a reactor with the aid of computational fluid dynamics software to maximize acoustic pressure zones inside the reactor and select appropriate ultrasound emitter frequency and geometry. This type of study has major limitations as the number of possible geometries and operating variables is nearly infinite as it involves, besides frequency, power, signal type and duty cycle (section 2.2.3): vessel/transducer diameter ratio, number and position of transducers, shape of the reactor. The computational time required may be another impediment and could reach several days. We recommend defining a type of

emitter(s) (either horn or plate) and their number and possibly location inside the reactor basing on pre-established process economics. These latter should be based on data collected with laboratory available equipment, which has its inherent limitations. Building the equipment at specific resonant frequencies also requires interfacing with companies specialized in manufacturing customized acoustic emitters.

- Computational methods combined with particle image velocimetry can be used to analyse high-speed imaging sequences for the characterization of acoustically-generated bubbles and their position in a sonochemical reactor to maximize both chemical and physical effects. This method limits to transparent media and requires specialized and expensive equipment tailored to the geometry of the ultrasound emitter and reactor.
- Physical methods such as calorimetry, temperature, and pressure (through hydrophones) mapping, and aluminum foil erosion may be adopted for a simple characterization of ultrasound reactors (section 3.1). These methods are normally easy to implement and require relatively inexpensive equipment. The electro-diffusional method determines the mass transfer coefficients relative to cavitation activity. The main limitation of these techniques is the possible damage ultrasound shock waves and bubble implosion may cause to the temperature and pressure probes. Protection sleeves can obviate the problem.
- Sonoluminescence and sonochemiluminescence imaging techniques (section 3.1), which are as well physical methods, may be used for characterizing cavitation bubble field. Sonoluminescence and sonochemiluminescence offer a semi-quantitative measure and visualize the extent of acoustic cavitation. Once again, these techniques are limited to transparent media.
- Characterize acoustic activity (quantify acoustically-generated radicals) in the reaction medium through chemical dosimetry (section 3.2.1). While there are several methods available for the quantification of ˙OH radicals in aqueous solutions, simple techniques to determine other radical types are still lacking. However, electron paramagnetic resonance (EPR) spectroscopy together with spin-

trapping agents appears suitable to identify and quantify organic radicals. The number of radical generated is a direct outcome of the temperature and pressure of collapse of the acoustically generated bubbles, which in turn depends on the composition of the system and the ultrasound operating variables (frequency, power, signal type and duty cycle), as well as reactor geometry. We recommend mapping acoustic activity for each system at a fixed composition, frequency and optimal power. Similarly, for ultrasound horn emitters, we recommend characterizing acoustic activity while changing the emitter immersion depth.

- Pursue research to find piezoelectric or magnostrictive transducer materials, as well as emitter and reaction geometries that minimize erosion and corrosion. This is unfortunately a major impediment to a more wide-spread commercial adoption of ultrasound technologies. It indeed directly impacts the process economics as it requires specialized personnel to perform regular maintenance or replace the parts damaged, as well as it involves reactor shut-down or purchasing back-up equipment.
- Consider altering the composition of the medium through (section 2.3): solvent selection – viscosity, vapor pressure and surface tension; temperature; static pressure; type and concentration of dissolved gases; type and concentration of salts; type and concentration of suspended solids and surfactants. All these elements have a role in determining physical and chemical effects of ultrasound and enhancing them.
- Consider continuous reactors (section 4.2) instead of batch reactors (section 4.1) when designing experiments at a laboratory scale, including ultrasound microreactors, to generate data of industrial interest and to prompt wide-spread application of ultrasound equipment at a commercial scale. Both batch and continuous reactors can be designed with multiple emitters operating each at different frequencies, in order to select the one(s) that suits different applications.
- Perform energy and techno-economic calculations for each target application: as we highlighted in section 6, several challenges remain when considering the scalability and commercialization of ultrasound as a technology.

References

(1) Crum, L. Acoustic cavitation series: part five rectified diffusion. *Ultrasonics* **1984,** *22* (5), 215.

(2) Wood, R. J.; Lee, J.; Bussemaker, M. J. A parametric review of sonochemistry: control and augmentation of sonochemical activity in aqueous solutions. *Ultrason Sonochem* **2017,** *38*, 351.

(3) Xu, H.; Zeiger, B. W.; Suslick, K. S. Sonochemical synthesis of nanomaterials. *Chem. Soc. Rev.* **2013,** *42* (7), 2555.

(4) Barber, B. P.; Hiller, R. A.; Löfstedt, R.; Putterman, S. J.; Weninger, K. R. Defining the unknowns of sonoluminescence. *Phys. Rep.* **1997,** *281* (2), 65.

(5) Schanz, D.; Metten, B.; Kurz, T.; Lauterborn, W. Molecular dynamics simulations of cavitation bubble collapse and sonoluminescence. New J. Phys. **2012,** *14* (11), 113019.

(6) Yasui, K. Effect of volatile solutes on sonoluminescence. *J. Chem. Phys.* **2002,** *116* (7), 2945.

(7) Flannigan, D. J.; Suslick, K. S. Plasma formation and temperature measurement during single-bubble cavitation. *Nature* **2005,** *434* (7029), 52.

(8) Flannigan, D. J.; Hopkins, S. D.; Camara, C. G.; Putterman, S. J.; Suslick, K. S. Measurement of pressure and density inside a single sonoluminescing bubble. Phys. Rev. Lett **2006,** *96* (20), 204301.

(9) Suslick, K. S.; Flannigan, D. J. Inside a collapsing bubble: sonoluminescence and the conditions during cavitation. *Annu. Rev. Phys. Chem.* **2008,** *59*, 659.

(10) Mahamuni, N. N.; Adewuyi, Y. G. Advanced oxidation processes (AOPs) involving ultrasound for waste water treatment: a review with emphasis on cost estimation. *Ultrason Sonochem* **2010,** *17* (6), 990.

(11) Gao, Y.; Wu, M.; Lin, Y.; Xu, J. Trapping and control of bubbles in various microfluidic applications. *Lab on a Chip* **2020,** *20* (24), 4512.

(12) Kim, H. N.; Suslick, K. S. Sonofragmentation of Organic Molecular Crystals vs Strength of Materials. *J. Org. Chem.* **2021**, XXXX, XXX, XXX-XXX

(13) Sander, J. R.; Zeiger, B. W.; Suslick, K. S. Sonocrystallization and sonofragmentation. *Ultrason Sonochem* **2014,** *21* (6), 1908.

(14) Weissler, A. Cavitation in ultrasonic depolymerization. *J. Acoust. Soc. Am.* **1951,** *23* (3), 370.

(15) Ruecroft, G.; Hipkiss, D.; Ly, T.; Maxted, N.; Cains, P. W. Sonocrystallization: the use of ultrasound for improved industrial crystallization. *Org. Process Res. Dev.* **2005,** *9* (6), 923.

(16) Li, H.; Li, H.; Guo, Z.; Liu, Y. The application of power ultrasound to reaction crystallization. *Ultrason Sonochem* **2006,** *13* (4), 359.

(17) Valoppi, F.; Salmi, A.; Ratilainen, M.; Barba, L.; Puranen, T.; Tommiska, O.; Helander, P.; Heikkilä, J.; Haeggström, E. Controlling oleogel crystallization using ultrasonic standing waves. *Sci. Rep.* **2020,** *10* (1), 1.

(18) Banerjee, B. Recent developments on ultrasound assisted catalyst-free organic synthesis. *Ultrason Sonochem* **2017,** *35*, 1.
(19) Sancheti, S. V.; Gogate, P. R. A review of engineering aspects of intensification of chemical synthesis using ultrasound. *Ultrason Sonochem* **2017,** *36*, 527.
(20) Boffito, D. C.; Leveque, J.-M.; Pirola, C.; Bianchi, C.; Vibert, R.; Perrier, A.; Patience, G. In *Production of Biofuels and Chemicals with Ultrasound*; Springer, 2015.
(21) Patience, N. A.; Galli, F.; Rigamonti, M. G.; Schieppati, D.; Boffito, D. C. Ultrasonic intensification to produce diester biolubricants. *Ind. Eng. Chem. Res.* **2019,** *58* (19), 7957.
(22) Thompson, L. H.; Doraiswamy, L. Sonochemistry: science and engineering. *Ind. Eng. Chem. Res.* **1999,** *38* (4), 1215.
(23) Bianchi, C.; Carli, R.; Lanzani, S.; Lorenzetti, D.; Vergani, G.; Ragaini, V. A new method to prepare highly dispersed supported metal catalysts. *Catal. Lett.* **1993,** *22* (4), 319.
(24) Djellabi, R.; Yang, B.; Sharif, H. M. A.; Zhang, J.; Ali, J.; Zhao, X. Sustainable and easy recoverable magnetic TiO_2-Lignocellulosic Biomass@Fe_3O_4 for solar photocatalytic water remediation. *J. Clean. Prod.* **2019,** *233*, 841.
(25) Bianchi, C.; Carli, R.; Lanzani, S.; Lorenzetti, D.; Vergani, G.; Ragaini, V. Influence of ultrasound on the preparation of ruthenium catalysts supported on alumina. *Ultrason Sonochem* **1994,** *1* (1), S47.
(26) Schieppati, D.; Galli, F.; Peyot, M.-L.; Yargeau, V.; Bianchi, C.; Boffito, D. An ultrasound-assisted photocatalytic treatment to remove an herbicidal pollutant from wastewaters. *Ultrason Sonochem* **2019,** *54*, 302.
(27) Stucchi, M.; Elfiad, A.; Rigamonti, M.; Khan, H.; Boffito, D. Water treatment: Mn-TiO_2 synthesized by ultrasound with increased aromatics adsorption. *Ultrason Sonochem* **2018,** *44*, 272.
(28) Stucchi, M.; Bianchi, C.; Pirola, C.; Vitali, S.; Cerrato, G.; Morandi, S.; Argirusis, C.; Sourkouni, G.; Sakkas, P.; Capucci, V. Surface decoration of commercial micro-sized TiO_2 by means of high energy ultrasound: A way to enhance its photocatalytic activity under visible light. *Appl. Catal. B* **2015,** *178*, 124.
(29) Zhang, M.; Shang, Q.; Wan, Y.; Cheng, Q.; Liao, G.; Pan, Z. Self-template synthesis of double-shell TiO_2@ZIF-8 hollow nanospheres via sonocrystallization with enhanced photocatalytic activities in hydrogen generation. *Appl. Catal. B* **2019,** *241*, 149.
(30) Haque, E.; Khan, N. A.; Park, J. H.; Jhung, S. H. Synthesis of a metal–organic framework material, iron terephthalate, by ultrasound, microwave, and conventional electric heating: a kinetic study. *Chem. Eur. J.* **2010,** *16* (3), 1046.
(31) Meroni, D.; Gasparini, C.; Di Michele, A.; Ardizzone, S.; Bianchi, C. L. Ultrasound-assisted synthesis of ZnO photocatalysts for gas phase pollutant remediation: Role of the synthetic parameters and of promotion with WO_3. *Ultrason Sonochem* **2020,** *66*, 105119.

(32) Djellabi, R.; Yang, B.; Xiao, K.; Gong, Y.; Cao, D.; Sharif, H. M. A.; Zhao, X.; Zhu, C.; Zhang, J. Unravelling the mechanistic role of Ti-O-C bonding bridge at titania/lignocellulosic biomass interface for Cr(VI) photoreduction under visible light. *J. Colloid Interface Sci.* **2019,** *553, 409-417.*.

(33) Jung, S.-H.; Oh, E.; Lee, K.-H.; Yang, Y.; Park, C. G.; Park, W.; Jeong, S.-H. Sonochemical preparation of shape-selective ZnO nanostructures. *Cryst. Growth Des.* **2008,** *8* (1), 265.

(34) Gogate, P. R. Improvements in catalyst synthesis and photocatalytic oxidation processing based on the use of ultrasound. *Heterogeneous Photocatalysis* **2020**, 71-105.

(35) Babu, S. G.; Ashokkumar, M.; Neppolian, B. The role of ultrasound on advanced oxidation processes. *Sonochemistry* **2017**, 117-148.

(36) Gągol, M.; Przyjazny, A.; Boczkaj, G. Wastewater treatment by means of advanced oxidation processes based on cavitation–a review. *Chem. Eng. J.* **2018,** *338: 599-627.*.

(37) Ragaini, V.; Selli, E.; Bianchi, C. L.; Pirola, C. Sono-photocatalytic degradation of 2-chlorophenol in water: kinetic and energetic comparison with other techniques. *Ultrason Sonochem* **2001,** *8* (3), 251.

(38) Selli, E.; Bianchi, C. L.; Pirola, C.; Bertelli, M. Degradation of methyl tert-butyl ether in water: effects of the combined use of sonolysis and photocatalysis. *Ultrason Sonochem* **2005,** *12* (5), 395.

(39) Damiri, F.; Dobaradaran, S.; Hashemi, S.; Foroutan, R.; Vosoughi, M.; Sahebi, S.; Ramavandi, B.; Boffito, D. C. Waste sludge from shipping docks as a catalyst to remove amoxicillin in water with hydrogen peroxide and ultrasound. *Ultrason Sonochem* **2020,** *68*, 105187.

(40) Khani, Z.; Schieppati, D.; Bianchi, C. L.; Boffito, D. C. The sonophotocatalytic degradation of pharmaceuticals in water by mnox-TiO_2 systems with tuned band-gaps. *Catalysts* **2019,** *9* (11), 949.

(41) Löning, J.-M.; Horst, C.; Hoffmann, U. Investigations on the energy conversion in sonochemical processes. *Ultrason Sonochem* **2002,** *9* (3), 169.

(42) Theerthagiri, J.; Madhavan, J.; Lee, S. J.; Choi, M. Y.; Ashokkumar, M.; Pollet, B. G. Sonoelectrochemistry for energy and environmental applications. *Ultrason Sonochem* **2020,** *63*, 104960.

(43) Capote, F. P.; De Castro, M. L. Ultrasound in analytical chemistry. *nal. Bioanal. Chem.* **2007,** *387* (1), 249.

(44) Banks, C. E.; Compton, R. G. Ultrasound: promoting electroanalysis in difficult real world media. *Analyst* **2004,** *129* (8), 678.

(45) Chemat, F.; Rombaut, N.; Sicaire, A.-G.; Meullemiestre, A.; Fabiano-Tixier, A.-S.; Abert-Vian, M. Ultrasound assisted extraction of food and natural products. Mechanisms, techniques, combinations, protocols and applications. A review. *Ultrason Sonochem* **2017,** *34*, 540.

(46) Bindes, M. M. M.; Reis, M. H. M.; Cardoso, V. L.; Boffito, D. C. Ultrasound-assisted extraction of bioactive compounds from green tea leaves and

clarification with natural coagulants (chitosan and Moringa oleífera seeds). *Ultrason Sonochem* **2019,** *51*, 111.

(47) Boffito, D.; Galli, F.; Pirola, C.; Bianchi, C.; Patience, G. Ultrasonic free fatty acids esterification in tobacco and canola oil. *Ultrason Sonochem* **2014,** *21* (6), 1969.

(48) Boffito, D.; Crocellà, V.; Pirola, C.; Neppolian, B.; Cerrato, G.; Ashokkumar, M.; Bianchi, C. Ultrasonic enhancement of the acidity, surface area and free fatty acids esterification catalytic activity of sulphated ZrO_2–TiO_2 systems. *J. Catal.* **2013,** *297*, 17.

(49) Kiss, A. A.; Geertman, R.; Wierschem, M.; Skiborowski, M.; Gielen, B.; Jordens, J.; John, J. J.; Van Gerven, T. Ultrasound ‐ assisted emerging technologies for chemical processes. *J. Chem. Technol. Biotechnol* **2018,** *93* (5), 1219.

(50) Boffito, D. C.; Galli, F.; Martinez, P. R.; Pirola, C.; Bianchi, C.; Patience, G. Transesterification of triglycerides in a new ultrasonic-assisted mixing device. **2015,** 427-432.

(51) Boffito, D. C.; Galli, F.; Pirola, C.; Patience, G. S. CaO and isopropanol transesterify and crack triglycerides to isopropyl esters and green diesel. *Energy Convers. Manag.* **2017,** *139*, 71.

(52) Fang, Y.; Yamamoto, T.; Komarov, S. Cavitation and acoustic streaming generated by different sonotrode tips. *Ultrason Sonochem* **2018,** *48*, 79.

(53) Panda, D.; Saharan, V. K.; Manickam, S. Controlled hydrodynamic cavitation: A review of recent advances and perspectives for greener processing. *Processes* **2020,** *8* (2), 220.

(54) Pétrier, C.; Gondrexon, N.; Boldo, P. ultrasons et sonochimie, techniques de l'ingénieur chimie verte: optimisation des modes de séparation. *D'activation Et De Synthèse Base Documentaire: Tıb493duo* **2008**.

(55) Ashokkumar, M. In *Ultrasonic synthesis of functional materials*; Springer, 2016.

(56) Toegel, R.; Gompf, B.; Pecha, R.; Lohse, D. Does water vapor prevent upscaling sonoluminescence? *Phys. Rev. Lett.* **2000,** *85* (15), 3165.

(57) Yasui, K. Effect of liquid temperature on sonoluminescence. *Phys. Rev. E* **2001,** *64* (1), 016310.

(58) Ashokkumar, M. The characterization of acoustic cavitation bubbles–an overview. *Ultrason Sonochem* **2011,** *18* (4), 864.

(59) Yasui, K.; Tuziuti, T.; Kozuka, T.; Towata, A.; Iida, Y. Relationship between the bubble temperature and main oxidant created inside an air bubble under ultrasound. *J. Chem. Phys.* **2007,** *127* (15), 154502.

(60) Koda, S.; Kimura, T.; Kondo, T.; Mitome, H. A standard method to calibrate sonochemical efficiency of an individual reaction system. *Ultrason Sonochem* **2003,** *10* (3), 149.

(61) Pétrier, C.; Francony, A. Ultrasonic waste-water treatment: incidence of ultrasonic frequency on the rate of phenol and carbon tetrachloride degradation. *Ultrason Sonochem* **1997,** *4* (4), 295.

(62) Jiang, Y.; Petrier, C.; Waite, T. D. Sonolysis of 4-chlorophenol in aqueous solution: effects of substrate concentration, aqueous temperature and ultrasonic frequency. *Ultrason Sonochem* **2006,** *13* (5), 415.
(63) Petrier, C.; Jeunet, A.; Luche, J. L.; Reverdy, G. Unexpected frequency effects on the rate of oxidative processes induced by ultrasound. *J. Am. Chem. Soc.* **1992,** *114* (8), 3148.
(64) Kanthale, P.; Ashokkumar, M.; Grieser, F. Sonoluminescence, sonochemistry (H2O2 yield) and bubble dynamics: frequency and power effects. *Ultrason Sonochem* **2008,** *15* (2), 143.
(65) Beckett, M. A.; Hua, I. Impact of ultrasonic frequency on aqueous sonoluminescence and sonochemistry. *J. Phys. Chem. A* **2001,** *105* (15), 3796.
(66) Mason, T. J.; Lorimer, J. P. *Applied sonochemistry: the uses of power ultrasound in chemistry and processing*; Wiley-Vch Weinheim, 2002.
(67) Kaur Bhangu, S.; Ashokkumar, M.; Lee, J. Ultrasound assisted crystallization of paracetamol: crystal size distribution and polymorph control. *Cryst. Growth Des.* **2016,** *16* (4), 1934.
(68) Kanthale, P. M.; Gogate, P. R.; Pandit, A. B. Modeling aspects of dual frequency sonochemical reactors. *Chem. Eng. J.* **2007,** *127* (1-3), 71.
(69) Matafonova, G.; Batoev, V. Dual-frequency ultrasound: Strengths and shortcomings to water treatment and disinfection. *Water Res.* **2020,** *182*, 116016.
(70) d'Auzay, S. d. L. R.; Blais, J.-F.; Naffrechoux, E. Comparison of characterization methods in high frequency sonochemical reactors of differing configurations. *Ultrason Sonochem* **2010,** *17* (3), 547.
(71) Rabiei, K.; Naeimi, H. Ultrasonic assisted synthesis of gem-dichloroaziridine derivatives using Mg/CCl4 under neutral conditions. *Ultrason Sonochem* **2015,** *24*, 150.
(72) Safari, J.; Javadian, L. Ultrasound assisted the green synthesis of 2-amino-4H-chromene derivatives catalyzed by Fe_3O_4-functionalized nanoparticles with chitosan as a novel and reusable magnetic catalyst. *Ultrason Sonochem* **2015,** *22*, 341.
(73) Dange, P.; Kulkarni, A.; Rathod, V. Ultrasound assisted synthesis of methyl butyrate using heterogeneous catalyst. *Ultrason Sonochem* **2015,** *26*, 257.
(74) Khan, N. R.; Jadhav, S. V.; Rathod, V. K. Lipase catalysed synthesis of cetyl oleate using ultrasound: optimisation and kinetic studies. *Ultrason Sonochem* **2015,** *27*, 522.
(75) Son, Y.; No, Y.; Kim, J. Geometric and operational optimization of 20-kHz probe-type sonoreactor for enhancing sonochemical activity. *Ultrason Sonochem* **2020,** *65*, 105065.
(76) van Iersel, M. M.; Benes, N. E.; Keurentjes, J. T. Importance of acoustic shielding in sonochemistry. *Ultrason Sonochem* **2008,** *15* (4), 294.
(77) Son, Y.; Lim, M.; Ashokkumar, M.; Khim, J. Geometric optimization of sonoreactors for the enhancement of sonochemical activity. *J. Phys. Chem. C* **2011,** *115* (10), 4096.

(78) Wu, X.; Zhang, X.; Zhao, S.; Gong, Y.; Djellabi, R.; Lin, S.; Zhao, X. Highly-efficient photocatalytic hydrogen peroxide production over polyoxometalates covalently immobilized onto titanium dioxide. *Appl Catal A-gen* **2020,** *591*, 117271.
(79) Demaerel, J.; Govaerts, S.; Paul, R. R.; Van Gerven, T.; De Borggraeve, W. M. Non-innocent probes in direct sonication: Metal assistance in oxidative radical CH functionalization. *Ultrason Sonochem* **2018,** *41*, 134.
(80) Dukane: https://www.dukane.com/
(81) Cravotto, G.; Boffa, L.; Mantegna, S.; Perego, P.; Avogadro, M.; Cintas, P. Improved extraction of vegetable oils under high-intensity ultrasound and/or microwaves. *Ultrason Sonochem* **2008,** *15* (5), 898.
(82) Cravotto, G.; Cintas, P. The combined use of microwaves and ultrasound: improved tools in process chemistry and organic synthesis. *Chem. Eur. J.* **2007,** *13* (7), 1902.
(83) Thangavadivel, K.; Okitsu, K.; Owens, G.; Lesniewski, P. J.; Nishimura, R. Influence of sonochemical reactor diameter and liquid height on methyl orange degradation under 200 kHz indirect sonication. *J. Environ. Chem. Eng.* **2013,** *1* (3), 275.
(84) Fukunaga, S.; Higashi, S.; Horie, T.; Sugiyama, H.; Kanda, A.; Hsu, T.-Y.; Tung, K.-L.; Taniya, K.; Nishiyama, S.; Ohmura, N. Effect of geometrical configuration of reactor on a ZrP nano-dispersion process using ultrasonic irradiation. *Ultrason Sonochem* **2019,** *52*, 157.
(85) Capelo, J.; Galesio, M.; Felisberto, G.; Vaz, C.; Pessoa, J. C. Micro-focused ultrasonic solid–liquid extraction (μFUSLE) combined with HPLC and fluorescence detection for PAHs determination in sediments: optimization and linking with the analytical minimalism concept. *Talanta* **2005,** *66* (5), 1272.
(86) Tudela, I.; Sáez, V.; Esclapez, M. D.; Díez-García, M. I.; Bonete, P.; González-García, J. Simulation of the spatial distribution of the acoustic pressure in sonochemical reactors with numerical methods: a review. *Ultrason Sonochem* **2014,** *21* (3), 909.
(87) Klima, J.; Frias-Ferrer, A.; González-García, J.; Ludvik, J.; Saez, V.; Iniesta, J. Optimisation of 20 kHz sonoreactor geometry on the basis of numerical simulation of local ultrasonic intensity and qualitative comparison with experimental results. *Ultrason Sonochem* **2007,** *14* (1), 19.
(88) Asakura, Y.; Nishida, T.; Matsuoka, T.; Koda, S. Effects of ultrasonic frequency and liquid height on sonochemical efficiency of large-scale sonochemical reactors. *Ultrason Sonochem* **2008,** *15* (3), 244.
(89) No, Y.; Son, Y. Effects of probe position of 20 kHz sonicator on sonochemical oxidation activity. *Jpn. J. Appl. Phys.* **2019,** *58* (SG), SGGD02.
(90) Mohod, A. V.; Gogate, P. R. Ultrasonic degradation of polymers: effect of operating parameters and intensification using additives for carboxymethyl cellulose (CMC) and polyvinyl alcohol (PVA). *Ultrason Sonochem* **2011,** *18* (3), 727.

(91) Laborde, J.-L.; Bouyer, C.; Caltagirone, J.-P.; Gérard, A. Acoustic cavitation field prediction at low and high frequency ultrasounds. *Ultrasonics* **1998,** *36* (1-5), 581.
(92) Little, C.; El-Sharif, M.; Hepher, M. The effect of solution level on calorific and dosimetric results in a 70 kHz tower type sonochemical reactor. *Ultrason Sonochem* **2007,** *14* (3), 375.
(93) Renaudin, V.; Gondrexon, N.; Boldo, P.; Pétrier, C.; Bernis, A.; Gonthier, Y. Method for determining the chemically active zones in a high-frequency ultrasonic reactor. *Ultrason Sonochem* **1994,** *1* (2), S81.
(94) Kojima, Y.; Imazu, H.; Nishida, K. Physical and chemical characteristics of ultrasonically-prepared water-in-diesel fuel: effects of ultrasonic horn position and water content. *Ultrason Sonochem* **2014,** *21* (2), 722.
(95) Ge, H.; Li, Y.; Chen, H. Ultrasonic cavitation noise in suspensions with ethyl cellulose nanoparticles. *J. Appl. Phys.* **2019,** *125* (22), 225301.
(96) Hallez, L.; Lee, J.; Touyeras, F.; Nevers, A.; Ashokkumar, M.; Hihn, J.-Y. Enhancement and quenching of high-intensity focused ultrasound cavitation activity via short frequency sweep gaps. *Ultrason Sonochem* **2016,** *29*, 194.
(97) Delacour, C.; Lutz, C.; Kuhn, S. Pulsed ultrasound for temperature control and clogging prevention in micro-reactors. *Ultrason Sonochem* **2019,** *55*, 67.
(98) Iida, Y.; Ashokkumar, M.; Tuziuti, T.; Kozuka, T.; Yasui, K.; Towata, A.; Lee, J. Bubble population phenomena in sonochemical reactor: II. Estimation of bubble size distribution and its number density by simple coalescence model calculation. *Ultrason Sonochem* **2010,** *17* (2), 480.
(99) Tuziuti, T.; Yasui, K.; Lee, J.; Kozuka, T.; Towata, A.; Iida, Y. Mechanism of enhancement of sonochemical-reaction efficiency by pulsed ultrasound. *J. Phys. Chem. A* **2008,** *112* (22), 4875.
(100) Casadonte Jr, D. J.; Flores, M.; Petrier, C. Enhancing sonochemical activity in aqueous media using power-modulated pulsed ultrasound: an initial study. *Ultrason Sonochem* **2005,** *12* (3), 147.
(101) Bussemaker, M. J.; Zhang, D. A phenomenological investigation into the opposing effects of fluid flow on sonochemical activity at different frequency and power settings. 1. Overhead stirring. *Ultrason Sonochem* **2014,** *21* (1), 436.
(102) Hatanaka, S.-i.; Mitome, H.; Yasui, K.; Hayashi, S. Multibubble sonoluminescence enhancement by fluid flow. *Ultrasonics* **2006,** *44*, e435.
(103) Pflieger, R.; Chave, T.; Vite, G.; Jouve, L.; Nikitenko, S. I. Effect of operational conditions on sonoluminescence and kinetics of H2O2 formation during the sonolysis of water in the presence of Ar/O2 gas mixture. *Ultrason Sonochem* **2015,** *26*, 169.
(104) Kojima, Y.; Asakura, Y.; Sugiyama, G.; Koda, S. The effects of acoustic flow and mechanical flow on the sonochemical efficiency in a rectangular sonochemical reactor. *Ultrason Sonochem* **2010,** *17* (6), 978.
(105) Waghmare, G. V.; Vetal, M. D.; Rathod, V. K. Ultrasound assisted enzyme catalyzed synthesis of glycerol carbonate from glycerol and dimethyl carbonate. *Ultrason Sonochem* **2015,** *22*, 311.

(106) Meroni, D.; Jiménez-Salcedo, M.; Falletta, E.; Bresolin, B. M.; Kait, C. F.; Boffito, D. C.; Bianchi, C. L.; Pirola, C. Sonophotocatalytic degradation of sodium diclofenac using low power ultrasound and micro sized TiO_2. *Ultrason Sonochem* **2020,** *67*, 105123.
(107) Vivekanand, P.; Wang, M.-L. Sonocatalyzed synthesis of 2-phenylvaleronitrile under controlled reaction conditions–A kinetic study. *Ultrason Sonochem* **2011,** *18* (5), 1241.
(108) Bansode, S. R.; Rathod, V. K. Ultrasound assisted lipase catalysed synthesis of isoamyl butyrate. *Process Biochem* **2014,** *49* (8), 1297.
(109) Khanal, S. K.; Grewell, D.; Sung, S.; Van Leeuwen, J. Ultrasound applications in wastewater sludge pretreatment: a review. *Crit. Rev. Environ. Sci. Technol.* **2007,** *37* (4), 277.
(110) Yasuda, K.; Matsuura, K.; Asakura, Y.; Koda, S. Effect of agitation condition on performance of sonochemical reaction. *Jpn J Appl Phys* **2009,** *48* (7S), 07GH04.
(111) Ginsburg, E.; Kinsley, M.; Quitral, A. The power of ultrasound. *Adm Radiol J.* **1998,** *17* (5), 17.
(112) Flannigan, D. J.; Suslick, K. S. Inertially confined plasma in an imploding bubble. *Nat. Phys.* **2010,** *6* (8), 598.
(113) Crum, L. A. Tensile strength of water. *Nature* **1979,** *278* (5700), 148.
(114) Bader, K. B.; Raymond, J. L.; Mobley, J.; Church, C. C.; Felipe Gaitan, D. The effect of static pressure on the inertial cavitation threshold. *J. Acoust. Soc. Am.* **2012,** *132* (2), 728.
(115) Van Iersel, M. M.; van den Manacker, J.-P. A.; Benes, N. E.; Keurentjes, J. T. Pressure-induced reduction of shielding for improving sonochemical activity. *J. Phys. Chem. B* **2007,** *111* (12), 3081.
(116) Henglein, A.; Gutierrez, M. Sonochemistry and sonoluminescence: effects of external pressure. *J. Phys. Chem. A* **1993,** *97* (1), 158.
(117) Merouani, S.; Hamdaoui, O.; Rezgui, Y.; Guemini, M. Computer simulation of chemical reactions occurring in collapsing acoustical bubble: dependence of free radicals production on operational conditions. *Res. Chem. Intermed.* **2015,** *41* (2), 881.
(118) Yasui, K. Influence of ultrasonic frequency on multibubble sonoluminescence. *J. Acoust. Soc. Am.* **2002,** *112* (4), 1405.
(119) Didenko, Y. T.; McNamara III, W. B.; Suslick, K. S. Effect of noble gases on sonoluminescence temperatures during multibubble cavitation. *Phys. Rev. Lett.* **2000,** *84* (4), 777.
(120) Gogate, P. R. Intensification of chemical processing applications using ultrasonic and microwave irradiations. *Curr. Opin. Chem. Eng.* **2017,** *17*, 9.
(121) Merouani, S.; Hamdaoui, O.; Al ‐ Zahrani, S. M. Toward understanding the mechanism of pure CO2 ‐ quenching sonochemical processes. *J. Chem. Technol. Biotechnol* **2020,** *95* (3), 553.

(122) Pflieger, R.; Lee, J.; Nikitenko, S. I.; Ashokkumar, M. Influence of He and Ar flow rates and NaCl concentration on the size distribution of bubbles generated by power ultrasound. *J. Phys. Chem. B* **2015,** *119* (39), 12682.
(123) Brotchie, A.; Statham, T.; Zhou, M.; Dharmarathne, L.; Grieser, F.; Ashokkumar, M. Acoustic bubble sizes, coalescence, and sonochemical activity in aqueous electrolyte solutions saturated with different gases. *Langmuir* **2010,** *26* (15), 12690.
(124) Browne, C.; Tabor, R. F.; Chan, D. Y.; Dagastine, R. R.; Ashokkumar, M.; Grieser, F. Bubble coalescence during acoustic cavitation in aqueous electrolyte solutions. *Langmuir* **2011,** *27* (19), 12025.
(125) Gogate, P. R.; Katekhaye, S. N. A comparison of the degree of intensification due to the use of additives in ultrasonic horn and ultrasonic bath. *Chem. Eng. Process* **2012,** *61*, 23.
(126) Pflieger, R.; Nikitenko, S. I.; Ashokkumar, M. Effect of NaCl salt on sonochemistry and sonoluminescence in aqueous solutions. *Ultrason Sonochem* **2019,** *59*, 104753.
(127) Weissenborn, P. K.; Pugh, R. J. Surface tension of aqueous solutions of electrolytes: relationship with ion hydration, oxygen solubility, and bubble coalescence. *J. Colloid Interface Sci* **1996,** *184* (2), 550.
(128) Rimoldi, L.; Meroni, D.; Falletta, E.; Pifferi, V.; Falciola, L.; Cappelletti, G.; Ardizzone, S. Emerging pollutant mixture mineralization by TiO_2 photocatalysts. The role of the water medium. *Photochem. Photobiol. Sci.* **2017,** *16* (1), 60.
(129) Khan, I.; Ali, S.; Mansha, M.; Qurashi, A. Sonochemical assisted hydrothermal synthesis of pseudo-flower shaped Bismuth vanadate ($BiVO_4$) and their solar-driven water splitting application. *Ultrason Sonochem* **2017,** *36*, 386.
(130) Suslick, K. S. *Ultrasound: its chemical, physical, and biological effects*; VCH Publishers, 1988.
(131) Hartmann, J.; Bartels, P.; Mau, U.; Witter, M.; Tümpling, W.; Hofmann, J.; Nietzschmann, E. Degradation of the drug diclofenac in water by sonolysis in presence of catalysts. *Chemosphere* **2008,** *70* (3), 453.
(132) Laajimi, H.; Mattia, M.; Stein, R. S.; Bianchi, C. L.; Boffito, D. C. Electron paramagnetic resonance of sonicated powder suspensions in organic solvents. *Ultrason Sonochem* **2021,** *73*, 105544.
(133) Madhavan, J.; Kumar, P. S. S.; Anandan, S.; Zhou, M.; Grieser, F.; Ashokkumar, M. Ultrasound assisted photocatalytic degradation of diclofenac in an aqueous environment. *Chemosphere* **2010,** *80* (7), 747.
(134) Ashokkumar, M.; Lee, J.; Kentish, S.; Grieser, F. Bubbles in an acoustic field: an overview. *Ultrason Sonochem* **2007,** *14* (4), 470.
(135) Leong, T.; Wu, S.; Kentish, S.; Ashokkumar, M. Growth of bubbles by rectified diffusion in aqueous surfactant solutions. *J. Phys. Chem. C* **2010,** *114* (47), 20141.
(136) Leong, T.; Collis, J.; Manasseh, R.; Ooi, A.; Novell, A.; Bouakaz, A.; Ashokkumar, M.; Kentish, S. The role of surfactant headgroup, chain length,

and cavitation microstreaming on the growth of bubbles by rectified diffusion. *J. Phys. Chem. C* **2011,** *115* (49), 24310.

(137) Mišík, V.; Riesz, P. In *Sonochemistry and sonoluminescence*; Springer, 1999.

(138) Chakraborty, J.; Sarkar, J.; Kumar, R.; Madras, G. Ultrasonic degradation of polybutadiene and isotactic polypropylene. *Polym. Degrad. Stab.* **2004,** *85* (1), 555.

(139) Harkal, U.; Gogate, P.; Pandit, A.; Shenoy, M. Ultrasonic degradation of poly (vinyl alcohol) in aqueous solution. *Ultrason Sonochem* **2006,** *13* (5), 423.

(140) Tran, K. V. B.; Asakura, Y.; Koda, S. Influence of Liquid Height on Mechanical and Chemical Effects in 20 kHz Sonication. *Jpn. J. Appl. Phys.* **2013,** *52* (7S), 07HE07.

(141) Ma, X.; Huang, B.; Wang, G.; Zhang, M. Experimental investigation of conical bubble structure and acoustic flow structure in ultrasonic field. *Ultrason Sonochem* **2017,** *34*, 164.

(142) Han, J. T.; Jang, J. I.; Kim, H.; Hwang, J. Y.; Yoo, H. K.; Woo, J. S.; Choi, S.; Kim, H. Y.; Jeong, H. J.; Jeong, S. Y. Extremely efficient liquid exfoliation and dispersion of layered materials by unusual acoustic cavitation. *Sci. Rep.* **2014,** *4* (1), 1.

(143) Kumar, A.; Kumaresan, T.; Pandit, A. B.; Joshi, J. B. Characterization of flow phenomena induced by ultrasonic horn. *Chem. Eng. Sci.* **2006,** *61* (22), 7410.

(144) Chouvellon, M.; Largillier, A.; Fournel, T.; Boldo, P.; Gonthier, Y. Velocity study in an ultrasonic reactor. *Ultrason Sonochem* **2000,** *7* (4), 207.

(145) Mandroyan, A.; Doche, M.; Hihn, J.; Viennet, R.; Bailly, Y.; Simonin, L. Modification of the ultrasound induced activity by the presence of an electrode in a sono-reactor working at two low frequencies (20 and 40 kHz). Part II: Mapping flow velocities by particle image velocimetry (PIV). *Ultrason Sonochem* **2009,** *16* (1), 97.

(146) Contamine, R. F.; Wilhelm, A.; Berlan, J.; Delmas, H. Power measurement in sonochemistry. *Ultrason Sonochem* **1995,** *2* (1), S43.

(147) Gogate, P. R.; Sutkar, V. S.; Pandit, A. B. Sonochemical reactors: important design and scale up considerations with a special emphasis on heterogeneous systems. *Chem. Eng. J.* **2011,** *166* (3), 1066.

(148) Orandrou, S.-V.; Roy, J.-C.; Bailly, Y.; Poncet, E.; Girardot, L.; Ramel, D. Determination of the heat transfer coefficients for the combined natural and streaming convection on an ultrasonic transducer. *Int. J. Heat Mass Transf.* **2013,** *62*, 402.

(149) Cintas, P.; Mantegna, S.; Gaudino, E. C.; Cravotto, G. A new pilot flow reactor for high-intensity ultrasound irradiation. Application to the synthesis of biodiesel. *Ultrason Sonochem* **2010,** *17* (6), 985.

(150) da Paz, J. A.; de Menezes, F. D.; Selva, T. M. G.; Navarro, M.; da Costa, J. Â. P.; da Silva, R. D.; Villa, A. A. O.; Vilar, M. Sonoelectrochemical hydrogenation of safrole: A reactor design, statistical analysis and computational fluid dynamic approach. *Ultrason Sonochem* **2020,** *63*, 104949.

(151) John, J. J.; Kuhn, S.; Braeken, L.; Van Gerven, T. Ultrasound assisted liquid–liquid extraction with a novel interval-contact reactor. *Chem. Eng. Process* **2017,** *113*, 35.
(152) Sutkar, V. S.; Gogate, P. R. Design aspects of sonochemical reactors: techniques for understanding cavitational activity distribution and effect of operating parameters. *Chem. Eng. J.* **2009,** *155* (1-2), 26.
(153) Dong, Z.; Delacour, C.; Mc Carogher, K.; Udepurkar, A. P.; Kuhn, S. Continuous ultrasonic reactors: design, mechanism and application. *Materials* **2020,** *13* (2), 344.
(154) Avvaru, B.; Pandit, A. B. Experimental investigation of cavitational bubble dynamics under multi-frequency system. *Ultrason Sonochem* **2008,** *15* (4), 578.
(155) Wei, Z.; Weavers, L. K. Combining COMSOL modeling with acoustic pressure maps to design sono-reactors. *Ultrason Sonochem* **2016,** *31*, 490.
(156) Koch, C.; Jenderka, K.-V. Measurement of sound field in cavitating media by an optical fibre-tip hydrophone. *Ultrason Sonochem* **2008,** *15* (4), 502.
(157) Wang, L.; Memoli, G.; Hodnett, M.; Butterworth, I.; Sarno, D.; Zeqiri, B. Towards a reference cavitating vessel Part III—design and acoustic pressure characterization of a multi-frequency sonoreactor. *Metrologia* **2015,** *52* (4), 575.
(158) Servant, G.; Laborde, J.-L.; Hita, A.; Caltagirone, J.-P.; Gérard, A. Spatio-temporal dynamics of cavitation bubble clouds in a low frequency reactor: comparison between theoretical and experimental results. *Ultrason Sonochem* **2001,** *8* (3), 163.
(159) Lebon, G. B.; Tzanakis, I.; Pericleous, K.; Eskin, D.; Grant, P. S. Ultrasonic liquid metal processing: The essential role of cavitation bubbles in controlling acoustic streaming. *Ultrason Sonochem* **2019,** *55*, 243.
(160) Barthes, M.; Mazue, G.; Bonnet, D.; Viennet, R.; Hihn, J.-Y.; Bailly, Y. Characterization of the activity of ultrasound emitted in a perpendicular liquid flow using Particle Image Velocimetry (PIV) and electrochemical mass transfer measurements. *Ultrasonics* **2015,** *59*, 72.
(161) Schenker, M.; Pourquié, M.; Eskin, D.; Boersma, B. PIV quantification of the flow induced by an ultrasonic horn and numerical modeling of the flow and related processing times. *Ultrason Sonochem* **2013,** *20* (1), 502.
(162) Hihn, J.-Y.; Doche, M.-L.; Hallez, L.; Taouil, A. E.; Pollet, B. G. Sonoelectrochemistry: both a tool for investigating mechanisms and for accelerating processes. *J. Electrochem. Soc.* **2018,** *27* (3), 47.
(163) Kim, E.; Son, Y. The Effect of Distance between Two Transducers on Sonochemical Reactions in Dual Irradiation Systems. *J. Soil Groundw. Environ.* **2013,** *18* (5), 39.
(164) Couto, A. B.; de Souza, D. C.; Sartori, E. R.; Jacob, P.; Klockow, D.; Neves, E. A. The catalytic cycle of oxidation of iodide ion in the oxygen/nitrous acid/nitric oxide system and its potential for analytical applications. *Anal. Lett.* **2006,** *39* (15), 2763.

(165) Sehested, K.; Bjergbakke, E.; Rasmussen, O.; Fricke, H. Reactions of H_2O_3 in the Pulse - Irradiated Fe (II) – O_2 System, Atomic Energy Commission Research Establishment Risoe, Denmark, 1969.
(166) Yasuda, K.; Torii, T.; Yasui, K.; Iida, Y.; Tuziuti, T.; Nakamura, M.; Asakura, Y. Enhancement of sonochemical reaction of terephthalate ion by superposition of ultrasonic fields of various frequencies. *Ultrason Sonochem* **2007,** *14* (6), 699.
(167) Zhao, Y.; Zhu, C.; Feng, R.; Xu, J.; Wang, Y. Fluorescence enhancement of the aqueous solution of terephthalate ion after bi-frequency sonication. *Ultrason Sonochem* **2002,** *9* (5), 241.
(168) Arrojo, S.; Nerin, C.; Benito, Y. Application of salicylic acid dosimetry to evaluate hydrodynamic cavitation as an advanced oxidation process. *Ultrason Sonochem* **2007,** *14* (3), 343.
(169) Chakinala, A. G.; Gogate, P. R.; Burgess, A. E.; Bremner, D. H. Intensification of hydroxyl radical production in sonochemical reactors. *Ultrason Sonochem* **2007,** *14* (5), 509.
(170) Hihn, J.-Y.; Doche, M.-L.; Mandroyan, A.; Hallez, L.; Pollet, B. Respective contribution of cavitation and convective flow to local stirring in sonoreactors. *Ultrason Sonochem* **2011,** *18* (4), 881.
(171) Niazi, S.; Hashemabadi, S. H.; Razi, M. M. CFD simulation of acoustic cavitation in a crude oil upgrading sonoreactor and prediction of collapse temperature and pressure of a cavitation bubble. *Chem. Eng. Res. Des.* **2014,** *92* (1), 166.
(172) Sutkar, V. S.; Gogate, P. R.; Csoka, L. Theoretical prediction of cavitational activity distribution in sonochemical reactors. *Chem. Eng. J.* **2010,** *158* (2), 290.
(173) Yasui, K.; Kozuka, T.; Tuziuti, T.; Towata, A.; Iida, Y.; King, J.; Macey, P. FEM calculation of an acoustic field in a sonochemical reactor. *Ultrason Sonochem* **2007,** *14* (5), 605.
(174) Dion, J.-L. Contamination-free high capacity converging waves sonoreactors for the chemical industry. *Ultrason Sonochem* **2009,** *16* (2), 212.
(175) Tangsopa, W.; Thongsri, J. Development of an industrial ultrasonic cleaning tank based on harmonic response analysis. *Ultrasonics* **2019,** *91*, 68.
(176) Mutasa, T.; Gachagan, A.; Nordon, A.; O'leary, R. IEEE International Ultrasonics Symposium, 2010; p 1470.
(177) Csoka, L.; Katekhaye, S. N.; Gogate, P. R. Comparison of cavitational activity in different configurations of sonochemical reactors using model reaction supported with theoretical simulations. *Chem. Eng. J.* **2011,** *178*, 384.
(178) Rashwan, S. S.; Dincer, I.; Mohany, A. Investigation of acoustic and geometric effects on the sonoreactor performance. *Ultrason Sonochem* **2020,** *68*, 105174.
(179) Dubus, B., and P. Mosbah. Modeling of power ultrasonic transducers. Power Ultrasonics. Woodhead Publishing, 2015. 219-239..
(180) Lais, H.; Lowe, P. S.; Gan, T.-H.; Wrobel, L. C. Numerical modelling of acoustic pressure fields to optimize the ultrasonic cleaning technique for cylinders. *Ultrason Sonochem* **2018,** *45*, 7.

(181) Mason, T. J. Ultrasonic cleaning: An historical perspective. *Ultrason Sonochem* **2016,** *29*, 519.
(182) Henglein, A. Sonochemistry: historical developments and modern aspects. *Ultrasonics* **1987,** *25* (1), 6.
(183) Choi, J.; Kim, T.-H.; Kim, H.-Y.; Kim, W. Ultrasonic washing of textiles. *Ultrason Sonochem* **2016,** *29*, 563.
(184) Bryson, L.; Fernandez Rivas, D.; Boutsioukis, C. Cleaning of used rotary nickel‐titanium files in an ultrasonic bath by locally intensified acoustic cavitation. *Int. Endod. J.* **2018,** *51* (4), 457.
(185) Lee, J.-H.; Choi, S. U.; Jang, S. P.; Lee, S. Y. Production of aqueous spherical gold nanoparticles using conventional ultrasonic bath. *Nanoscale research letters* **2012,** *7* (1), 1.
(186) Muthoosamy, K.; Manickam, S. State of the art and recent advances in the ultrasound-assisted synthesis, exfoliation and functionalization of graphene derivatives. *Ultrason Sonochem* **2017,** *39*, 478.
(187) Djellabi, R.; Zhang, L.; Yang, B.; Haider, M. R.; Zhao, X. Sustainable self-floating lignocellulosic biomass-TiO_2@Aerogel for outdoor solar photocatalytic Cr (VI) reduction. *Sep. Purif. Technol.* **2019,** *229*, 115830.
(188) Plattes, M.; Koehler, C.; Gallé, T. Purely ultrasonic enzyme extraction from activated sludge in an ultrasonic cleaning bath. *MethodsX* **2017,** *4*, 214.
(189) Bizzi, C. A.; Santos, D.; Sieben, T. C.; Motta, G. V.; Mello, P. A.; Flores, E. M. Furfural production from lignocellulosic biomass by ultrasound-assisted acid hydrolysis. *Ultrason Sonochem* **2019,** *51*, 332.
(190) Huang, X.; Zhou, C.; Suo, Q.; Zhang, L.; Wang, S. Experimental study on viscosity reduction for residual oil by ultrasonic. *Ultrason Sonochem* **2018,** *41*, 661.
(191) Costa, J. M.; de Almeida Neto, A. F. Ultrasound-assisted electrodeposition and synthesis of alloys and composite materials: A review. *Ultrason Sonochem* **2020,** *68*, 105193.
(192) Zhou, Z.; Yang, Y.; Li, X.; Zhang, Y.; Guo, X. Characterization of drinking water treatment sludge after ultrasound treatment. *Ultrason Sonochem* **2015,** *24*, 19.
(193) Gogate, P. R.; Mujumdar, S.; Pandit, A. B. Sonochemical reactors for waste water treatment: comparison using formic acid degradation as a model reaction. *Adv. Environ. Res.* **2003,** *7* (2), 283.
(194) Mason, T. J.; Peters, D. *Practical sonochemistry: Power ultrasound uses and applications*; Woodhead Publishing, 2002.
(195) Iervolino, G.; Zammit, I.; Vaiano, V.; Rizzo, L. Limitations and prospects for wastewater treatment by UV and visible-light-active heterogeneous photocatalysis: a critical review. *Heterogeneous Photocatalysis* **2020**, 225-264.
(196) Li, C.; Guo, Y.; Tang, D.; Guo, Y.; Wang, G.; Jiang, H.; Li, J. Optimizing electron structure of Zn-doped $AgFeO_2$ with abundant oxygen vacancies to boost photocatalytic activity for Cr(VI) reduction and organic pollutants

decomposition: DFT insights and experimental. *Chem. Eng. J.* **2021,** *411*, 128515.

(197) Bruze, Magnus. "The use of ultrasonic bath extracts in the diagnostics of contact allergy and allergic contact dermatitis." *Patch Testing Tips. Springer, Berlin, Heidelberg*, **2014**. 129-142..

(198) Qin, D.-D.; Zhu, Y.-J.; Chen, F.-F.; Yang, R.-L.; Xiong, Z.-C. Self-floating aerogel composed of carbon nanotubes and ultralong hydroxyapatite nanowires for highly efficient solar energy-assisted water purification. *Carbon* **2019,** *150*, 233-243.

(199) Gogate, P. R. Cavitational reactors for process intensification of chemical processing applications: a critical review. *Chem. Eng. Process* **2008,** *47* (4), 515.

(200) Doğruel, S.; Özgen, A. S. Effect of ultrasonic and microwave disintegration on physico-chemical and biodegradation characteristics of waste-activated sludge. *Environ. Technol.* **2017,** *38* (7), 844.

(201) Delmas, H.; Le, N. T.; Barthe, L.; Julcour-Lebigue, C. Optimization of hydrostatic pressure at varied sonication conditions–power density, intensity, very low frequency–for isothermal ultrasonic sludge treatment. *Ultrason Sonochem* **2015,** *25*, 51-59.

(202) Kentish, S.; Feng, H. Applications of power ultrasound in food processing. *Annu. Rev. Food Sci. Technol.* **2014,** *5*, 263-284.

(203) Tao, Y.; Sun, D.-W. Enhancement of food processes by ultrasound: a review. *Crit. Rev. Food Sci. Nutr.* **2015,** *55* (4), 570-594.

(204) Petošić, A.; Horvat, M.; Jambrak, A. R. Electromechanical, acoustical and thermodynamical characterization of a low-frequency sonotrode-type transducer in a small sonoreactor at different excitation levels and loading conditions. *Ultrason Sonochem* **2017,** *39*, 219.

(205) Islam, M. H.; Paul, M. T.; Burheim, O. S.; Pollet, B. G. Recent developments in the sonoelectrochemical synthesis of nanomaterials. *Ultrason Sonochem* **2019,** *59*, 104711.

(206) Comazzi, A.; Pirola, C.; Longhi, M.; Bianchi, C. L.; Suslick, K. S. Fe-based heterogeneous catalysts for the Fischer-Tropsch reaction: Sonochemical synthesis and bench-scale experimental tests. *Ultrason Sonochem* **2017,** *34*, 774-780.

(207) Stucchi, M.; Bianchi, C. L.; Argirusis, C.; Pifferi, V.; Neppolian, B.; Cerrato, G.; Boffito, D. Ultrasound assisted synthesis of Ag-decorated TiO_2 active in visible light. *Ultrason Sonochem* **2018,** *40*, 282-288.

(208) Comazzi, A.; Livraghi, N.; Pirola, C.; Bianchi, C.; Di Michele, A.; Demartin, F.; Suslick, K. DGMK-International Conference on Catalysis-Novel Aspects in Petrochemistry and Refining, **2016**; 83.

(209) Eskin, D. G.; Al-Helal, K.; Tzanakis, I. Application of a plate sonotrode to ultrasonic degassing of aluminum melt: acoustic measurements and feasibility study. *J. Mater. Process. Technol.* **2015,** *222*, 148.

(210) Naddeo, V.; Belgiorno, V.; Kassinos, D.; Mantzavinos, D.; Meric, S. Ultrasonic degradation, mineralization and detoxification of diclofenac in water: optimization of operating parameters. *Ultrason Sonochem* **2010,** *17* (1), 179.
(211) Wu, Z.; Abramova, A.; Nikonov, R.; Cravotto, G. Sonozonation (sonication/ozonation) for the degradation of organic contaminants–A review. *Ultrason Sonochem* **2020,** *68*, 105195.
(212) Martín-García, B.; Pasini, F.; Verardo, V.; Díaz-de-Cerio, E.; Tylewicz, U.; Gómez-Caravaca, A. M.; Caboni, M. F. Optimization of sonotrode ultrasonic-assisted extraction of proanthocyanidins from brewers' spent grains. *Antioxidants* **2019,** *8* (8), 282.
(213) Rani, M. R.; Prakasan, K.; Rudramoorthy, R. Studies on thermo-elastic heating of horns used in ultrasonic plastic welding. *Ultrasonics* **2015,** *55, 123-132*.
(214) Nguyen, H.-T.; Nguyen, H.-D.; Uan, J.-Y.; Wang, D.-A. A nonrational B-spline profiled horn with high displacement amplification for ultrasonic welding. *Ultrasonics* **2014,** *54* (8), 2063.
(215) Ma, Z.; Zhang, Y. Characterization of multilayer ultrasonic welding based on the online monitoring of sonotrode displacement. *J. Manuf. Process.* **2020,** *54, 138-147*.
(216) Yu, J.; Luo, H.; Nguyen, T. V.; Huang, L.; Liu, B.; Zhang, Y. Eigenfrequency characterization and tuning of Ti-$_6$Al-4V ultrasonic horn at high temperatures for glass molding. *Ultrasonics* **2020,** *101*, 106002.
(217) Kim, S.-R.; Lee, J. H.; Yoo, C. D.; Song, J.-Y.; Lee, S. S. Design of highly uniform spool and bar horns for ultrasonic bonding. *IEEE transactions on ultrasonics, ferroelectrics, and frequency control* **2011,** *58* (10), 2194.
(218) Li, D.; Soar, R. Influence of sonotrode texture on the performance of an ultrasonic consolidation machine and the interfacial bond strength. *J. Mater. Process. Technol.* **2009,** *209* (4), 1627.
(219) Son, Y. Simple design strategy for bath-type high-frequency sonoreactors. *Chem. Eng. J.* **2017,** *328*, 654-664.
(220) Son, Y.; Lim, M.; Song, J.; Khim, J. Liquid height effect on sonochemical reactions in a 35 kHz sonoreactor. *Jpn. J. Appl. Phys.* **2009,** *48* (7S), 07GM16.
(221) Thokchom, B.; Pandit, A. B.; Qiu, P.; Park, B.; Choi, J.; Khim, J. A review on sonoelectrochemical technology as an upcoming alternative for pollutant degradation. *Ultrason Sonochem* **2015,** 27, 210-234.
(222) Birkin, P. R.; Offin, D. G.; Leighton, T. G. Experimental and theoretical characterisation of sonochemical cells. Part 2: cell disruptors (Ultrasonic horns) and cavity cluster collapse. *Phys. Chem. Chem. Phys.* **2005,** *7* (3), 530-537.
(223) Xiao, C.-f.; Han, B. Research and design of ultra-long ultrasonic horn. *J. Inst. Eng. (India): C* **2019,** *100* (6), 1015-1022.
(224) Shu, K.-M.; Chen, J.-W. The design of acoustic horns for ultrasonic aided tube double side flange making. *International Journal of Mechanical, Aerospace, Industrial, Mechatronic and Manufacturing Engineering* **2015,** *9* (5).

(225) He, T.; Ye, X.-Q.; Zhao, Y. Optimization design for ultrasonic horn with large amplitude based on genetic algorithm. *J. Vibroengineering* **2015,** 17(3), 1157-1168.
(226) Wei, Z.; Kosterman, J. A.; Xiao, R.; Pee, G.-Y.; Cai, M.; Weavers, L. K. Designing and characterizing a multi-stepped ultrasonic horn for enhanced sonochemical performance. *Ultrason Sonochem* **2015,** *27*, 325-333.
(227) Peshkovsky, S. L.; Peshkovsky, A. S. Matching a transducer to water at cavitation: Acoustic horn design principles. *Ultrason Sonochem* **2007,** *14* (3), 314-322.
(228) Mottyll, S.; Skoda, R. Numerical 3D flow simulation of ultrasonic horns with attached cavitation structures and assessment of flow aggressiveness and cavitation erosion sensitive wall zones. *Ultrason Sonochem* **2016,** *31*, 570-589.
(229) Dong, F.; Li, X.; Zhang, L.; Ma, L.; Li, R. Cavitation erosion mechanism of titanium alloy radiation rods in aluminum melt. *Ultrason Sonochem* **2016,** *31*, 150-156..
(230) Grabalosa, J.; Ferrer, I.; Martínez-Romero, O.; Elías-Zúñiga, A.; Plantá, X.; Rivillas, F. Assessing a stepped sonotrode in ultrasonic molding technology. *Journal of Materials Processing Technology* **2016,** *229*, 687-696.
(231) Tian, Y.; Liu, Z.; Li, X.; Zhang, L.; Li, R.; Jiang, R.; Dong, F. The cavitation erosion of ultrasonic sonotrode during large-scale metallic casting: Experiment and simulation. *Ultrason Sonochem* **2018,** *43*, 29-37.
(232) Rosett, T. Cooling device for use with a sonic oscillator. *Applied microbiology* **1965,** *13* (2), 254-256.
(233) Davidson, E. A.; Theodore, R.; Process and apparatus for treating heat sensitive material with sonic vibrations, Patent: US3246881A, United States 1966.
(234) Yasumitsu, T.; Liu, G.; Leveque, J.-M.; Aonuma, S.; Duclaux, L.; Kimura, T.; Komatsu, N. A rosette cooling cell: More effective container for solubilization of single-walled carbon nanotubes under probe-type ultrasonic irradiation. *Ultrason Sonochem* **2013,** *20* (1), 37.
(235) NAMAL, Imge. Fabrication and Optical and Electronic Characterization of Conjugated Polymer-Stabilized Semiconducting Single-Wall Carbon Nanotubes in Dispersions and Thin Films. **2018**. PhD thesis, Universität Würzburg.
(236) Levêque, J.-M.; Duclaux, L.; Rouzaud, J.-N.; Reinert, L.; Komatsu, N.; Desforges, A.; Afreen, S.; Sivakumar, M.; Kimura, T. Ultrasonic treatment of glassy carbon for nanoparticle preparation. *Ultrason Sonochem* **2017,** *35*, 615-622.
(237) Lu, Y.; Riyanto, N.; Weavers, L. K. Sonolysis of synthetic sediment particles: particle characteristics affecting particle dissolution and size reduction. *Ultrason Sonochem* **2002,** *9* (4), 181-188.
(238) Sun, S.; Li, P.; Liang, S.; Yang, Z. Diversified copper sulfide ($Cu_{2-x}S$) micro-/nanostructures: a comprehensive review on synthesis, modifications and applications. *Nanoscale* **2017,** *9* (32), 11357.

(239) Ghim, D.; Jiang, Q.; Cao, S.; Singamaneni, S.; Jun, Y.-S. Mechanically interlocked 1T/2H phases of MoS2 nanosheets for solar thermal water purification. *Nano energy* **2018,** *53*, 949-957.
(240) Song, L.; Zhang, X.-F.; Wang, Z.; Zheng, T.; Yao, J. Fe_3O_4/polyvinyl alcohol decorated delignified wood evaporator for continuous solar steam generation. *Desalination* **2021,** *507*, 115024.
(241) Andrés, R.; Riera, E.; Gallego-Juárez, J.; Mulet, A.; García-Pérez, J.; Cárcel, J. Airborne power ultrasound for drying process intensification at low temperatures: Use of a stepped-grooved plate transducer. *Dry. Technol.* **2021,** *39* (2), 245-258.
(242) Beck, S. M.; Sabarez, H.; Gaukel, V.; Knoerzer, K. Enhancement of convective drying by application of airborne ultrasound–a response surface approach. *Ultrason Sonochem* **2014,** *21* (6), 2144-2150.
(243) Charoux, C. M.; O'Donnell, C. P.; Tiwari, B. K. Effect of airborne ultrasonic technology on microbial inactivation and quality of dried food ingredients. *Ultrason Sonochem* **2019,** *56*, 313-317.
(244) Riera, E.; Golas, Y.; Blanco, A.; Gallego, J.; Blasco, M.; Mulet, A. Mass transfer enhancement in supercritical fluids extraction by means of power ultrasound. *Ultrason Sonochem* **2004,** *11* (3-4), 241-244.
(245) Riera, E.; Blanco, A.; García, J.; Benedito, J.; Mulet, A.; Gallego-Juárez, J. A.; Blasco, M. High-power ultrasonic system for the enhancement of mass transfer in supercritical CO_2 extraction processes. *Phys. Procedia* **2010,** *3* (1), 141-146.
(246) Riera, E.; Gallego Juárez, J. A.; Montoya Vitini, F.; Blanco Blanco, A.; Mulet Pons, A.; Benedito Fort, J. J.; Peña Cervero, R.; Golás Sánchezet al. Separation or extraction method using supercritical fluids assisted by high-intensity ultrasound. Patent: EP1547679B1, **2005**.
(247) Riera, E.; Cardoni, A.; Gallego-Juárez, J.; Acosta, V.; Blanco, A.; Rodríguez, G.; Blasco, M.; Herranz, L. Recent advances in the development and application of power plate transducers in dense gas extraction and aerosol agglomeration processes. *Phys. Procedia* **2015,** *63*, 67-72.
(248) Riera, E.; González-Gomez, I.; Rodríguez, G.; Gallego-Juárez, J. Ultrasonic agglomeration and preconditioning of aerosol particles for environmental and other applications. *Power Ultrasonics* **2015**, 1023-1058.
(249) Riera, E.; Gallego-Juárez, J. A.; Mason, T. J. Airborne ultrasound for the precipitation of smokes and powders and the destruction of foams. *Ultrason Sonochem* **2006,** *13* (2), 107-116.
(250) Gallego-Juárez, J.; Rodríguez, G.; Acosta-Aparicio, V.; Riera, E.; Cardoni, A. Power ultrasonic transducers with vibrating plate radiators. In : Power Ultrasonics. Woodhead Publishing, 2015. p. 159-193.
(251) Juárez, J. A. G., Corral, G. R., Vitini, F. M., Aparicio, V. A., De Sarabia, E. R. F., & Blanco, A. B. (2010). Macrosonic generator for the air-based industrial defoaming of liquids.In: US Patent (US 7719924 B2), USA.

(252) Andrés, R.; Acosta, V.; Lucas, M.; Riera, E. Modal analysis and nonlinear characterization of an airborne power ultrasonic transducer with rectangular plate radiator. *Ultrasonics* **2018,** *82*, 345-356.
(253) Charoux, C. M.; Ojha, K. S.; O'Donnell, C. P.; Cardoni, A.; Tiwari, B. K. Applications of airborne ultrasonic technology in the food industry. *J. Food Eng.* **2017,** *208*, 28-36.
(254) Cardoni, A.; de Sarabia, E. R. F.; Blanco-Blanco, A.; Gallego-Juarez, J.; Acosta-Aparicio, V. 2009 IEEE International Ultrasonics Symposium, 2009; 2576.
(255) Gallego-Juárez, J. A.; Rodriguez, G.; Acosta, V.; Riera, E. Power ultrasonic transducers with extensive radiators for industrial processing. *Ultrason Sonochem* **2010,** *17* (6), 953-964.
(256) De La Calle, I.; Cabaleiro, N.; Lavilla, I.; Bendicho, C. Analytical evaluation of a cup-horn sonoreactor used for ultrasound-assisted extraction of trace metals from troublesome matrices. *Spectrochim. Acta B* **2009,** *64* (9), 874-883.
(257) Bizzi, C. A.; Zanatta, R. C.; Santos, D.; Giacobe, K.; Dallago, R. M.; Mello, P. A.; Flores, E. M. Ultrasound-assisted extraction of chromium from residual tanned leather: An innovative strategy for the reuse of waste in tanning industry. *Ultrason Sonochem* **2020,** *64*, 104682.
(258) Teixeira, L. S.; Vieira, H. P.; Windmöller, C. C.; Nascentes, C. C. Fast determination of trace elements in organic fertilizers using a cup-horn reactor for ultrasound-assisted extraction and fast sequential flame atomic absorption spectrometry. *Talanta* **2014,** *119*, 232-239.
(259) Santos, D.; Silva, U. F.; Duarte, F. A.; Bizzi, C. A.; Flores, E. M.; Mello, P. A. Ultrasound-assisted acid hydrolysis of cellulose to chemical building blocks: Application to furfural synthesis. *Ultrason Sonochem* **2018,** *40*, 81-88.
(260) Zargazi, M.; Entezari, M. H. Sonochemical versus hydrothermal synthesis of bismuth tungstate nanostructures: Photocatalytic, sonocatalytic and sonophotocatalytic activities. *Ultrason Sonochem* **2019,** *51*, 1-11.
(261) Cappelletti, L.; Vaghi, L.; Rinaldi, L.; Rotolo, L.; Palmisano, G.; Cravotto, G.; Penoni, A. One-pot sonochemical synthesis of ferrocenyl derivatives via a three-component reaction in aqueous media. *Ultrason Sonochem* **2015,** *27*, 30-36.
(262) Gogate, P. R.; Pandit, A. B.; Wilhelm, A.; Ratsimba, B.; Delmas, H. Destruction of formic acid using high frequency cup horn reactor. *Water Res.* **2006,** *40* (8), 1697-1705.
(263) Giannakoudakis, D. A.; Łomot, D.; Colmenares, J. C. When sonochemistry meets heterogeneous photocatalysis: designing a sonophotoreactor towards sustainable selective oxidation. *Green Chem.* **2020,** *22* (15), 4896-4905.
(264) Lippert, T.; Bandelin, J.; Musch, A.; Drewes, J. E.; Koch, K. Energy-positive sewage sludge pre-treatment with a novel ultrasonic flatbed reactor at low energy input. *Bioresour. Technol.* **2018,** *264*, 298-305.

(265) Bandelin, J.; Lippert, T.; Drewes, J. E.; Koch, K. Cavitation field analysis for an increased efficiency of ultrasonic sludge pre-treatment using a novel hydrophone system. *Ultrason Sonochem* **2018,** *42*, 672-678.
(266) Lippert, T.; Bandelin, J.; Schlederer, F.; Drewes, J. E.; Koch, K. Impact of ultrasound-induced cavitation on the fluid dynamics of water and sewage sludge in ultrasonic flatbed reactors. *Ultrason Sonochem* **2019,** *55*, 217-222.
(267) Bandelin, J.; Lippert, T.; Drewes, J. E.; Koch, K. Assessment of sonotrode and tube reactors for ultrasonic pre-treatment of two different sewage sludge types. *Ultrason Sonochem* **2020,** *64*, 105001.
(268) Koch, K.; Lippert, T.; Sabadini, N. H.; Drewes, J. E. Tube reactors as a novel ultrasonication system for trouble-free treatment of sludges. *Ultrason Sonochem* **2017,** *37*, 464-470.
(269) Kumar, A.; Gogate, P. R.; Pandit, A. B. Mapping the efficacy of new designs for large scale sonochemical reactors. *Ultrason Sonochem* **2007,** *14* (5), 538-544.
(270) Vibert, R.; Perrier, A. Ultrasonic device for continuous flow production (SONITUBE® 20-35 kHz). **2012**.
(271) Ozmen, F. K.; Koparal, A. S. Hybrid water disinfection system with silver ion in continuous flow ultrasonic reactor. *Desalin. Water Treat.* **2021,** *213*, 64-74.
(272) Somnuk, K.; Prasit, T.; Phanyusoh, D.; Prateepchaikul, G. Continuous methyl ester production with low frequency ultrasound clamps on a tubular reactor. *Biofuels* **2021,** *12* (5), 589-595.
(273) Abramova, A. V.; Bayazitov, V. M.; Fedulov, I. S.; Nikonov, R. V.; Sister, V. G.; Cravotto, G. Influence of Acoustic Oscillations on Continuous-Flow Water Disinfection. *Processes* **2020,** *8* (10), 1259.
(274) Servili, M.; Veneziani, G.; Taticchi, A.; Romaniello, R.; Tamborrino, A.; Leone, A. Low-frequency, high-power ultrasound treatment at different pressures for olive paste: Effects on olive oil yield and quality. *Ultrason Sonochem* **2019,** *59*, 104747.
(275) Vernes, L.; Abert-Vian, M.; El Maâtaoui, M.; Tao, Y.; Bornard, I.; Chemat, F. Application of ultrasound for green extraction of proteins from spirulina. Mechanism, optimization, modeling, and industrial prospects. *Ultrason Sonochem* **2019,** *54*, 48-60.
(276) K.N. Uwe Neis, F. S. Ultrasonic treatment device for biogas plants, DE102013206492A1, 2013, Germany.
(277) Nickel, K.; Neis, U. Ultrasonic disintegration of biosolids for improved biodegradation. *Ultrason Sonochem* **2007,** *14* (4), 450-455.
(278) Nickel, K.; Yang, S.; Klingspor, G.; Neis, U. Sonication of sludge by innovative high-power ultrasound technology–Practical Experiences.
(279) NEIS, U. The use of power ultrasound for wastewater and biomass treatment. In : Power ultrasonics. Woodhead Publishing, **2015**. 973-996.
(280) Wolff, H.; Nickel, K.; Houy, A.; Lunden, A.; Neis, U. 11th IWA World Congress on Anaerobic Digestion, Session PP9C-Biosolids, Brisbane, Australia, September, **2007**,23.

(281) Le, N. T.; Julcour-Lebigue, C.; Delmas, H. An executive review of sludge pretreatment by sonication. *J. Environ. Sci.* **2015,** *37*, 139-153.
(282) Cravotto, G.; Cintas, P. Power ultrasound in organic synthesis: moving cavitational chemistry from academia to innovative and large-scale applications. *Chem. Soc. Rev.* **2006,** *35* (2), 180-196.
(283) Chatel, G.; Varma, R. S. Ultrasound and microwave irradiation: contributions of alternative physicochemical activation methods to Green Chemistry. *Green Chem.* **2019,** *21* (22), 6043-6050.
(284) Leonelli, C.; Mason, T. J. Microwave and ultrasonic processing: now a realistic option for industry. *Chem. Eng. Process* **2010,** *49* (9), 885-900.
(285) Cravotto, G.; Di Carlo, S.; Curini, M.; Tumiatti, V.; Roggero, C. A new flow reactor for the treatment of polluted water with microwave and ultrasound. *J. Chem. Technol. Biotechnol.* **2007,** *82* (2), 205-208.
(286) Martina, K.; Tagliapietra, S.; Barge, A.; Cravotto, G. Combined microwaves/ultrasound, a hybrid technology. *Sonochemistry* **2017**, 175-201.
(287) Dong, Z.; Zhao, S.; Zhang, Y.; Yao, C.; Yuan, Q.; Chen, G. Mixing and residence time distribution in ultrasonic microreactors. *AIChE Journal* **2017,** *63* (4), 1404-1418.
(288) Fernandez Rivas, D.; Kuhn, S. Synergy of microfluidics and ultrasound: Process intensification challenges and opportunities. *Top. Curr. Chem.* **2016,** *374* (5).
(289) Dong, Z.; Yao, C.; Zhang, X.; Xu, J.; Chen, G.; Zhao, Y.; Yuan, Q. A high-power ultrasonic microreactor and its application in gas–liquid mass transfer intensification. *Lab on a Chip* **2015,** *15* (4), 1145-1152.
(290) Zhao, S.; Yao, C.; Dong, Z.; Liu, Y.; Chen, G.; Yuan, Q. Intensification of liquid-liquid two-phase mass transfer by oscillating bubbles in ultrasonic microreactor. *Chem. Eng. Sci.* **2018,** *186*, 122-134.
(291) Feng, H.; Barbosa-Cánovas, G. V.; Weiss, J. *Ultrasound technologies for food and bioprocessing*; Springer, **2011**.
(292) Freitas, S.; Gander, B.; Lehmann, N. Verfahren und Durchflusszelle zur kontinuierlichen Bearbeitung von fliessfähigen Zusammensetzungen mittels Ultraschall. **2002,** *102* (43), 837.
(293) Freitas, S.; Hielscher, G.; Merkle, H. P.; Gander, B. Continuous contact-and contamination-free ultrasonic emulsification—a useful tool for pharmaceutical development and production. *Ultrason Sonochem* **2006,** *13* (1), 76-85.
(294) Dubey, S. P.; Abhyankar, H. A.; Marchante, V.; Brighton, J. L.; Bergmann, B. Mathematical modeling for continuous reactive extrusion of poly lactic acid formation by ring opening polymerization considering metal/organic catalyst and alternative energies. *Catalyst* **2015,** *5*, 9.
(295) Dubey, S. P.; Abhyankar, H. A.; Marchante, V.; Brighton, J. L.; Blackburn, K.; Temple, C.; Bergmann, B.; Trinh, G.; David, C. Modelling and validation of synthesis of poly lactic acid using an alternative energy source through a continuous reactive extrusion process. *Polymers* **2016,** *8* (4), 164.

(296) Dion, J.-L.; Agbossou, K.; Method for the production of amines by reductive amination of carbonyl compounds under transfer-hydrogenation conditions, Patent: WO2003014061A, **2002**.
(297) John, J. J.; Kuhn, S.; Braeken, L.; Van Gerven, T. Temperature controlled interval contact design for ultrasound assisted liquid–liquid extraction. *Chem. Eng. Res. Des.* **2017,** *125*, 146-155.
(298) John, J. J.; Kuhn, S.; Braeken, L.; Van Gerven, T. Ultrasound assisted liquid–liquid extraction in microchannels—A direct contact method. *Chem. Eng. Process* **2016,** *102*, 37-46.
(299) Leong, T.; Coventry, M.; Swiergon, P.; Knoerzer, K.; Juliano, P. Ultrasound pressure distributions generated by high frequency transducers in large reactors. *Ultrason Sonochem* **2015,** *27*, 22-29.
(300) Juliano, P.; Augustin, M. A.; Xu, X.-Q.; Mawson, R.; Knoerzer, K. Advances in high frequency ultrasound separation of particulates from biomass. *Ultrason Sonochem* **2017,** *35*, 577-590.
(301) Juliano, P.; Bainczyk, F.; Swiergon, P.; Supriyatna, M. I. M.; Guillaume, C.; Ravetti, L.; Canamasas, P.; Cravotto, G.; Xu, X.-Q. Extraction of olive oil assisted by high-frequency ultrasound standing waves. *Ultrason Sonochem* **2017,** *38*, 104-114.
(302) Pilli, S.; Bhunia, P.; Yan, S.; LeBlanc, R.; Tyagi, R.; Surampalli, R. Ultrasonic pretreatment of sludge: a review. *Ultrason Sonochem* **2011,** *18* (1), 1-18.
(303) Gallipoli, A.; Braguglia, C. High-frequency ultrasound treatment of sludge: combined effect of surfactants removal and floc disintegration. *Ultrason Sonochem* **2012,** *19* (4), 864-871.
(304) Mohammadi, P.; Karami, N.; Zinatizadeh, A. A.; Falahi, F.; Aghamohammadi, N.; Almasi, A. Using high frequency and low-intensity ultrasound to enhance activated sludge characteristics. *Ultrason Sonochem* **2019,** *54*, 274-280.
(305) Dong, Z.; Udepurkar, A. P.; Kuhn, S. Synergistic effects of the alternating application of low and high frequency ultrasound for particle synthesis in microreactors. *Ultrason Sonochem* **2020,** *60*, 104800.
(306) Zielewicz, E. Effects of ultrasonic disintegration of excess sewage sludge. *Sonochemistry* **2017**, 149-174.
(307) Lippert, T.; Bandelin, J.; Schlederer, F.; Drewes, J. E.; Koch, K. Effects of ultrasonic reactor design on sewage sludge disintegration. *Ultrason Sonochem* **2020,** *68*, 105223.
(308) Wang, Q.; Wei, W.; Gong, Y.; Yu, Q.; Li, Q.; Sun, J.; Yuan, Z. Technologies for reducing sludge production in wastewater treatment plants: state of the art. *Sci. Total Environ.* **2017,** *587*, 510-521.
(309) Van Leeuwen, J.; Akin, B.; Khanal, S. K.; Sung, S.; Grewell, D.; van Leeuwen, J. Ultrasound pre-treatment of waste activated sludge. *Water Sci. Tech. Water* **2006,** *6* (6), 35-42.
(310) Dauknys, R.; Mažeikienė, A.; Paliulis, D. Effect of ultrasound and high voltage disintegration on sludge digestion process. *J. Environ. Manage.* **2020,** *270*, 110833.

(311) Xu, X.; Cao, D.; Wang, Z.; Liu, J.; Gao, J.; Sanchuan, M.; Wang, Z. Study on ultrasonic treatment for municipal sludge. *Ultrason Sonochem* **2019,** *57*, 29-37.
(312) Mobaraki, M.; Semken, R. S.; Mikkola, A.; Pyrhönen, J. Enhanced sludge dewatering based on the application of high-power ultrasonic vibration. *Ultrasonics* **2018,** *84*, 438-445.
(313) Na, S.; Kim, Y.-U.; Khim, J. Physiochemical properties of digested sewage sludge with ultrasonic treatment. *Ultrason Sonochem* **2007,** *14* (3), 281-285.
(314) Meegoda, J. N.; Perera, R. Ultrasound to decontaminate heavy metals in dredged sediments. *J. Hazard. Mater.* **2001,** *85* (1-2), 73-89.
(315) Wang, Y.; Pan, Y.; Li, X.; Zhang, K.; Zhu, T. Ultrasonic treatment enhances sludge disintegration and degradation in a photosynthetic bacteria - bioelectrochemical system. *Water Environ. Res.* **2019,** *91* (8), 665-671.
(316) Lizama, A. C.; Figueiras, C. C.; Herrera, R. R.; Pedreguera, A. Z.; Espinoza, J. E. R. Effects of ultrasonic pretreatment on the solubilization and kinetic study of biogas production from anaerobic digestion of waste activated sludge. *Int. Biodeterior. Biodegradation* **2017,** *123*, 1-9.
(317) Xie, G.-J.; Liu, B.-F.; Wang, Q.; Ding, J.; Ren, N.-Q. Ultrasonic waste activated sludge disintegration for recovering multiple nutrients for biofuel production. *Water Res.* **2016,** *93*, 56-64.
(318) Zheng, M.; Liu, Y.-C.; Xin, J.; Zuo, H.; Wang, C.-W.; Wu, W.-M. Ultrasonic treatment enhanced ammonia-oxidizing bacterial (AOB) activity for nitritation process. *Environ. Sci. Technol.* **2016,** *50* (2), 864-871.
(319) Huang, S.; Zhu, Y.; Zhang, G.; Lian, J.; Liu, Z.; Zhang, L.; Tian, S. Effects of low-intensity ultrasound on nitrite accumulation and microbial characteristics during partial nitrification. *Sci. Total Environ.* **2020,** *705*, 135985.
(320) Huang, S.; Zhu, Y.; Lian, J.; Liu, Z.; Zhang, L.; Tian, S. Enhancement in the partial nitrification of wastewater sludge via low-intensity ultrasound: Effects on rapid start-up and temperature resilience. *Bioresour. Technol.* **2019,** *294*, 122196.
(321) Avvaru, B.; Venkateswaran, N.; Uppara, P.; Iyengar, S. B.; Katti, S. S. Current knowledge and potential applications of cavitation technologies for the petroleum industry. *Ultrason Sonochem* **2018,** *42*, 493-507.
(322) Pukale, D. D.; Maddikeri, G. L.; Gogate, P. R.; Pandit, A. B.; Pratap, A. P. Ultrasound assisted transesterification of waste cooking oil using heterogeneous solid catalyst. *Ultrason Sonochem* **2015,** *22*, 278-286.
(323) Kuna, E.; Behling, R.; Valange, S.; Chatel, G.; Colmenares, J. C. Sonocatalysis: a potential sustainable pathway for the valorization of lignocellulosic biomass and derivatives. *Chemistry and Chemical Technologies in Waste Valorization* **2017**, 1.
(324) Esclapez, M.; García-Pérez, J. V.; Mulet, A.; Cárcel, J. Ultrasound-assisted extraction of natural products. *Food Eng. Rev.* **2011,** *3* (2), 108-120.
(325) Pingret, D.; Fabiano-Tixier, A.-S.; Chemat, F. Ultrasound-assisted extraction. Natural product extraction: principles and applications. *RSC Green Chem.* **2013,** *21*, 89-112.

(326) Wen, C.; Zhang, J.; Zhang, H.; Dzah, C. S.; Zandile, M.; Duan, Y.; Ma, H.; Luo, X. Advances in ultrasound assisted extraction of bioactive compounds from cash crops–A review. *Ultrason Sonochem* **2018,** *48*, 538-549.

(327) Chemat, S.; Aissa, A.; Boumechhour, A.; Arous, O.; Ait-Amar, H. Extraction mechanism of ultrasound assisted extraction and its effect on higher yielding and purity of artemisinin crystals from Artemisia annua L. leaves. *Ultrason Sonochem* **2017,** *34*, 310-316.

(328) Dzah, C. S.; Duan, Y.; Zhang, H.; Wen, C.; Zhang, J.; Chen, G.; Ma, H. The effects of ultrasound assisted extraction on yield, antioxidant, anticancer and antimicrobial activity of polyphenol extracts: A review. *Food Biosci.* **2020,** *35*, 100547.

(329) Umego, E. C.; He, R.; Ren, W.; Xu, H.; Ma, H. Ultrasonic-assisted enzymolysis: Principle and applications. *Process Biochem* **2020**.

(330) Vickers, N. J. Animal communication: when i'm calling you, will you answer too? *Curr. Biol.* **2017,** *27* (14), R713-R715.

(331) Dabbour, M.; He, R.; Mintah, B.; Golly, M. K.; Ma, H. Ultrasound pretreatment of sunflower protein: Impact on enzymolysis, ACE ‐ inhibition activity, and structure characterization. *J. Food Process. Preserv.* **2020,** *44* (4), e14398.

(332) Rahman, M. M.; Byanju, B.; Grewell, D.; Lamsal, B. P. High-power sonication of soy proteins: Hydroxyl radicals and their effects on protein structure. *Ultrason Sonochem* **2020,** *64*, 105019.

(333) Zhu, Z.; Zhu, M.; Wu, Z. Pretreatment of sugarcane bagasse with NH_4OH–H_2O_2 and ionic liquid for efficient hydrolysis and bioethanol production. *Bioresour. Technol.* **2012,** *119*, 199-207.

(334) Montalbo-Lomboy, M.; Grewell, D. Rapid dissolution of switchgrass in 1-butyl-3-methylimidazolium chloride by ultrasonication. *Ultrason Sonochem* **2015,** *22*, 588-599.

(335) Pananun, T.; Montalbo-Lomboy, M.; Noomhorm, A.; Grewell, D.; Lamsal, B. High-power ultrasonication-assisted extraction of soybean isoflavones and effect of toasting. *LWT-Food Science and Technology* **2012,** *47* (1), 199.

(336) Yu, L.; Sun, J.; Liu, S.; Bi, J.; Zhang, C.; Yang, Q. Ultrasonic-assisted enzymolysis to improve the antioxidant activities of peanut (Arachin conarachin L.) antioxidant hydrolysate. *Int. J. Mol. Sci.* **2012,** *13* (7), 9051-9068.

(337) Vallejo, A.; Usobiaga, A.; Ortiz-Zarragoitia, M.; Cajaraville, M. P.; Fernández, L. A.; Zuloaga, O. Focused ultrasound-assisted acceleration of enzymatic hydrolysis of alkylphenols and 17β-oestradiol glucuronide in fish bile. *Anal. Bioanal. Chem.* **2010,** *398* (5), 2307-2314.

(338) M. Sango, D.; Abela, D.; McElhatton, A.; Valdramidis, V. Assisted ultrasound applications for the production of safe foods. *J. Appl. Microbiol.* **2014,** *116* (5), 1067-1083.

(339) Deora, N.; Misra, N.; Deswal, A.; Mishra, H.; Cullen, P.; Tiwari, B. Ultrasound for improved crystallisation in food processing. *Food Eng. Rev.* **2013,** *5* (1), 36-44.

(340) Chen, F.; Zhang, M.; Yang, C.-h. Application of ultrasound technology in processing of ready-to-eat fresh food: A review. *Ultrason Sonochem* **2020,** *63*, 104953.
(341) Delmas, H.; Barthe, L. In *Power Ultrasonics*; Elsevier, 2015.
(342) Ojha, K. S.; Mason, T. J.; O'Donnell, C. P.; Kerry, J. P.; Tiwari, B. K. Ultrasound technology for food fermentation applications. *Ultrason Sonochem* **2017,** *34*, 410-417.
(343) Leong, T. S.; Martin, G. J.; Ashokkumar, M. Ultrasonic encapsulation–a review. *Ultrason Sonochem* **2017,** *35*, 605-614.
(344) del Rosario Cuéllar-Villarreal, M.; Ortega-Hernández, E.; Becerra-Moreno, A.; Welti-Chanes, J.; Cisneros-Zevallos, L.; Jacobo-Velázquez, D. A. Effects of ultrasound treatment and storage time on the extractability and biosynthesis of nutraceuticals in carrot (Daucus carota). *Postharvest Biol. Technol* **2016,** *119*, 18-26.
(345) Yildiz, G.; Palma, S.; Feng, H. Ultrasonic Cutting as a New Method to Produce Fresh‐Cut Red Delicious and Golden Delicious Apples. *J. Food Sci.* **2019,** *84* (12), 3391-3398.
(346) Huang, D.; Men, K.; Li, D.; Wen, T.; Gong, Z.; Sunden, B.; Wu, Z. Application of ultrasound technology in the drying of food products. *Ultrason Sonochem* **2020,** *63*, 104950.
(347) Alarcon-Rojo, A.; Janacua, H.; Rodriguez, J.; Paniwnyk, L.; Mason, T. J. Power ultrasound in meat processing. *Meat Sci.* **2015,** *107*, 86-93.
(348) Paniwnyk, L. Applications of ultrasound in processing of liquid foods: A review. *Ultrason Sonochem* **2017,** *38*, 794.
(349) Cao, X.; Zhang, M.; Mujumdar, A. S.; Zhong, Q.; Wang, Z. Effects of ultrasonic pretreatments on quality, energy consumption and sterilization of barley grass in freeze drying. *Ultrason Sonochem* **2018,** *40*, 333-340.
(350) Patist, A.; Bates, D. Ultrasonic innovations in the food industry: From the laboratory to commercial production. *Innovative food science & emerging technologies* **2008,** *9* (2), 73-83.
(351) Chandrapala, J.; Oliver, C.; Kentish, S.; Ashokkumar, M. Ultrasonics in food processing–Food quality assurance and food safety. *Trends Food Sci. Technol.* **2012,** *26* (2), 88-98.
(352) Arvanitoyannis, I. S.; Kotsanopoulos, K. V.; Savva, A. G. Use of ultrasounds in the food industry–Methods and effects on quality, safety, and organoleptic characteristics of foods: A review. *Crit. Rev. Food Sci. Nutr.* **2017,** *57* (1), 109-128.
(353) Dolatowski, Z. J.; Stadnik, J.; Stasiak, D. Applications of ultrasound in food technology. *Acta Sci. Pol. Technol. Aliment.* **2007,** *6* (3), 88-99.
(354) Awada, T.; Moharram, H.; Shaltout, O.; Asker, D.; Youssef, M. Applications of ultrasound in analysis, processing and quality control of food. *Food Res. Int.* **2012,** *48* (2), 410-427.

(355) Li, M.; Fogler, H. Acoustic emulsification. Part 1. The instability of the oil-water interface to form the initial droplets. *J. Fluid Mechanics* **1978,** *88* (3), 499-511.
(356) Li, M.; Fogler, H. Acoustic emulsification. Part 2. Breakup of the large primary oil droplets in a water medium. *J. Fluid Mechanics* **1978,** *88* (3), 513-528.
(357) Mason, T.; Graves, S.; Wilking, J.; Lin, M. Extreme emulsification: formation and structure of nanoemulsions. *Condens. Matter Phys.* **2006**.
(358) Pongsawatmanit, R.; Harnsilawat, T.; McClements, D. J. Influence of alginate, pH and ultrasound treatment on palm oil-in-water emulsions stabilized by β-lactoglobulin. *Colloids Surf. A Physicochem Eng. Asp.* **2006,** *287* (1-3), 59-67.
(359) de Moraes, D. P.; Antes, F. G.; Pereira, J. S.; dos Santos, M. d. F. P.; Guimarães, R. C.; Barin, J. S.; Mesko, M. r. F.; Paniz, J. N.; Flores, E. r. M. Microwave-assisted procedure for salinity evaluation of heavy crude oil emulsions. *Energy Fuels* **2010,** *24* (4), 2227-2232.
(360) Li, W.; Leong, T. S.; Ashokkumar, M.; Martin, G. J. A study of the effectiveness and energy efficiency of ultrasonic emulsification. *Phys. Chem. Chem. Phys.* **2018,** *20* (1), 86-96.
(361) O'sullivan, J.; Murray, B.; Flynn, C.; Norton, I. Comparison of batch and continuous ultrasonic emulsification processes. *J. Food Eng.* **2015,** *167*, 114-121.
(362) Ramisetty, K. A.; Pandit, A. B.; Gogate, P. R. Ultrasound assisted preparation of emulsion of coconut oil in water: understanding the effect of operating parameters and comparison of reactor designs. *Chem. Eng. Process* **2015,** *88*, 70-77.
(363) Shanmugam, A.; Ashokkumar, M. Functional properties of ultrasonically generated flaxseed oil-dairy emulsions. *Ultrason Sonochem* **2014,** *21* (5), 1649-1657.
(364) Abbas, S.; Karangwa, E.; Bashari, M.; Hayat, K.; Hong, X.; Sharif, H. R.; Zhang, X. Fabrication of polymeric nanocapsules from curcumin-loaded nanoemulsion templates by self-assembly. *Ultrason Sonochem* **2015,** *23*, 81-92.
(365) Ashokkumar, M. Applications of ultrasound in food and bioprocessing. *Ultrason Sonochem* **2015,** *25*, 17-23.
(366) Chemat, F.; Grondin, I.; Sing, A. S. C.; Smadja, J. Deterioration of edible oils during food processing by ultrasound. *Ultrason Sonochem* **2004,** *11* (1), 13-15.
(367) Pingret, D.; Durand, G. g.; Fabiano-Tixier, A.-S.; Rockenbauer, A.; Ginies, C.; Chemat, F. Degradation of edible oil during food processing by ultrasound: electron paramagnetic resonance, physicochemical, and sensory appreciation. *J. Agric. Food Chem.* **2012,** *60* (31), 7761-7768.
(368) Tao, Y.; Cai, J.; Huai, X.; Liu, B. Global average hydroxyl radical yield throughout entire lifetime of cavitation bubbles.
(369) Pradhan, A. A.; Gogate, P. R. Degradation of p-nitrophenol using acoustic cavitation and Fenton chemistry. *J. Hazard. Mater.* **2010,** *173* (1-3), 517-522.

TOC image

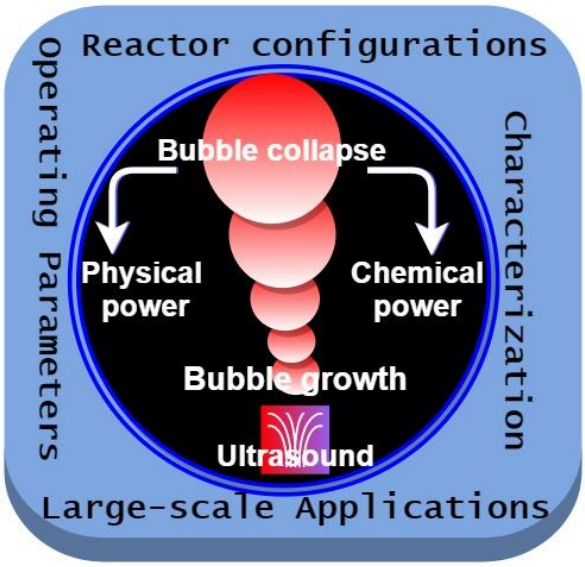
Reactor configurations
Operating Parameters
Characterization
Large-scale Applications
Bubble collapse
Physical power
Chemical power
Bubble growth
Ultrasound